

**Meteorological Model Performance Evaluation of an
Annual 2002 MM5 (version 3.6.3) Simulation**

**Matthew T. Johnson
Iowa Department of Natural Resources**

2004 - 2007

v2.0.4

Table of Contents

1. Introduction	3
1.1 Background.....	3
1.2 Model Selection	3
2. Sensitivity Projects	4
3. Modeling System Configuration	5
3.1 Overview.....	5
3.1.1 Terrain.....	5
3.1.2 PREGRID/REGRIDDER	5
3.1.3 LIITLE_R	10
3.1.4 INTERPF	10
3.2 MM5	12
3.3 Computational Summary	13
4. Model Performance Evaluation.....	14
4.1 Background.....	14
4.2 Methods.....	14
4.3 Statistical Measures	15
5. Surface Evaluation (36 km).....	18
5.1 Great Lakes	18
5.2 Northern and Southern Cenrap	18
5.3 Ohio Valley.....	19
5.4 Iowa.....	19
5.5 Eastern Regions	19
5.6 Western Regions	19
6. Twelve Kilometer Evaluation	30
6.1 Daily Averaged Statistics.....	30
6.2 Hourly Statistics.....	39
7. Upper Air Evaluation	43
7.1 Soundings.....	43
7.2 Precipitation	43
7.3 PBL Depths.....	45
8. Conclusions	48
9. References	49
Appendix A.....	51
Appendix B	52
Eastern Subdomains.....	52
Western Subdomains	58
Appendix C	66
CenrapN: January 2002	66
CenrapN: June 2002	68
OhioVal: January 2002.....	70
OhioVal: June 2002	72
Iowa: January 2002.....	74
Iowa: June 2002.....	76

1. INTRODUCTION

1.1 BACKGROUND

Projects pursuing PM_{2.5}, 8-hour ozone, and regional haze are generating modeling requirements at spatial and temporal scales only recently confronted within the regulatory air quality community. The scope of recent legislative and executive decisions has created the need to implement sophisticated models developed for regional scale multi-pollutant environments encompassing diverse climatological regimes. Computational limitations have historically bound the modeler's ability to investigate broad and complex scenarios with sufficient resolution. Exponential growth in computational efficiency has partially minimized this hurdle. As scientific theory and model complexity evolve, computational innovations remain moderately offset. Currently, a balance has been achieved which permits the development of large modeling databases such as annual continental scale simulations.

Annual continental scale air quality simulations require the implementation of a triumvirate modeling system composed of meteorological, emissions, and air quality models. Meteorological modeling is the first component addressed as meteorological data supports both the emissions and air quality models. In preparation for regulatory requirements involving regional haze, PM_{2.5}, and ozone, the Iowa Department of Natural Resources (IDNR) developed a continental scale annual meteorological dataset designed for use in air quality applications. This document details the methods employed to create the annual meteorological simulation and provides performance evaluation results.

1.2 MODEL SELECTION

Due to scientific progression, historical application, community support, and availability, the Fifth Generation Penn State University/National Center for Atmospheric Research Mesoscale Model (MM5) was selected for the development of an annual meteorological dataset. Originally formulated in the 1970s at Penn State and first documented by Anthes and Warner (1978), the MM5 modeling system maintains its status as a state-of-the-science¹ model through enhancements provided by a broad user community (*e.g.* Chen and Dudhia, 2001; Dudhia, 1993; Stauffer and Seaman, 1990; Stauffer and Seaman, 1991; Xiu and Pleim, 2000). The MM5 modeling system is routinely employed in operational forecasting frameworks as well as research applications spanning meteorological disciplines from synoptic to mesoscale. Utilization of MM5 within air quality applications is also a conventional practice. The MM5 modeling system was recently selected to generate three continental scale annual simulations: 1996, 2001, and 2002. The 1996 and 2001 simulations were conducted through EPA contracts (Olerud et al., 2000; McNally, 2003). The 2002 simulation was conducted in support of regional haze modeling for the Visibility Improvement – State and Tribal Association of the Southeast (VISTAS) regional planning organization (RPO) (Olerud and Sims, 2004). This list is not exhaustive as both public and private organizations continue to pursue annual meteorological modeling episodes.

Additional information regarding MM5 is available at: <http://www.mmm.ucar.edu/mm5/>

¹ True during project implementation. MM5 is no longer regularly updated as the focus has shifted to WRF.

2. SENSITIVITY PROJECTS

The MM5 modeling system consists of several pre-processors, the core prognostic model, and post-processing tools. Each component contains highly configurable control files; together they control the aspects of grid structure, first-guess fields, model physics, temporal operation, and ultimately results visualization. The inherent complexity of the MM5 modeling system complicates the development of a sound model configuration suitable for regional scale annual episode air quality applications. Although the complete matrix of configuration options reduces in size as inappropriate options are eliminated, a large matrix of potentially acceptable model configurations remains with most applications. The first step in developing the annual MM5 dataset was therefore completion of a series of sensitivities studies designed to identify the configuration yielding optimum results.

The first sensitivity study project began in 2002 and involved a collaborative project lead by Kirk Baker with the Lake Michigan Air Directors Consortium (LADCO) and Matthew Johnson (IDNR). Wyatt Appel and Mike Abraczkas with the North Carolina Division of Air Quality participated through the generation of a summary analysis for select sensitivity runs. The project was conducted in coordination with sensitivity work performed by Dennis McNally (with Alpine Geophysics). Components evaluated included, for example, PBL schemes, microphysical schemes, convective parameterizations, land surface parameterizations, and snow models. Two one-month long episodes were selected for evaluation, January and July of 2001. The performance evaluation of each sensitivity run included, but was not limited to, temperatures, wind vectors, cloud cover, precipitation, and mixing ratios.

Following the sensitivity study, the IDNR completed a 2002 annual simulation. This simulation utilized surface moisture and temperature nudging. Within implementation of the Pleim-Xiu (PX) land surface model (LSM), soil moisture and soil temperatures were modeled in continuum from one 5-day episode block to the next. The model performance evaluation revealed an extreme cold bias over the Central U.S. While unrelated to the cold bias, utilization of surface nudging techniques was abandoned following discussion with the modeling community, as this practice has led to the generation of super-adiabatic lapse rates near the surface. The optimum IDNR/LADCO configuration was thus modified accordingly and this annual simulation was deemed unsuitable for use in air quality modeling projects.

In a similar timeframe, VISTAS contracted with Baron Advanced Meteorological Systems, LLC (BAMS) for the development of an annual MM5 dataset (Olerud and Sims, 2004). The work of VISTAS (through Olerud and Sims, 2004) also included a series of sensitivity studies. Independent results from the VISTAS project yielded findings similar to the conclusions reached by IDNR and LADCO. The compilation of all project results subsequently produced the configuration utilized by the IDNR in development of an annual metrological dataset suitable for regional scale air quality modeling.

3. MODELING SYSTEM CONFIGURATION

3.1 OVERVIEW

Version 3.6.3 of the MM5 modeling system was utilized in the second¹ (and final) 2002 IDNR annual meteorological simulation. The 3.6.3 release represented the most current version available at the time of project inception. Other than the necessary configuration parameters, no modeling system code modifications capable of altering results were rendered.

3.1.1 TERRAIN

The terrain processor is used to define grid structure and assign various surface features. Terrain elevation, the dominant landuse category, and vegetative and soil data were assigned using the 2-minute 24-category USGS data. The horizontal grid structure consists of a 36 km domain conforming to the RPO meteorological grid specifications. A nested 12 km grid was also included. The RPO 36 km meteorological domain consists of a Lambert Conic Conformal projection centered at 90° W longitude, 40° N latitude, with true latitudes of 33 and 45° N. The horizontal extent of the RPO domain was engineered according to the bounds of the Eta 212 grid. Domain development involved the implementation of TERRAIN through a series of sensitivity runs designed to extract the largest domain which remains within the borders of the Eta 212 grid. The 12 km grid was designed to achieve a balance between computational resources while maximizing coverage of Iowa-centric upwind and downwind flows. Both grid structures are described in Table 3.1 and depicted in Figure 3.1.

Table 3.1. Grid data, referencing MM5 terminology specifications refer to dot points.

Grid	Resolution (km)	NX	NY	Nest Location (x,y)	Southwest Coordinate (km offset)
1	36	165	129	1,1	(-2952, -2304)
2	12	193	199	66,30	(-612, -1260)

3.1.2 PREGRID/REGRIDDER

The PREGRID processor prepares archived gridded meteorological data for use within MM5 through conversion to an intermediate data format readable by MM5. REGRIDDER invokes a horizontal interpolation scheme to translate data to the MM5 domain. The 3-hour Eta analysis and surface fields (ds609.2) were used to supply initial and boundary conditions to MM5. As the Eta analysis fields obtained from NCAR are a compressed (tar) file, the data were first uncompressed prior to use within PREGRID. The tar files also include the undesirable 12 hourly cold start files. All cold start files (*.tm12) were deleted prior to running PREGRID.

¹ The first simulation was deemed unsuitable for use in air quality modeling projects and has been deleted.

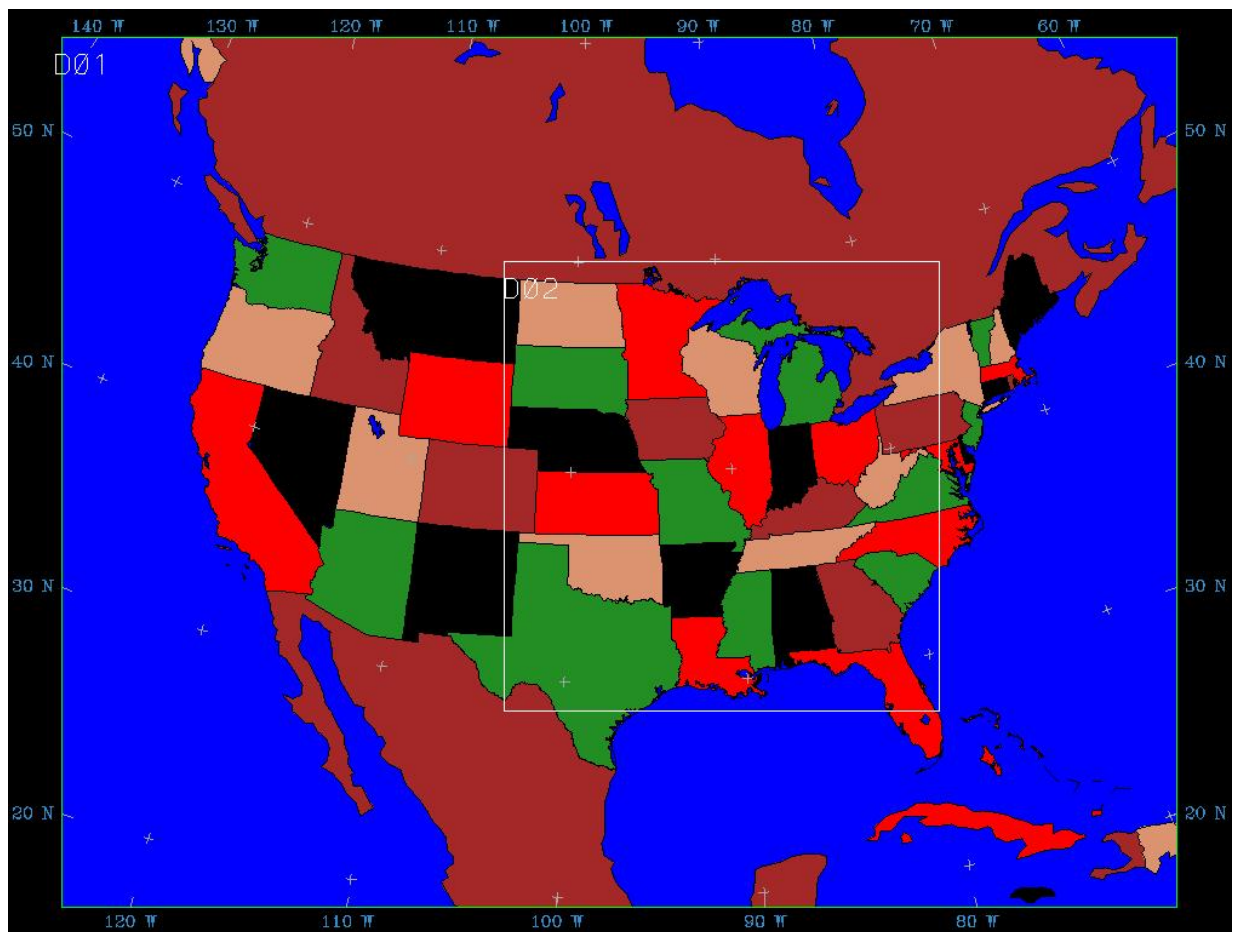


Figure 3.1. Twelve and 36 km domains utilized in the IDNR 2002 MM5v363 annual simulation.

In the first IDNR 2002 MM5 simulation, NCEP data was included in PREGRID to supply time-variant sea-surface temperature (SST) data, as the Eta surface files supply only a time-invariant SST approximation known as skin-temperature. Upon further examination of SST data sources, the temporally variable NCEP SST data was found to lead to unrealistic diurnal temperature profiles over the Great Lakes and near shorelines. Figure 3.2 shows the NCEP-based Great Lakes SSTs for July 4, 2002, at 12 and 18Z. Over this 6-hour span, temperature fluctuations over many areas of the Great Lakes (particularly Lake Erie, and most shorelines) reach 20° F. While some variability is expected along shorelines and other shallow areas, the magnitudes observed through use of the NCEP data are unrealistic. Observed SST data from buoy 45007 (located in the southern end of Lake Michigan yet far removed from the shoreline, see Figure 3.3) for the period July 4 – July 9 are provided in Figure 3.4. The maximum temperature variation throughout July 4 at this site was less than 3° F. Figure 3.5 depicts the 5-day SST timeseries produced using the NCEP SST data within REGRIDDER for the 36 km grid cell corresponding to the location of buoy 45007. The NCEP data yields a diurnal temperature range of approximately 7° F in this cell on July 4. The NCEP data also generates unrealistic diurnal profiles with a net upward trend in SST over this five-day period. In contrast, the observed data show less variability and a downward trend in SST. Utilization of the Eta skin-temperature data produces the constant SST boundary conditions shown in Figure 3.6. The corresponding Eta

skin-temperature for the location of buoy 45007 is ~294 K. While this yields warmer surface temperatures than observed throughout the July 4 – July 9 period, no questionable diurnal variability or artificial warming trends are present.

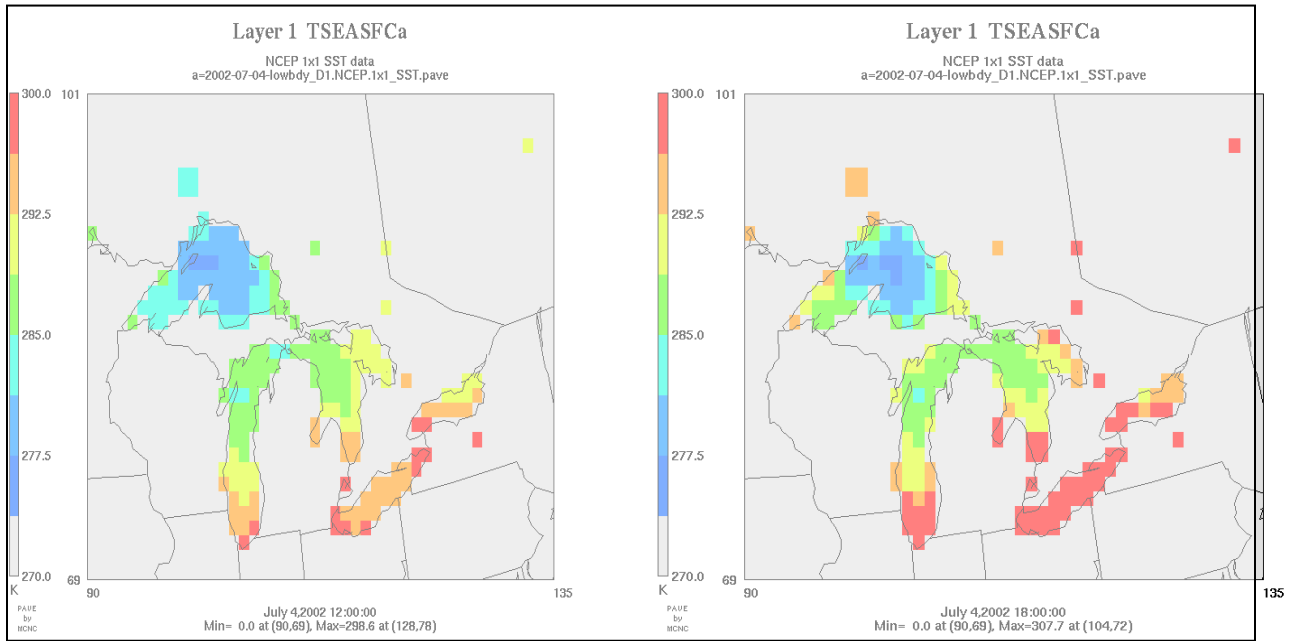


Figure 3.2. Lake temperature variability across a 6 hour span, from 12Z 7/4/2002 to 18Z 7/4/2002, using the NCEP SST data.

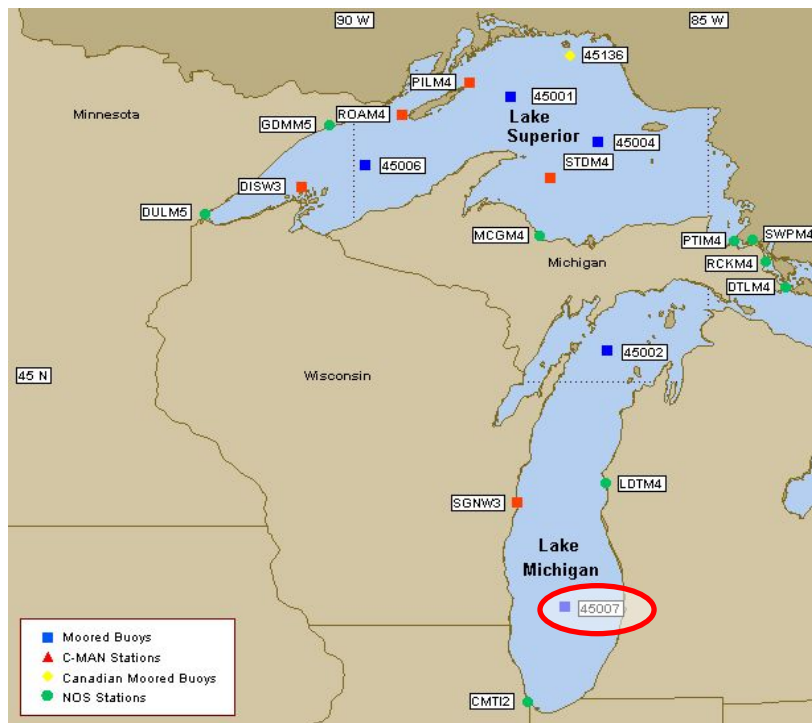


Figure 3.3. Great Lake buoy locations.

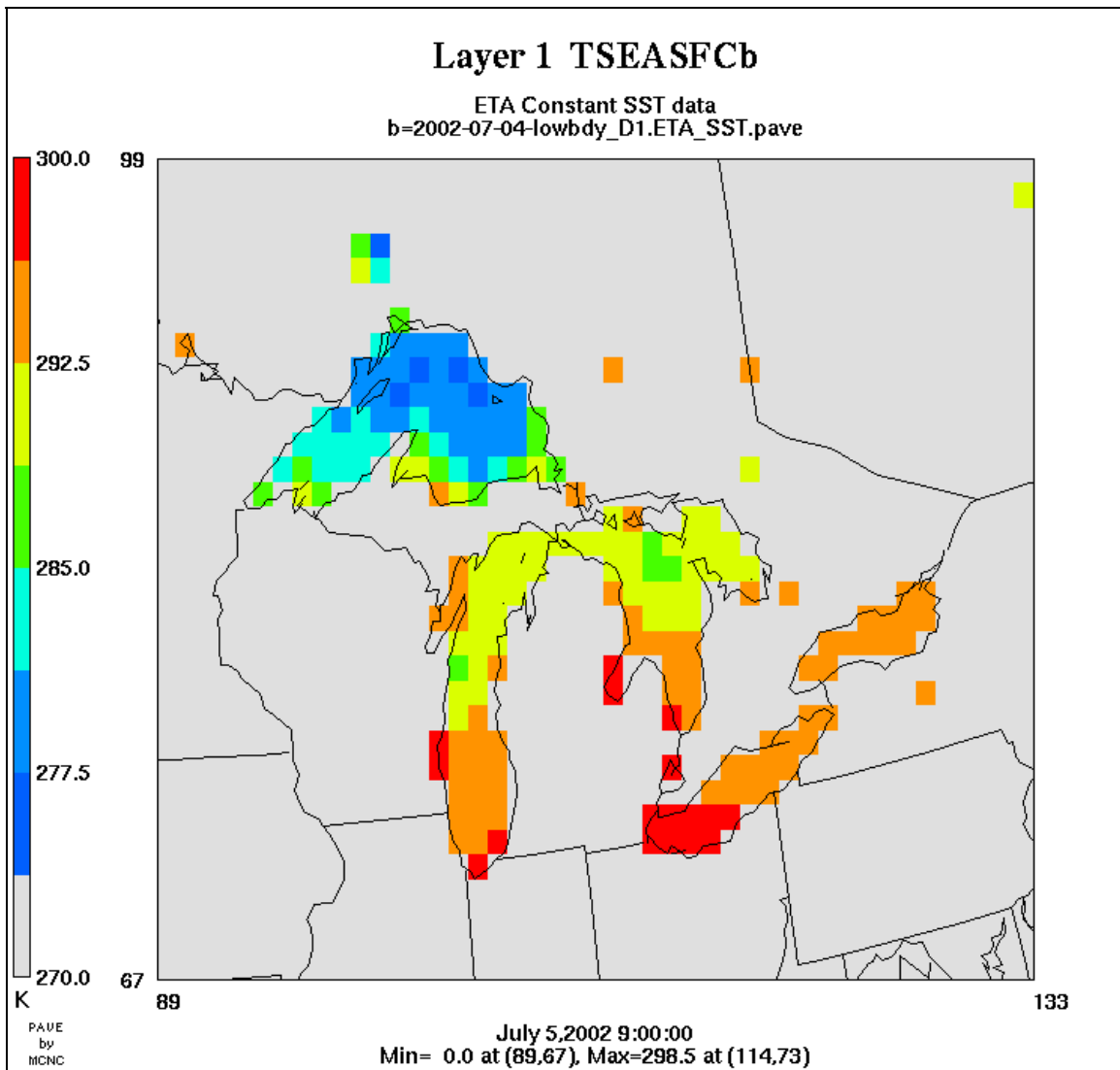


Figure 3.6. Constant SST data derived from Eta skin-temperatures for the period 12Z 7/4/2002 through 12Z 7/9/2002.

3.1.3 LITTLE_R

LITTLE_R was originally designed to improve the REGRIDDER output by using objective analysis techniques to blend observational data into the gridded first-guess fields. Following traditional practices, the NWS upper air (ds353.4) and surface (ds464.0) datasets supply the observations. As the Eta fields already contain these NWS datasets, the implementation of LITTLE_R is viewed as partially redundant. However, LITTLE_R also generates the files used in both the four-dimensional data assimilation (FDDA) and Pleim-Xiu soil moisture nudging schemes and therefore must be invoked. The implementation of LITTLE_R does not negatively affect model performance when the Eta surface and analysis data provide the first-guess fields (Baker, 2002).

3.1.4 INTERPF

The IDNR 2002MM5v363 simulation uses a 34 vertical layer structure defined through the INTERPF preprocessor. The layer interfaces, provided in Table 3.2, were designed through coordination with Dennis McNally to parallel the vertical structure in use by EPA. INTERPF interpolates the pressure level data developed in the previous preprocessors to MM5's native vertical system - terrain following sigma coordinates. Sigma levels are defined according to Eq. 3.1, where p_s equals the surface pressure, and p_t equals the pressure at model top. The model top was defined at 100 mb, or approximately 14,662 meters above ground level. Approximate sigma heights are calculated using Eqs. 3.1 – 3.3, with the user-defined variables assigned the following values: $p_s = 1000$ mb; $p_t = 100$ mb; $T_s = 275$ K; $A = 50$ K. R and g represent the gas and gravitational constants of 287 J/(kg K) and 9.8 m/s², respectively.

$$\sigma = \frac{p - p_t}{p_s - p_t} \quad (3.1)$$

$$p = \sigma \cdot (p_s - p_t) + p_t \quad (3.2)$$

$$z = - \left[\frac{R \cdot A}{2g} \cdot \ln \left(\frac{p}{p_s} \right)^2 + \frac{R \cdot T_s}{g} \ln \left(\frac{p}{p_s} \right) \right] \quad (3.3)$$

Table 3.2. Details of the 34-layer vertical structure.

Level	Sigma	Height (m)	p (mb)	Depth (m)
34	0.000	14662	100	1841
33	0.050	12822	145	1466
32	0.100	11356	190	1228
31	0.150	10127	235	1062
30	0.200	9066	280	939
29	0.250	8127	325	843
28	0.300	7284	370	767
27	0.350	6517	415	704
26	0.400	5812	460	652
25	0.450	5160	505	607
24	0.500	4553	550	569
23	0.550	3984	595	536
22	0.600	3448	640	506
21	0.650	2942	685	480
20	0.700	2462	730	367
19	0.740	2095	766	266
18	0.770	1828	793	259
17	0.800	1569	820	169
16	0.820	1400	838	166
15	0.840	1235	856	163
14	0.860	1071	874	160
13	0.880	911	892	158
12	0.900	753	910	78
11	0.910	675	919	77
10	0.920	598	928	77
9	0.930	521	937	76
8	0.940	445	946	76
7	0.950	369	955	75
6	0.960	294	964	74
5	0.970	220	973	74
4	0.980	146	982	37
3	0.985	109	987	37
2	0.990	73	991	36
1	0.995	36	996	36
0	1.000	0	1000	0

3.2 MM5

An overview of the physics parameterization configuration used in the IDNR 2002MM5v363 simulation is provided in Table 3.3. As previously discussed, the configuration emerges from the cumulative efforts of several sensitivity studies, in combination with guidance from the Ad-Hoc Meteorological Modeling community. In comparison with the original IDNR 2002 simulation, the cessation of continuous soil field techniques within the PX LSM is one of the most notable modifications.¹ With the PX LSM no longer restricted to sequential operation, the annual simulation was generated from 95 independent simulations initialized at 12Z and integrated through five days (versus 5-day blocks arranged in quarterly sequential simulations in the original run). This temporal structure allows maximum air quality modeling flexibility as photochemical simulations can be initialized using midnight local time or midnight GMT without the need to split any given 24-hour period across multiple MM5 simulation blocks. While this methodology does increase the number of runs required to complete an annual simulation (versus initialization at 00Z with a 5.5 day run time), the increased computational requirements are not prohibitive. An example of the temporal structure is provided in Appendix A. To allow for approximately a two week photochemical model spin-up period, the simulation started at 12/16/2001 12Z. The completion date occurred at 12Z on 1/1/2003. A 90 second timestep was used with output written every hour. The output files were split every 24 hours to simplify the post-processing (and photochemical pre-processing) stages.

Table 3.3 Description of the options selected within the IDNR 2002 annual MM5v363 run.

Option	Configuration	Details
Microphysics	Mixed-Phase (Reisner I)	
Cumulus Scheme	Kain-Fritsch 2	
PBL	Asymmetric Convective Model *	Required by Pleim-Xiu LSM
Radiation	RRTM	Calculated every 15 minutes
Land Surface Model	Pleim-Xiu	No continuous soil fields
Shallow Convection	Not enabled	
SST Data source	Eta Skin-Temperature	
Snow Cover Effects	Considered	IFSNOV=1
Timestep	90 seconds	(PX uses an internal 40s timestep)

*The Asymmetric Convective Model (ACM) is also referred to as the Pleim-Chang PBL. The ACM parameterization is a derivative of the Blackadar scheme (Pleim and Chang, 1992).

¹ While discussion of the complete list of configuration variability between the original and 2020MM5v363 simulations is beyond the scope of this document, additional key updates include: the abandonment of NCEP SST data in favor of Eta-Skin temperatures; the addition of the 12 km domain; use of a more recent modeling system release; and a new temporal structure.

Additional configuration details include the following: Sea surface temperatures remained constant during the simulation as Eta skin temperatures were used as surrogate sea surface temperatures. Snow cover effects were considered. Analysis nudging of the temperature, mixing ratio, and wind fields was applied above the PBL. At the surface only the wind field was nudged. The default nudging strengths of 2.5×10^{-4} and 1.0×10^{-4} were used for the temperature and wind fields at 36 and 12 km, respectively. A nudging coefficient of 1.5×10^{-5} was established for the mixing ratios at both 36 and 12 km. The rotational wind field was not nudged, nor were observational nudging techniques applied. Optimal observational nudging methods require a station density not available across a continental scale annual simulation.

Referencing Baker et al. (2004) the following details are provided:

Vertical moisture and temperature advection are set to use linear interpolation. Other options incorporated include: moist vertical diffusion in clouds, temperature advection using potential temperature, diffusion using perturbation temperature, and an upper radiative boundary condition. The Pleim-Xiu land surface module requires the addition of three variables in the MM5 deck: ISMRD, NUDGE, and IFGROW. ISMRD was set to use soil moisture fields from the ETA analyses. NUDGE was assigned to adjust the soil moisture data to the analyses fields. Finally, IFGROW was set to option 2, which takes vegetative growth into account based on vegetative fraction data from the TERRAIN file.

The configuration of the 12 km grid pictured in Figure 3.1 closely resembles the 36 km grid methodology. The explicit exceptions include a decrease in the wind and temperature nudging strengths. While the terminology is questionable, the nesting technique employed is commonly referred to as “a two-way nested run without feedback”. In this method, the 12 km model solution is not feed back to the master domain, but the grids are run simultaneously to allow the fine grid to receive boundary condition updates at every timestep.

3.3 COMPUTATIONAL SUMMARY

Seven dual CPU Linux workstations were acquired to complete the annual simulation. Six machines were equipped with dual 3.06 GHz Intel Pentium Xeon processors, with the final machine a dual 2.0 GHz processor. Each machine¹ was equipped with 2 Gb of RAM, and Ultra 320 SCSI local hard drives for model I/O. Upon completion of each run, output data was transferred via NFS to a SCSI-IDE RAID array. In summation, 41 wall-clock days were required to complete the annual simulation. This represents each machine computing two independent simulations simultaneously (essentially each CPU was tasked with one simulation at any given time). Open MP was not an available option due to the implementation of PX. Approximately 100 wall-clock hours was required for a 3.06 GHz machine to complete two simulations running simultaneously. Storage requirements reached 1.1 terabytes, with the 36 km simulation occupying 400 Gb and the 12 km data using 700 Gb.

¹ The 2.0 GHz machine had only 1 Gb of onboard RAM.

4. MODEL PERFORMANCE EVALUATION

4.1 BACKGROUND

No rigid guidelines exist for systematically and objectively evaluating the quality of meteorological simulations. However, sound comprehensive philosophies exist. A seven point approach outlined by Tesche (1994) provides the framework for a thorough model performance evaluation. The framework can be classified into two components: an operational evaluation and a scientific evaluation (Emery and Tai, 2001). The scientific evaluation requires rigorous examinations of model formulation and algorithm development, methods beyond the scope of most modeling projects. Historical development and applications of MM5 within the scientific community (including air quality and prognostic projects published through peer-reviewed journal articles) must then serve to support the scientific evaluation. Thus the performance evaluation of the IDNR 2002MM5v363 annual simulation will focus upon operational criteria.

4.2 METHODS

Climatic variability, complex mesoscale meteorological phenomena, and scientific unknowns contribute to meteorological modeling difficulties and force modelers to take a subjective approach to model performance. Objective statistical measures which offer a quantitative model assessment exist, but implementation of the metrics is subjective to a degree. For example, defining the area over which domain averaged metrics are calculated is a subjective decision, buffered only through guidelines. In general, metrics averaged over large meteorological modeling domain are avoided, as error cancellation dilutes relevance. Conversely, splitting the modeling domain into small subdomains renders sample sizes unrepresentative. The logical approach falls well within the bounds of the extremes, leaving optimum subdomain definition open to interpretation. As one means of addressing the issue, a subjective grid decomposition technique was applied, resulting in the twelve rectangular¹ subdomains pictured in Figure 4.1.

Model performance measures must also minimally include a review of upper air features in tandem with surface statistics. Upper air features are key variables in terms of air quality modeling given the importance of fields such as three dimension wind flows and PBL depths. Evaluation of the upper atmosphere also introduces a level of complexity exceeding the difficulty associated with assessing surface features. The sheer volume of upper air model data, in combination with a relatively sparse observing network gathering only twice daily soundings, creates problems in terms of scale. A limited set of data analysis tools also restricts the review process. In an attempt to achieve a balance between available resources and the level of detailed review, the upper air evaluation includes review of PBL features and focuses upon observed versus modeled soundings. To improve the efficiency and simplify the review of soundings, a new software tool was developed in-house: RAOBLOT. In the final aspect of the upper air evaluation, an independent review of precipitation prediction, conducted by Kirk Baker, is briefly summarized. While technically a surface feature, the precipitation evaluation indirectly enhances the upper air review given the three dimensional nature of precipitation events.

¹ Processing requirements necessitated that subdomains be simple rectangles defined only through a southwest and northeast grid coordinate.

Metstat Subdomains

12 Domains Total

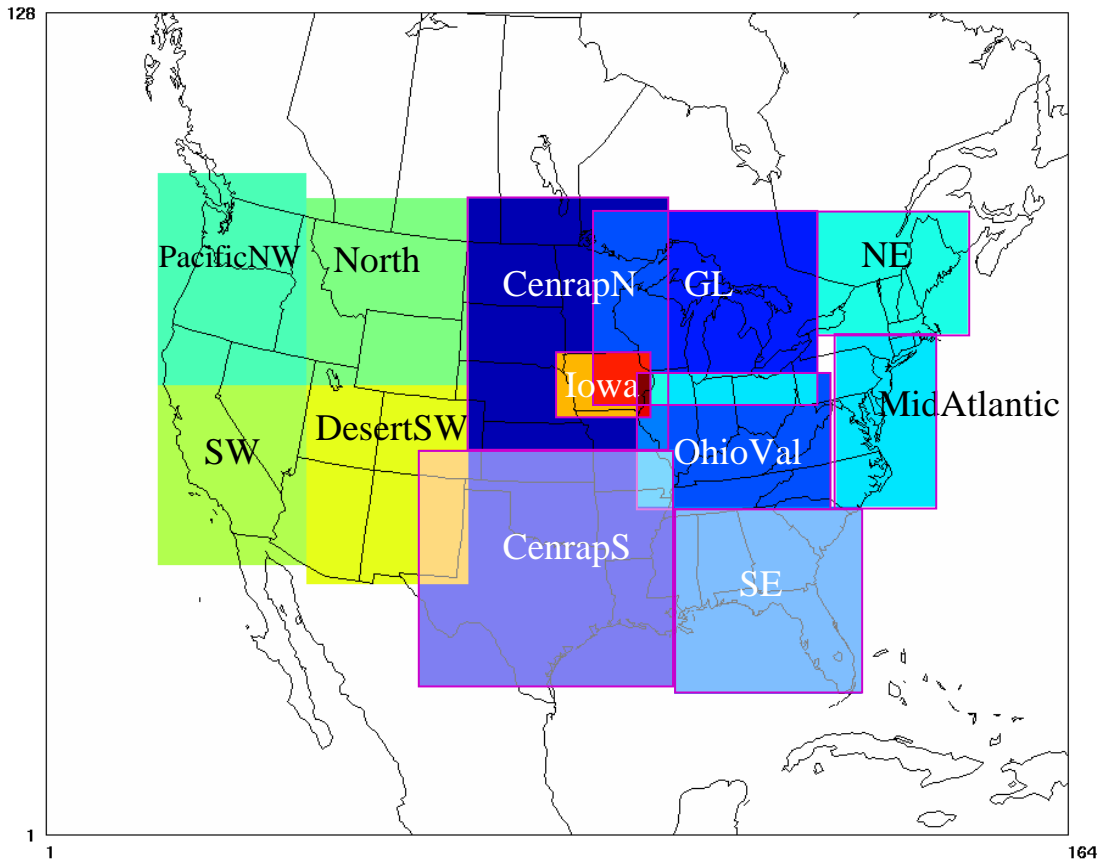


Figure 4.1. Decomposition of the continental scale MM5 domain into simple rectangular subregions designed for targeted model performance evaluation. Areas of overlap are shaded differently and outlines have been added to highlight individual subdomain boundaries.

4.3 STATISTICAL MEASURES

Within the statistical degrees of freedom available to the meteorological modeler, a subset of standard statistical measures has emerged, outlined in Table 4.1. These metrics are calculated based upon data contained within a given subdomain (See Figure 4.1). Metrics are calculated using hourly and daily averages. While no strict criteria establishing acceptable model performance exist, the general guidelines established by Emery and Tai (2001) provide a community adopted frame of reference. A summary of the guidelines is provided in Table 4.2.

Table 4.1. List of statistical measures commonly discussed in meteorological model evaluations. The DH designation represents that both daily and hourly averaged values are calculated for a particular metric. Conversely, D or H indicates that the value is available only on a daily or hourly average, respectively.

Statistical Measure	Wind Speed	Wind Direction	Temperature	Humidity
Obs. vs Predicted Timeline	DH	DH	DH	DH
Bias	DH	DH	DH	DH
Gross Error	D	D	D	D
Total RMSE	DH		DH	DH
Systematic RMSE	DH		DH	DH
Unsystematic RMSE	DH		DH	DH
Index of Agreement	DH		DH	DH

Table 4.2. Guidelines for meteorological model performance. Source: *Meteorological Modeling and Performance Evaluation of the September 13-20, 1999 Ozone Episode* (Emery and Tai, 2001). Data pertain to daily averaged values.

Wind Speed		Wind Direction		Temperature		Humidity	
RMSE	≤ 2 m/s	Gross Error	≤ 30 deg	Gross Error	≤ 2 K	Gross Error	≤ 2 g/kg
Mean Bias	≤ ±0.5 m/s	Mean Bias	≤ ± 10 deg	Mean Bias	≤ ±0.5 K	Mean Bias	≤ ±1 g/kg
IOA	≥ 0.6			IOA	≥ 0.8	IOA	≥ 0.6

An overview of the significance for each metric is provided by Baker et al. (2004):

“*Bias error* (bias) is the degree of correspondence between the mean prediction and the mean observation, with lower numbers indicative of better performance. Values less than 0 indicate under-prediction. The *gross error*, or mean absolute error, is the mean of the absolute value of the residuals from a fitted statistical model. Lower numbers indicate better model performance.

Root Mean Square Error (RMSE) is a good overall measure of model performance. The weighting of (prediction-observation) by its square tends to inflate RMSE, particularly when extreme values are present. With respect to a good model the root mean square error should approach zero. RMSE can be divided into a systematic and unsystematic component by least-squares regression. Since differences described by systematic RMSE can be described by a linear function, they should be relatively easy to dampen by a new parameterization of the model. Unsystematic RMSE can be interpreted as a measure of potential accuracy or noise level (Emery et al., 2001). With respect to a good model the systematic difference should approach zero while the unsystematic difference approaches RMSE.

Index of Agreement is a relative measure of the degree of which predictions are error-free. The denominator accounts for the model's deviation from the mean of the observations as well as to the observations deviation from their mean. It does not provide information regarding systematic and unsystematic errors. The index of agreement approaches one when model performance is best.”

The basis of the statistical analysis is formed through a comparison of the modeled fields with the Techniques Data Laboratory U.S. and Canada surface hourly observations (ds472.0). Hourly and daily averaged bias, error, RMSE (total, systematic, and unsystematic), and index of agreement metrics for wind speed, wind direction, temperature and humidity were generated using the Metstat program and MS Excel post-processing macro developed by Environ. Time series of modeled and observed conditions were also prepared via Metstat. As continental-scale domain averaged statistical measures are susceptible to error cancellation, metrics were calculated over the twelve subdomains illustrated in Fig. 4.1.

The volume of data associated with the annual simulation can quickly overwhelm standard time series displays or similar attempts at numerical data presentation. As a solution Kirk Baker developed an ingenious method of data display. PAVE is used to plot daily metrics, aligned vertically by month, and horizontally by date. This allows for an annual graphical display of daily averaged metrics in a single plot, simplifying the identification of error trends or pervasive biases. Even with this method of simplification, a detailed discussion of all twelve subdomains becomes excessive. The statistical analysis therefore focuses upon those regions encompassing the CENRAP and Midwest RPO states, primarily the regions: CenrapN, CenrapS, GL (Great Lakes), OhioVal (Ohio Valley), and Iowa.

5. SURFACE EVALUATION (36 KM)

The daily averaged metrics described below are provided graphically in the form of a “Bakergram”. The Bakergram, developed by Kirk Baker, allows for the meaningful depiction of an annual set of daily averaged statistical values in a single plot. For example, Figure 5.1 consists of a compilation of four Bakergrams, one each for the wind speed bias, wind speed error, wind direction bias, and wind direction error. Focusing on the wind speed bias Bakergram in Figure 5.1 (top left), 365 daily averaged metrics are provided. Twelve columns are provided, which each column containing a monthly dataset. The individual days are provided in rows, with the first of the month displayed at the top, with days descending from top to bottom. The concept is repeated (for example, see Figure 5.2) with temperature and mixing ratio metrics plotted.

5.1 GREAT LAKES

In previous sensitivity studies, the Pleim-Chang/Pleim-Xiu PBL/LSM configuration was found to improve wind vector performance versus the use of alternative PBL parameterizations. Consistent with this discovery, the wind vector performance in the GL region is encouraging. Wind speed metrics are generally favorable, and no clear trends in error or bias are evident (see Figure 5.1). A notable caveat, daily metrics may hide inconsistencies occurring within the diurnal profile.¹ Turning to the wind direction evaluation, again results are satisfactory, with one exception found, an increase in the summertime gross error.

In the Great Lakes region, the problems of greatest concern lie in the wintertime cold temperature biases, the warm summertime biases, and the summertime positive moisture biases (See Figure 5.2). Examining the temperature biases from a diurnal² perspective, the warm bias is predominantly caused by nighttime temperatures remaining warmer than observed. The cold wintertime temperature bias is often traced to underpredicted high temperatures, evening temperatures falling too rapidly, and nighttime lows often colder than observed. Caution should be exercised when generalizing the wintertime bias trends though, as exceptions are more abundant than with the summertime warm biases. Turning to the mixing ratio (humidity) evaluation (see Figure 5.2), although the gross error metrics are generally within the statistical guidelines, the summertime positive bias is a concerning trend. Only on rare occasions do negative biases occur. The likely culprit is MM5’s tendency to overpredict precipitation.

5.2 NORTHERN AND SOUTHERN CENRAP

In general, the statistical evaluation for the CenrapN subdomain (Figures 5.3 - 5.4) yields results similar to the Great Lakes region. A notable exception being the nearly consistently negatively biased wind speeds. Examining the wind speed bias in greater detail (through diurnal profiles), this fault is predominantly influenced by the underprediction in the daily peak wind speeds. Keeping these errors in perspective, the magnitude of the underprediction typically remains below 1 m/s. Examining the mixing ratio performance, the most serious issue remains the abundance of summertime surface moisture. While arguable trivial, CenrapN does differ from the GL subdomain during May, where several surface moisture underpredictions occur.

¹ Diurnal metrics are examined in Chapter 6.

² Ibid.

Turning to the Southern CENRAP subdomain (Figures 5.5 - 5.6), wind direction performance remains encouraging, similar to the performance for the CenrapN and GL regions. As found in CenrapN, wind speeds are generally negatively biased, but more pronounced in this region. The mixing ratio biases reveal excess moisture, although a drier than observed fall was predicted. Examining temperature performance, late winter/early spring temperatures yielded positively biased trends, in contrast to the pervasive cold winter biases found in the CenrapN and GL regions. Examination of the diurnal profiles revealed the biases were attributable to warm nighttime lows.

5.3 OHIO VALLEY

Once again, the wind speeds are generally too low, however, the associated error is well within the acceptable guidelines. Wind directions errors are also generally small, but an increase in error is found in the summer months. Mixing ratios are consistently too moist, except in the mid-October timeframe. As in the Great Lakes regions, a cold winter bias is found, while summer temperatures remain too warm (predominantly over the nighttime hours). The results are depicted in Figures 5.7 - 5.8.

5.4 IOWA

Within the Iowa subdomain wind vector performance is favorable, with wind speed bias and error measures predominantly meeting the statistical goals. Wind directions exhibit greater errors in the late summer/early fall timeframe versus the CenrapN and GL subdomains, but are not cause for severe alarm (see Figure 5.9). As is common, cold winter and warm summer biases are present (Figure 5.10). In terms of the moisture bias, the Iowa domain exhibits greater springtime negative moisture bias versus CenrapN, otherwise similar performance is shown (this result is not unexpected, given the superposition of the Iowa subdomain over CenrapN).

5.5 EASTERN REGIONS

A detailed discussion of model performance for all areas is beyond the scope of this document. Alternatively, summary remarks are provided. Over the MidAtlantic, no serious abnormalities are found beyond the errors identified previously in Central U.S. subdomains. As is common to MM5, a positive moisture bias exists, affecting both the MidAtlantic and SE regions. Examining the NE region, wind speed, and wind direction errors approach the upper extreme of acceptable performance. Again, the moisture bias is positively biased, with errors maximized over the summer months. Given moisture carrying capacity is a non-linear function of temperature, the relatively small mixing ratio gross errors occurring in the wintertime of regions with colder climates should not be interpreted as superior model performance. The daily averaged statistical results are provided in Appendix B for each of the individual Eastern subregions.

5.6 WESTERN REGIONS

The daily averaged statistical results for the western subdomains are also provided in Appendix B. The complex topography found in the Western United States clearly introduces a degree of modeling difficulty not found in other regions. Performance metrics are discouraging when viewed initially, however, the appropriateness of the statistical measures are questionable as model resolution is not designed to capture the topographically induced near-field flows affecting many of the local observations.

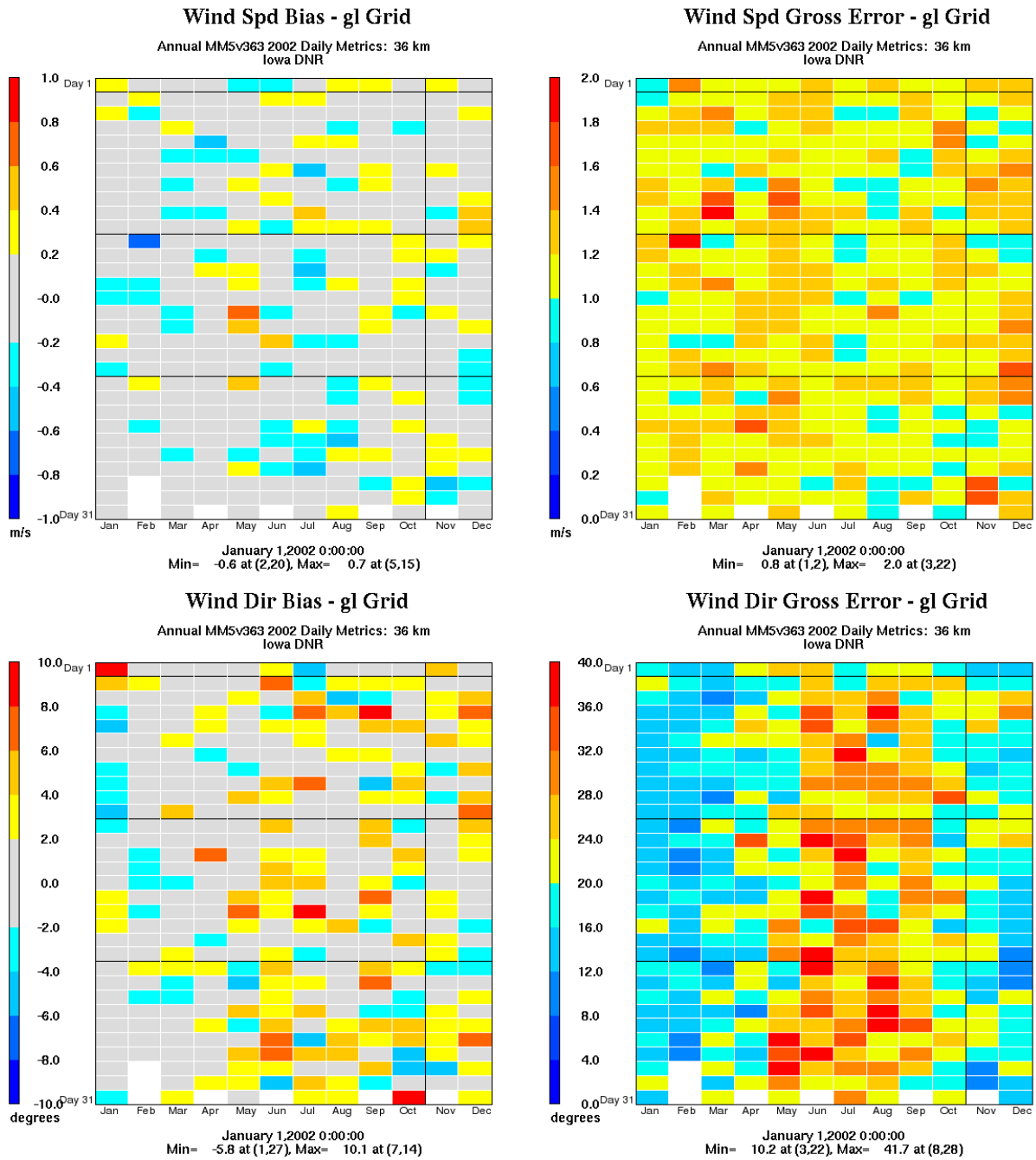


Figure 5.1. Daily averaged wind speed/direction metrics for the Great Lakes (GL) subdomain.

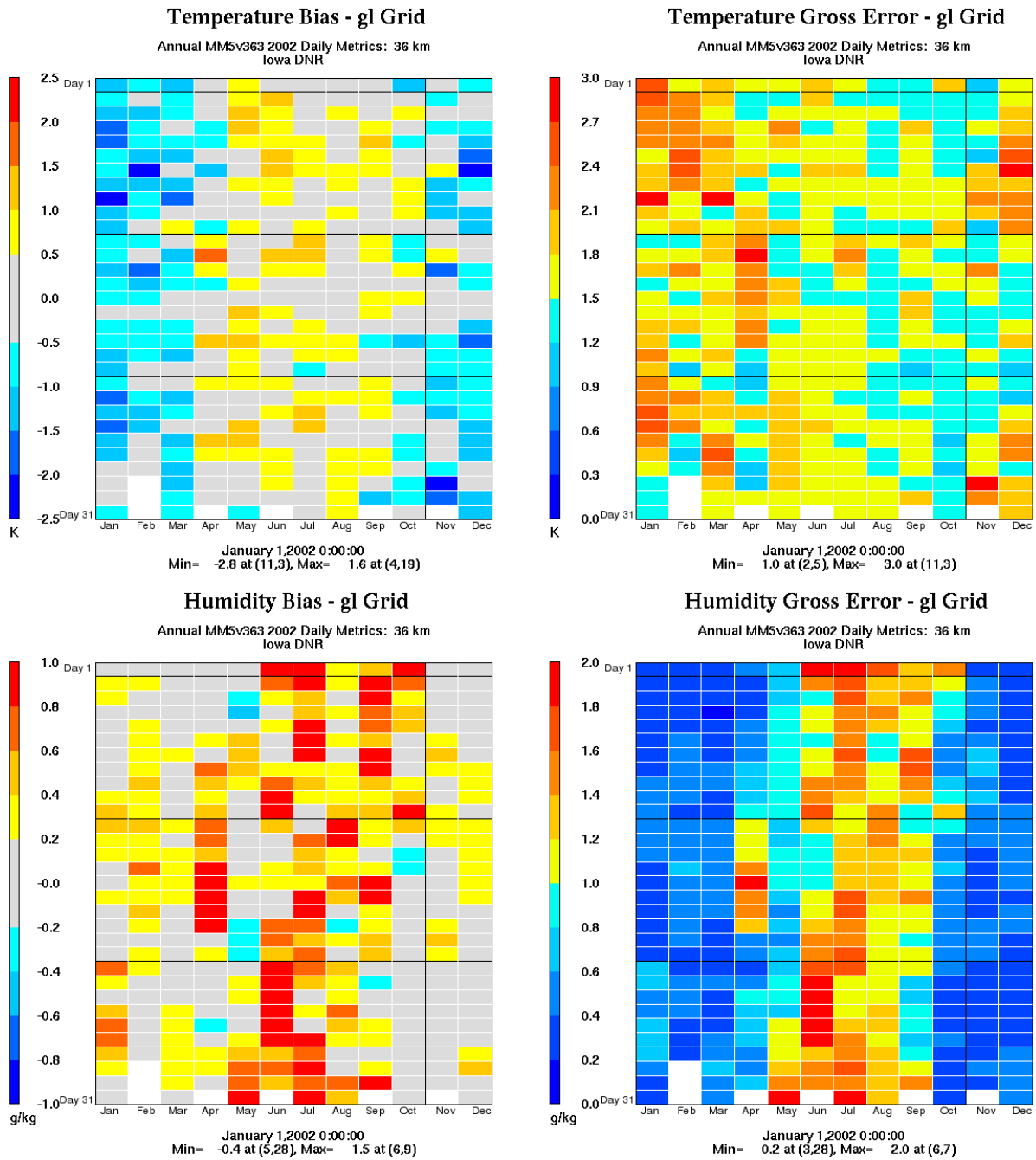


Figure 5.2. Daily averaged temperature and mixing ratio metrics for the Great Lakes (GL) subdomain.

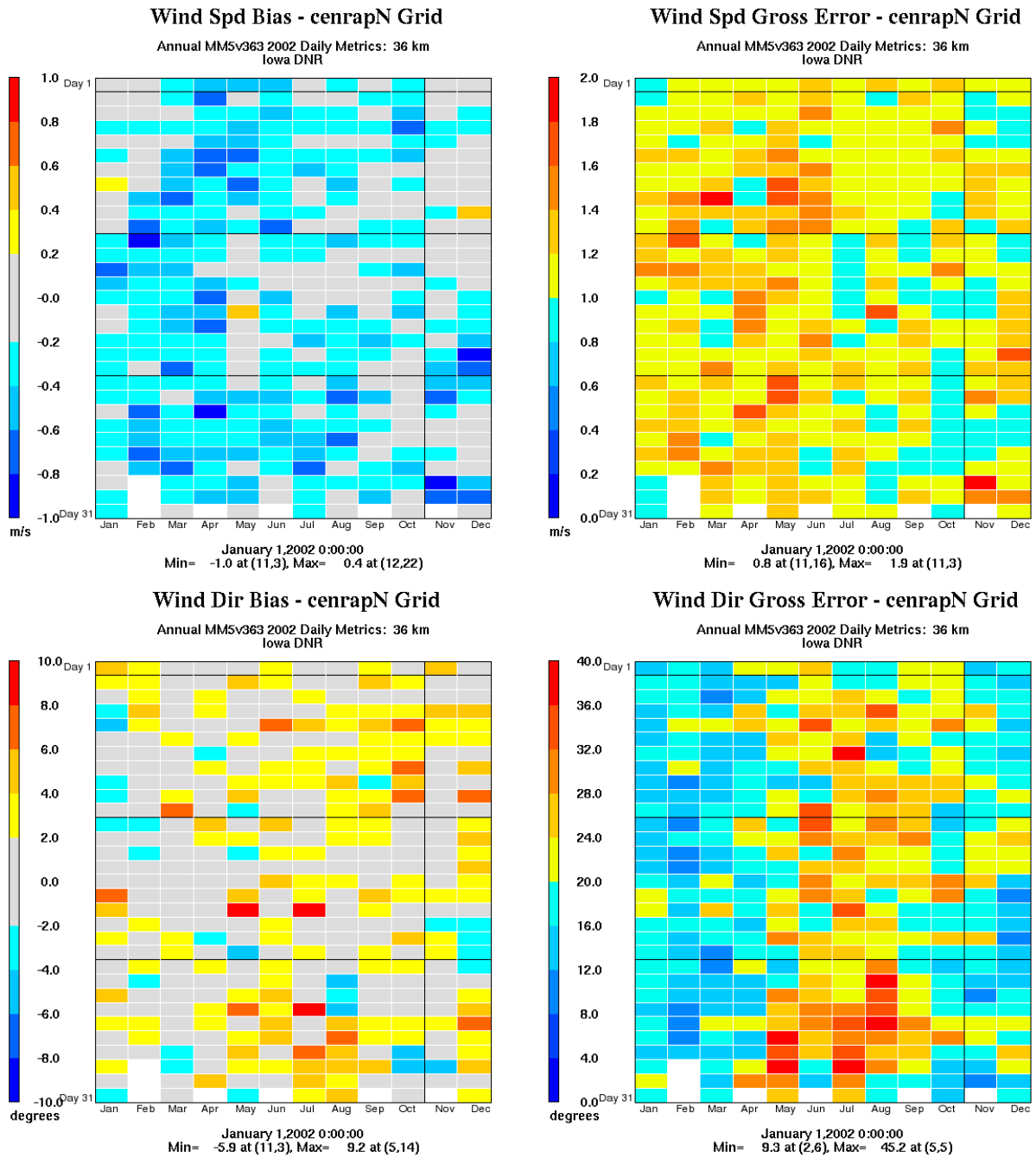


Figure 5.3. Daily averaged wind speed/direction metrics for the CenrapN subdomain.

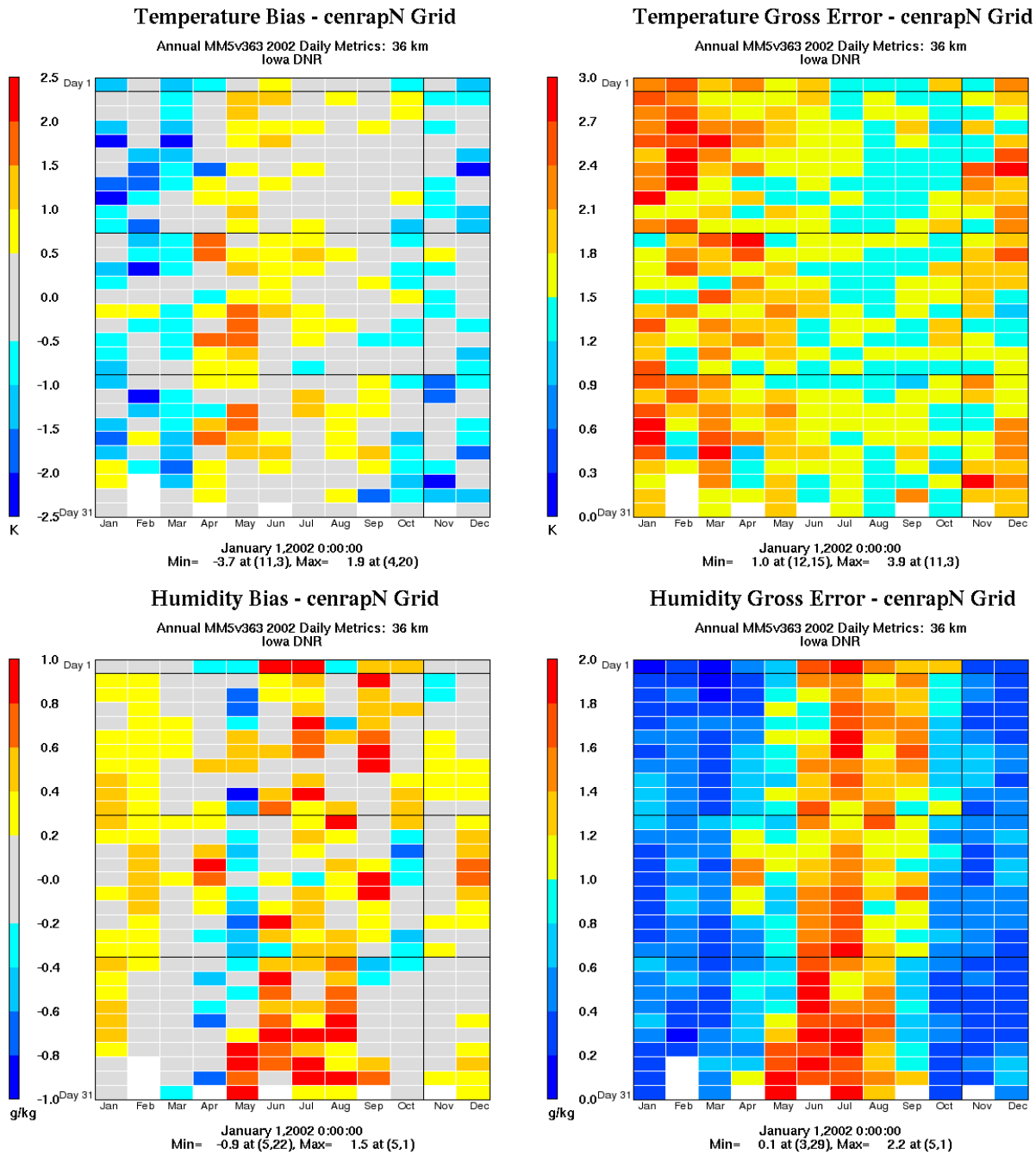


Figure 5.4. Daily averaged temperature and mixing ratio metrics for the CenrapN subdomain.

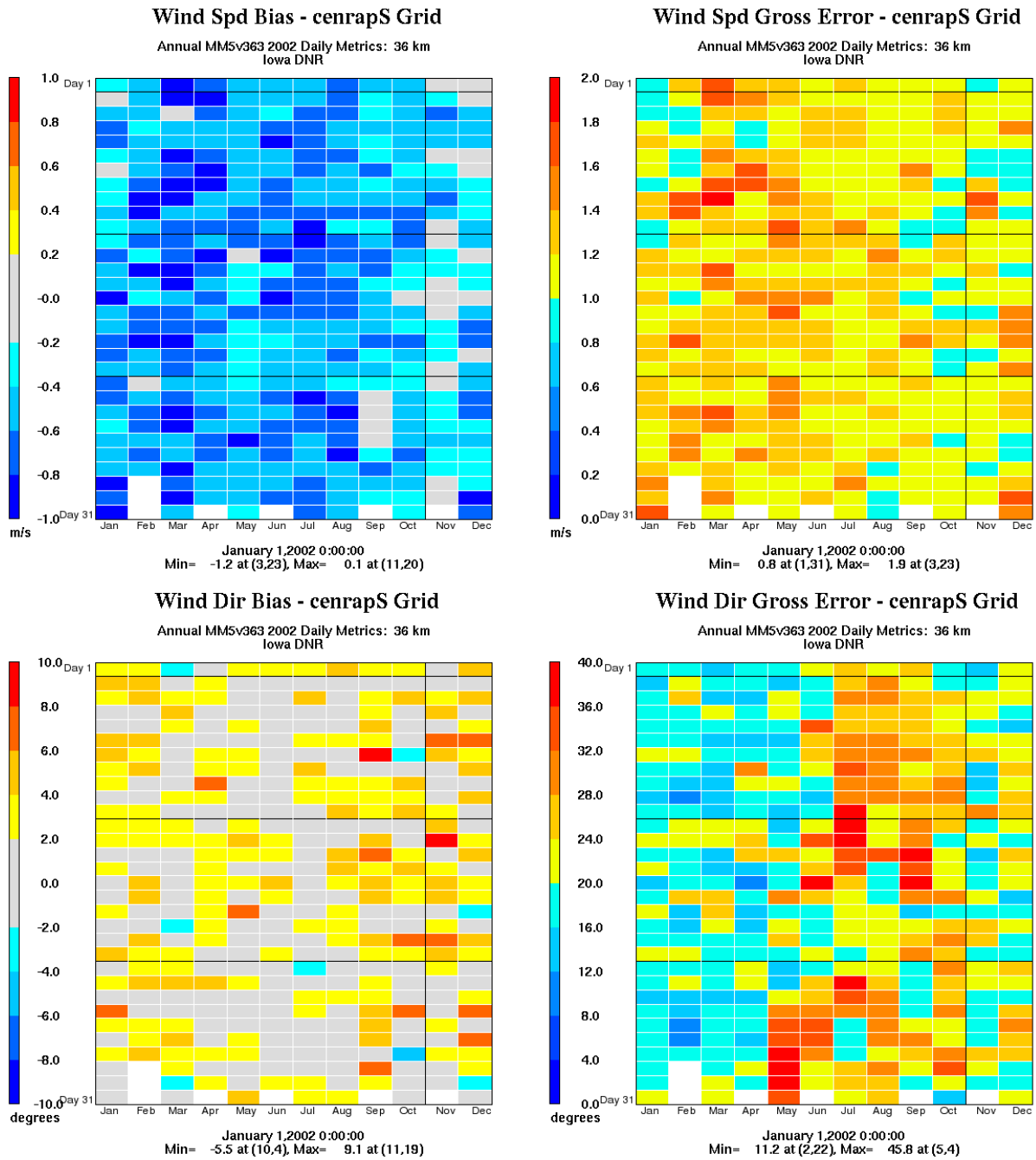


Figure 5.5. Daily averaged wind speed/direction metrics for the CenrapS subdomain

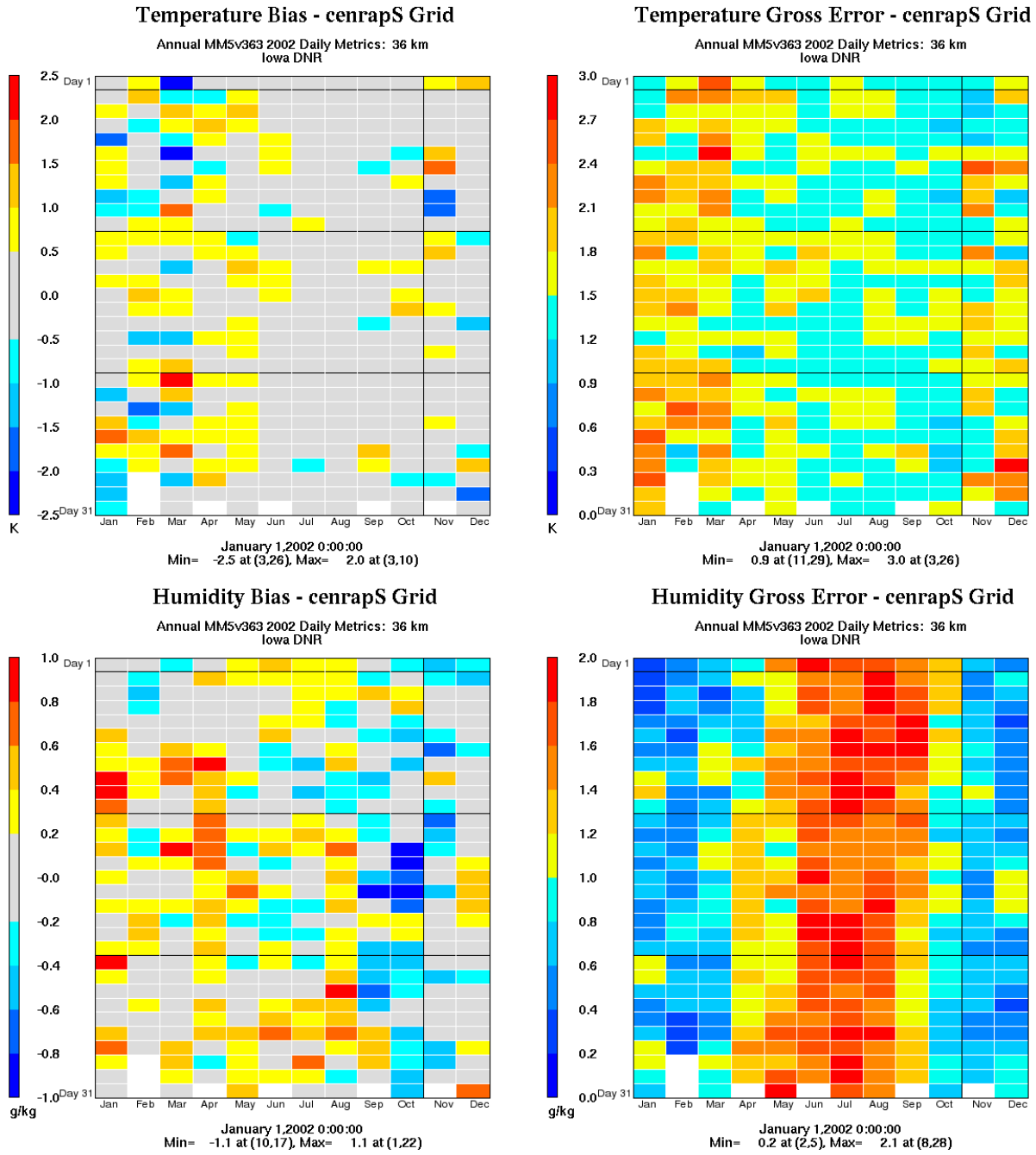


Figure 5.6. Daily averaged temperature and mixing ratio metrics for the CenrapS subdomain.

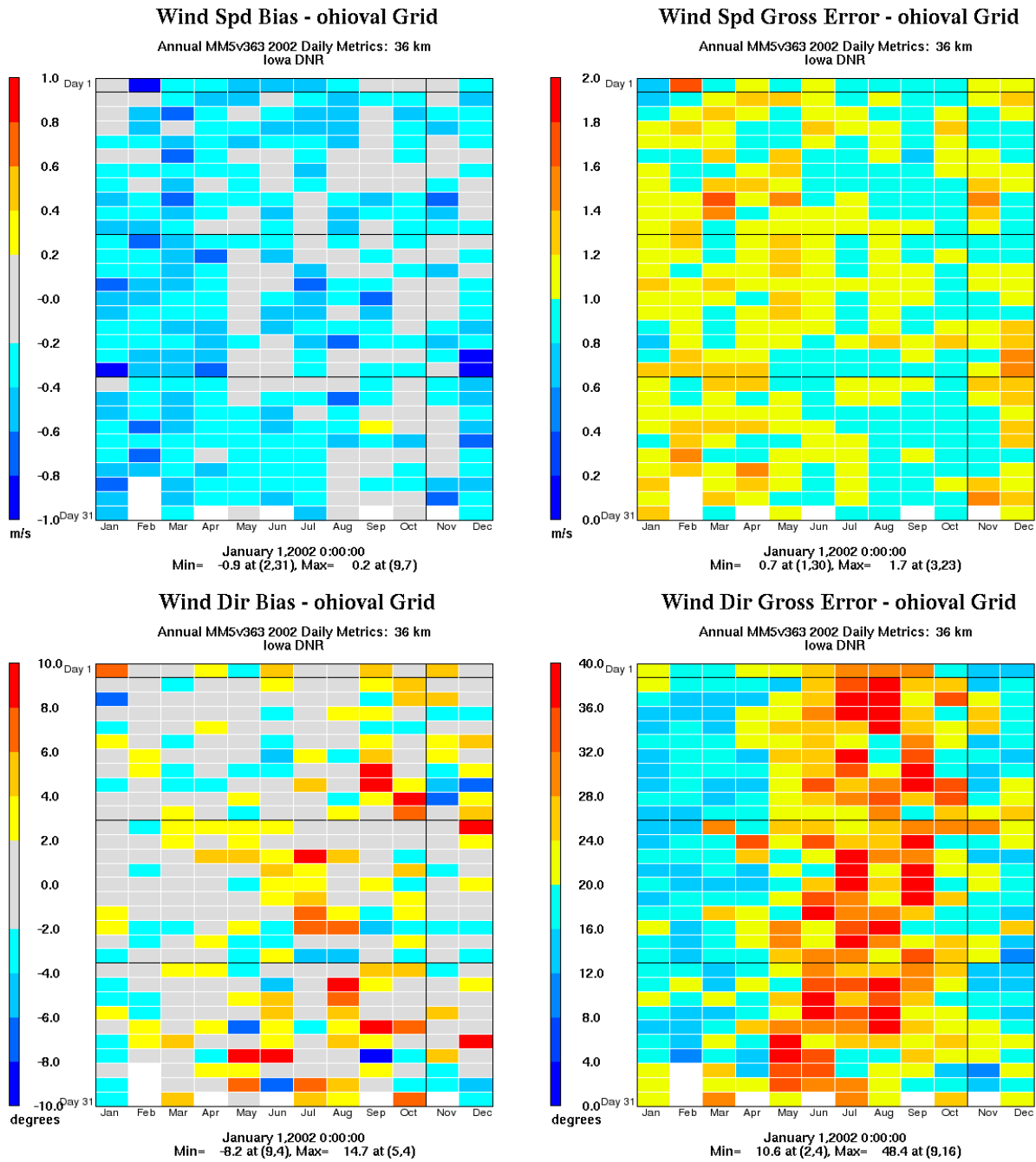


Figure 5.7. Daily averaged wind speed/direction metrics for the OhioVal subdomain.

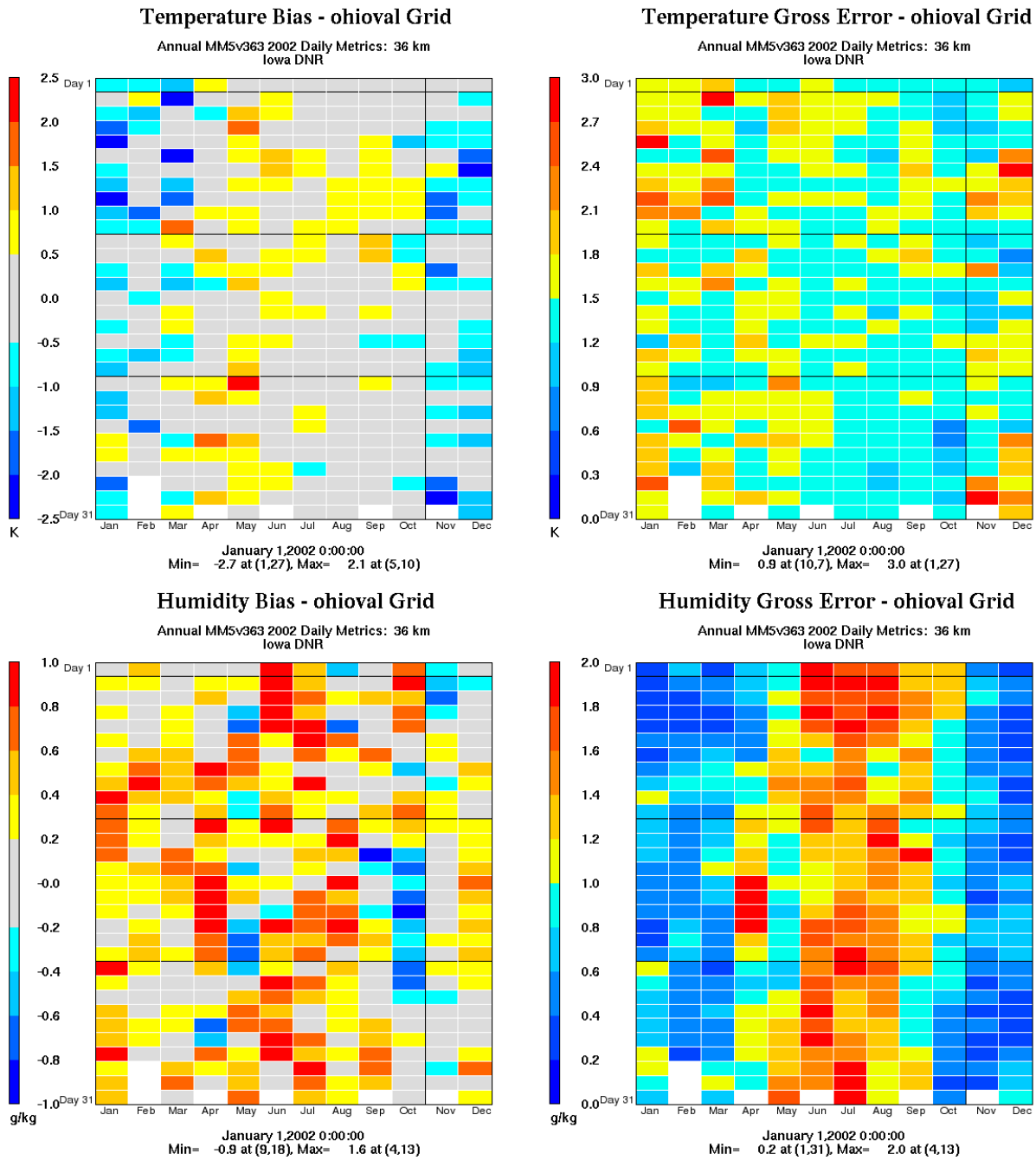


Figure 5.8. Daily averaged temperature and mixing ratio metrics for the OhioVal subdomain.

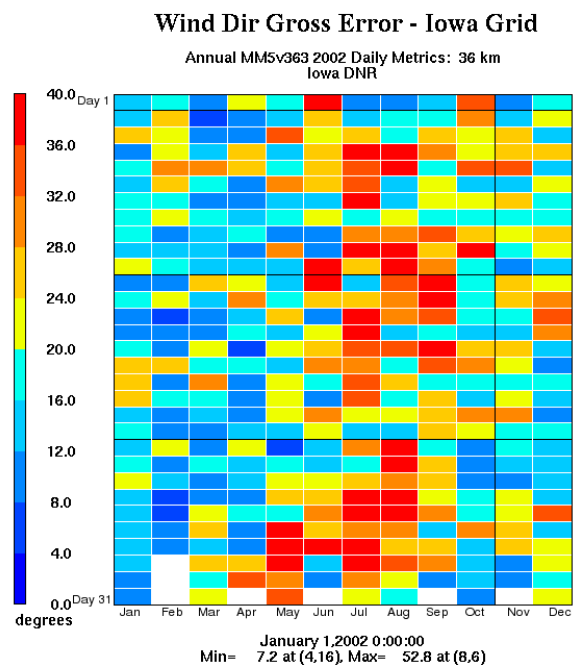
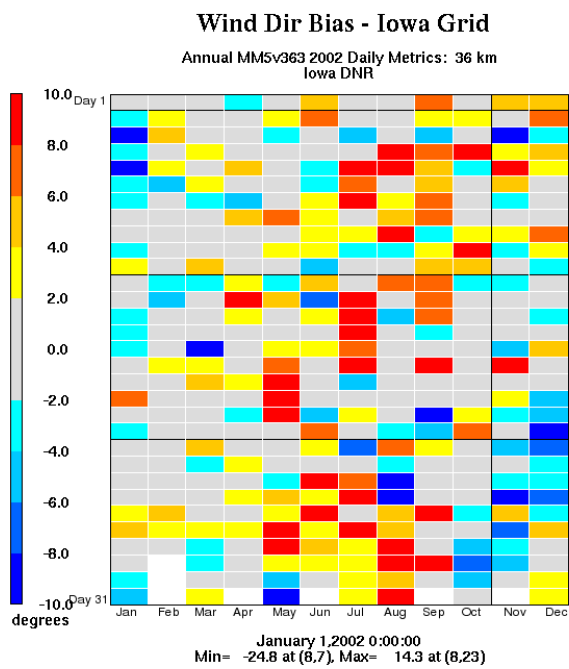
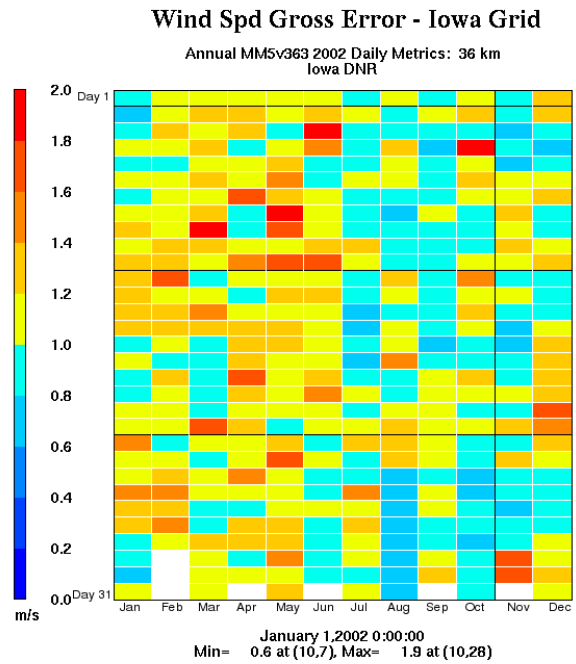
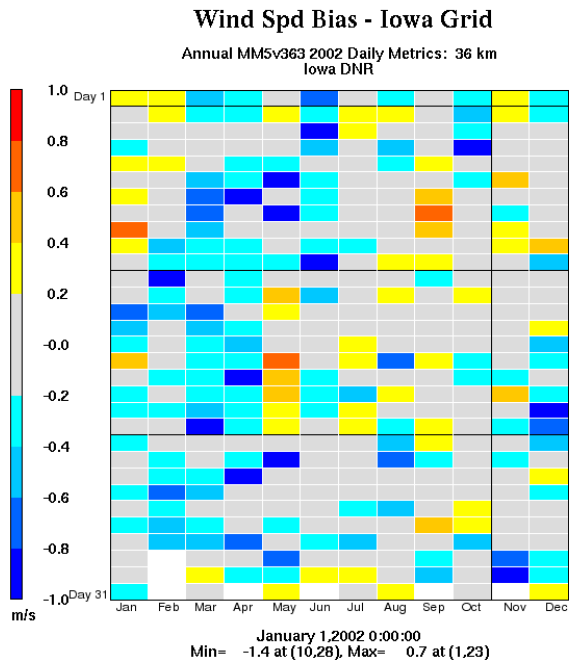


Figure 5.9. Daily averaged wind speed/direction metrics for the Iowa subdomain.

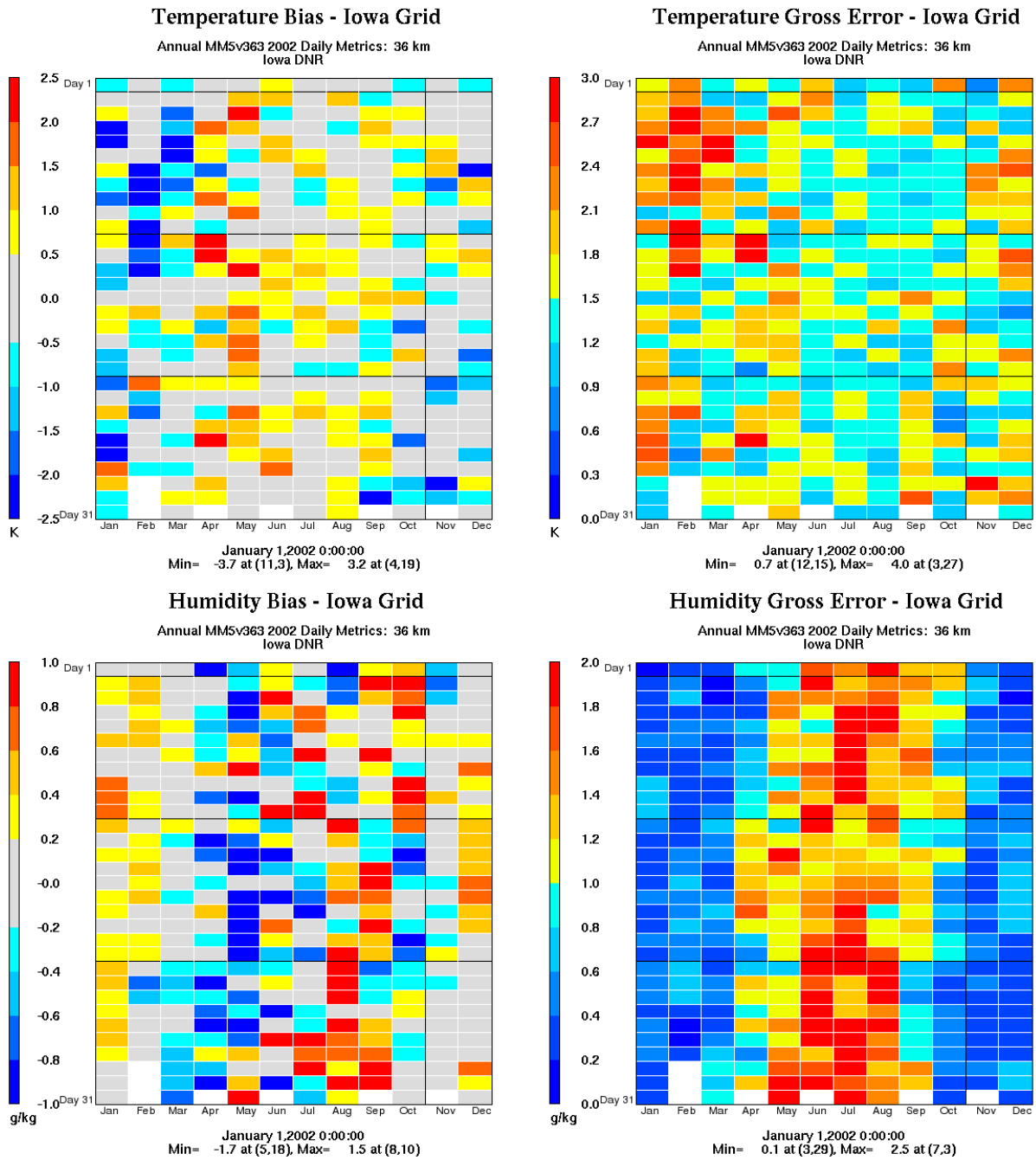


Figure 5.10. Daily averaged temperature and mixing ratio metrics for the Iowa subdomain.

6. TWELVE KILOMETER EVALUATION

6.1 DAILY AVERAGED STATISTICS

Generalizing the impacts of the 12 km domain upon the Great Lakes region, in terms of daily averaged metrics, a decrease in simulation accuracy during the winter months is found, while only negligible changes occur across the remainder of the year. This trend is prevalent for wind speed, wind direction¹ and temperature errors. The wintertime temperature cold bias (found at 36 km resolution) is thus even more pronounced in the 12 km domain. Mixing ratio statistics were generally uninfluenced by domain resolution. These results are depicted in Figures 6.1 – 6.2, where the Bakergram concept is maintained, however, the results are presented in terms of the differences between the 36 and 12 km results. The plots were generated by subtracting the 36 km daily averaged statistical values from the 12 km data. As the comparison only involves gross and root mean square error metrics, negative values indicate an improvement in model performance at 12 km resolution. This methodology is maintained for Figures 6.1 - 6.8.

The CenrapN regions shows only minor variations in the temperature fields, with the greatest change concentrated to the cooler months, with slight performance disbenefits. Wind direction metrics produced a drastically different trend, as nearly all days showed poorer performance. Figures 6.3 – 6.4 provide a graphical depiction of the 12 km domain impacts upon the daily averaged metrics for this subdomain.

Over the Ohio Valley, only minor differences were calculated between the 12 and 36 km daily averaged statistical results, in general. A slight improvement in the mixing ratio fields was computed. As in CenrapN, wind direction gross errors encountered widespread performance degradation during the winter and early spring months. Keeping the increasing errors in perspective, additional error remained below 3.5 degrees. See Figures 6.5 - 6.6.

In terms of daily averaged statistical measures, the Iowa subdomain receives few benefits from increased resolution. Wind speeds generally exhibit slightly greater error in the winter, spring, and fall, while demonstrating little variability during the summer. Consistent with nearby subdomains, wind direction performance suffers. While mixing ratios impacts were negligible, most months exhibited days with increased temperature error, particularly in the winter. Fortunately, gross error degradation remained below 0.5 K. The results are depicted in Figures 6.7 - 6.8.

Due to the spatial extent of the 12 km domain, neither the CenrapS domain, nor any other subdomain, is eligible for comparison.

¹ With additional errors occurring into the early spring months.

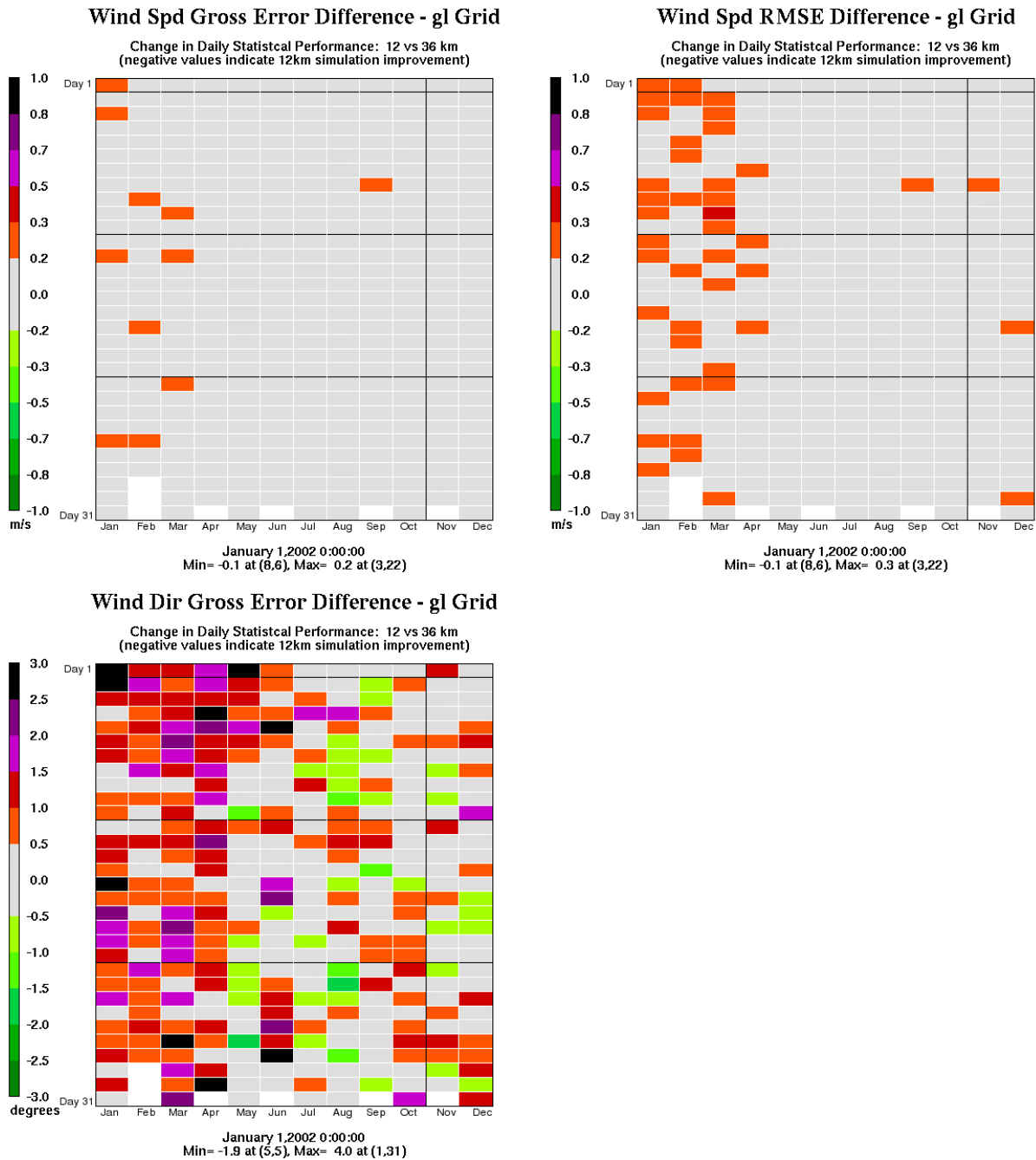


Figure 6.1. Twelve km domain daily averaged statistical performance for selected wind metrics in relation to the 36 km grid for the Great Lakes (GL) subdomain.

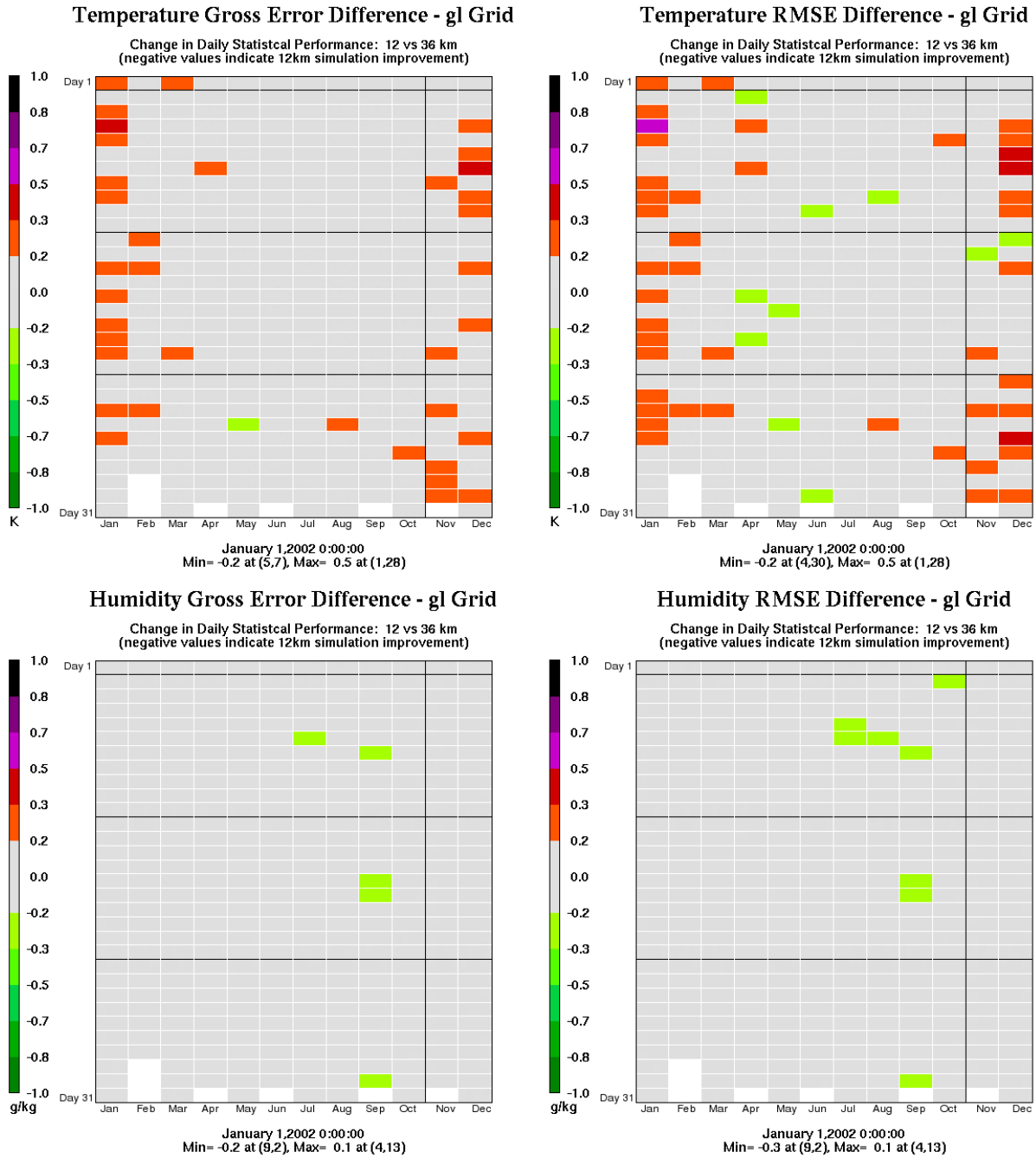


Figure 6.2. Twelve km domain daily averaged statistical performance for selected temperature and mixing ratio metrics in relation to the 36 km grid for the Great Lakes (GL) subdomain.

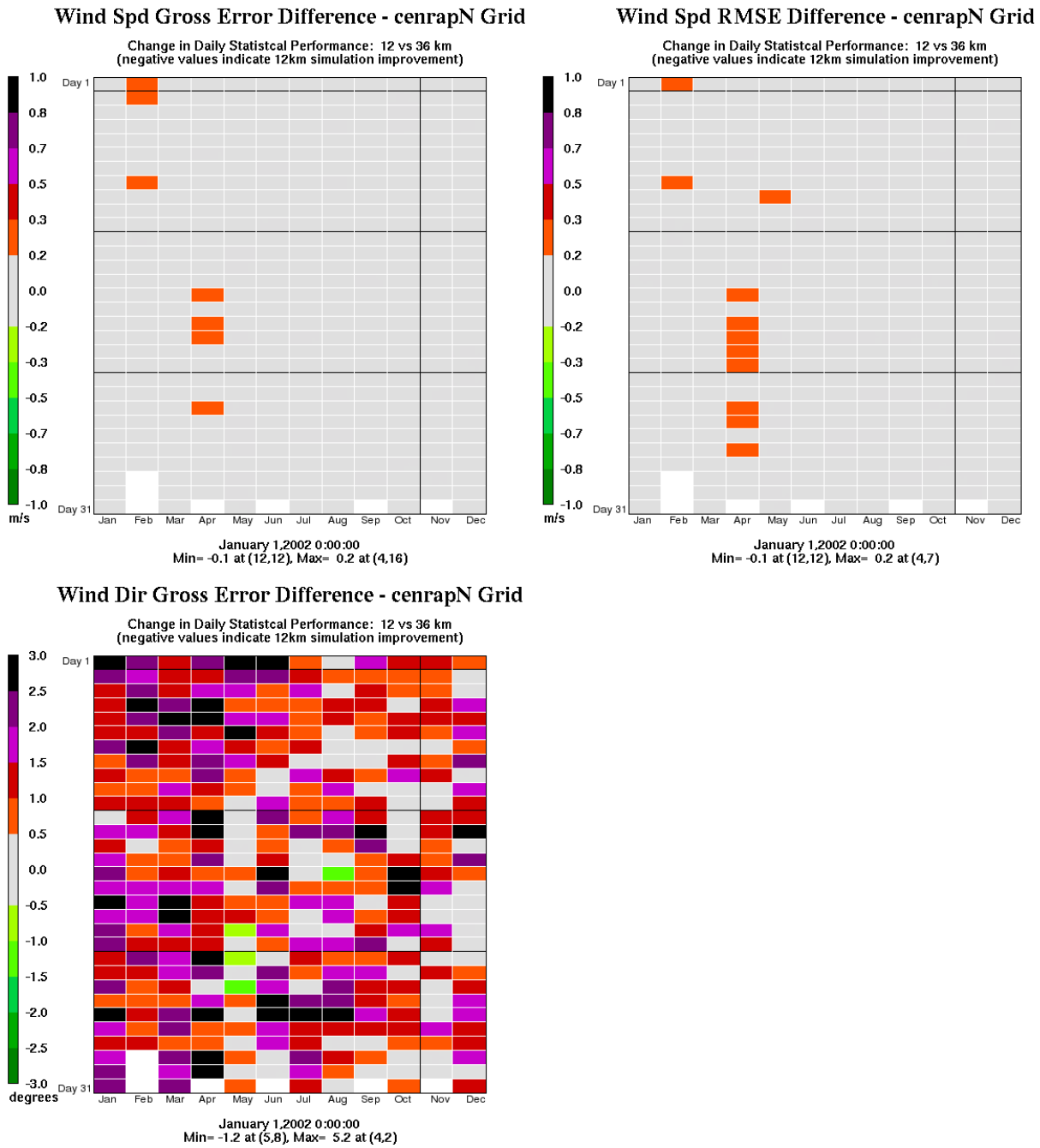
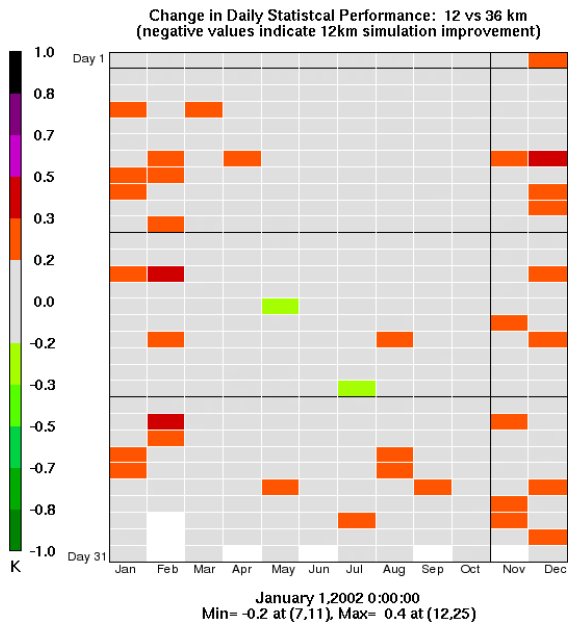
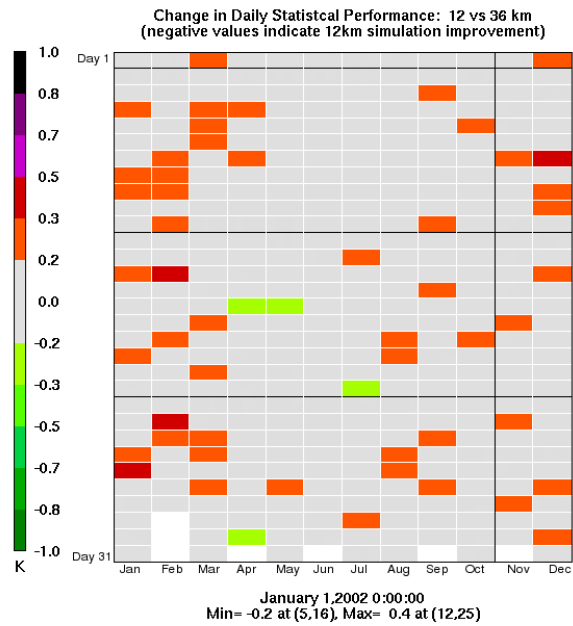


Figure 6.3. Twelve km domain daily averaged statistical performance for selected wind metrics in relation to the 36 km grid for the CenrapN subdomain.

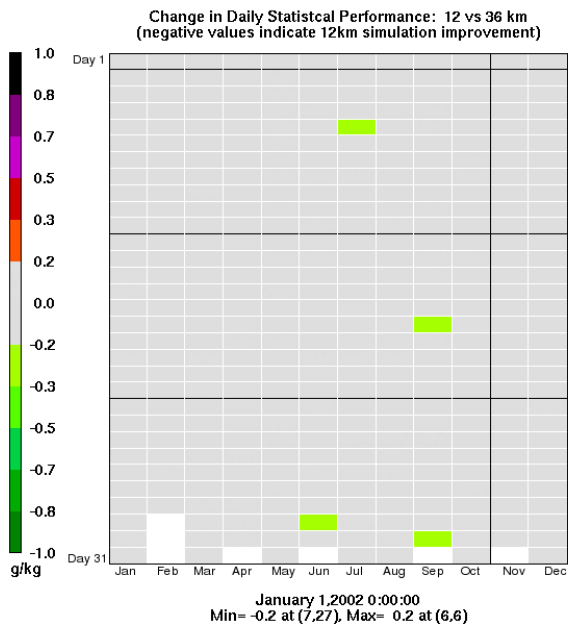
Temperature Gross Error Difference - cenrapN Grid



Temperature RMSE Difference - cenrapN Grid



Humidity Gross Error Difference - cenrapN Grid



Humidity RMSE Difference - cenrapN Grid

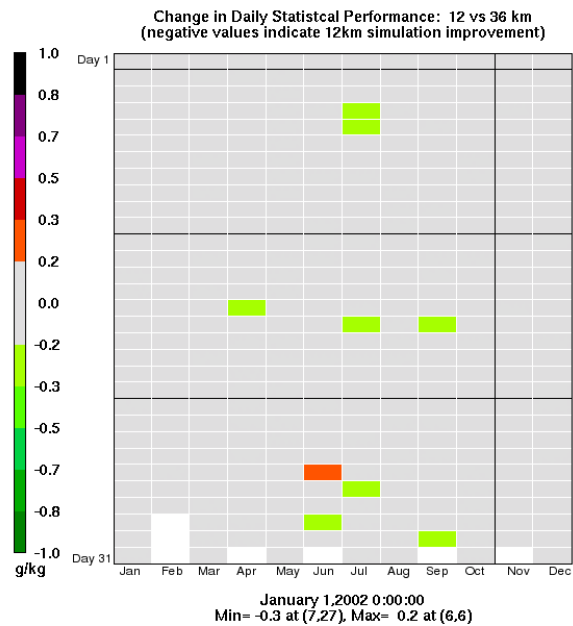


Figure 6.4. Twelve km domain daily averaged statistical performance for selected temperature and mixing ratio metrics in relation to the 36 km grid for the CenrapN subdomain.

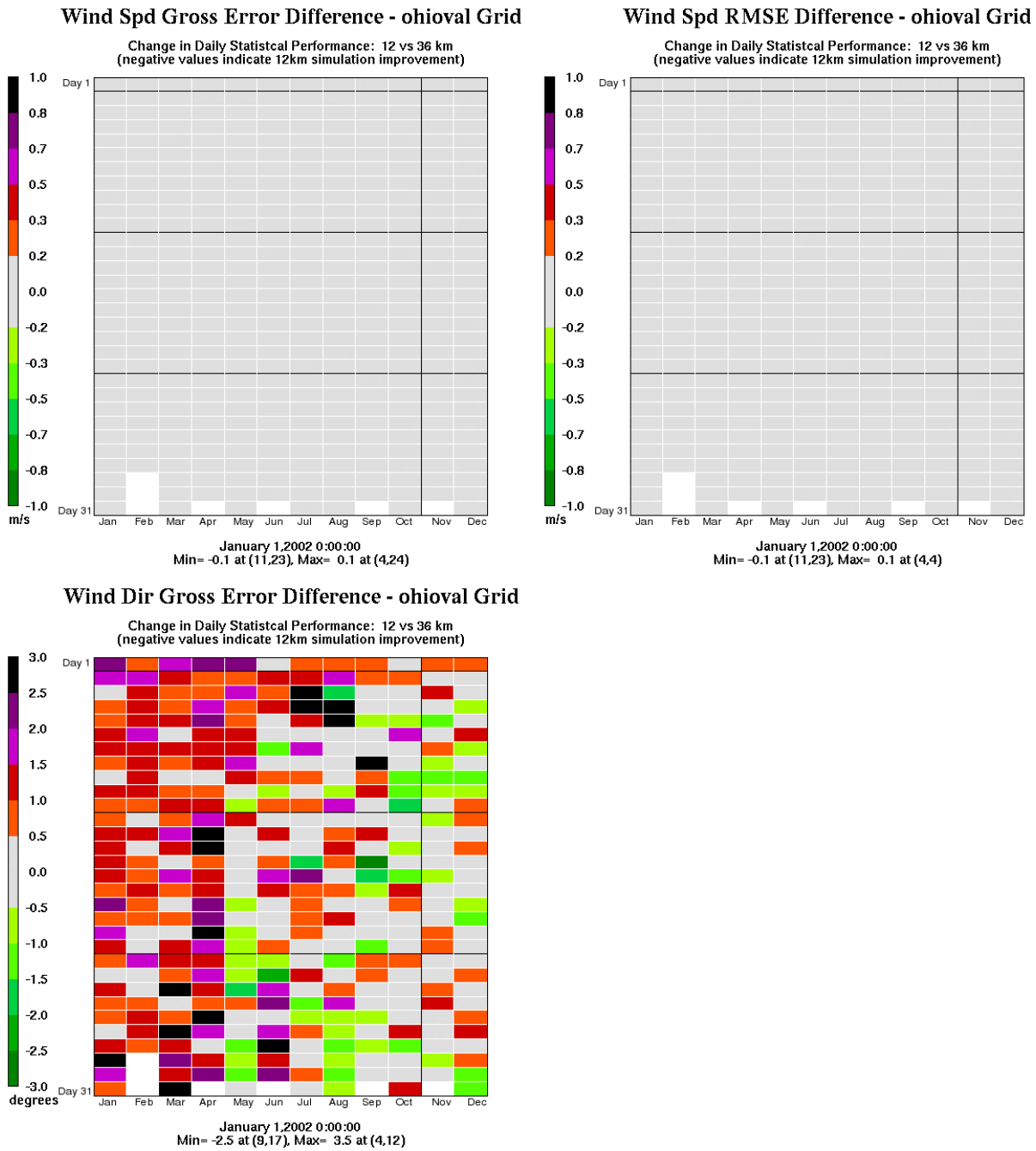
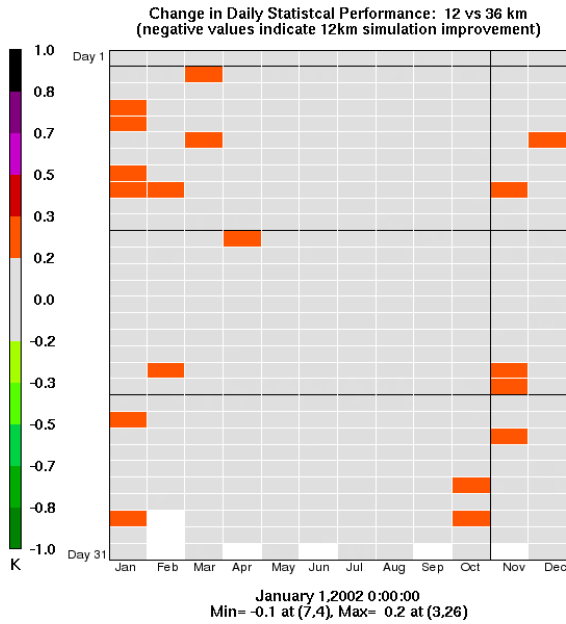
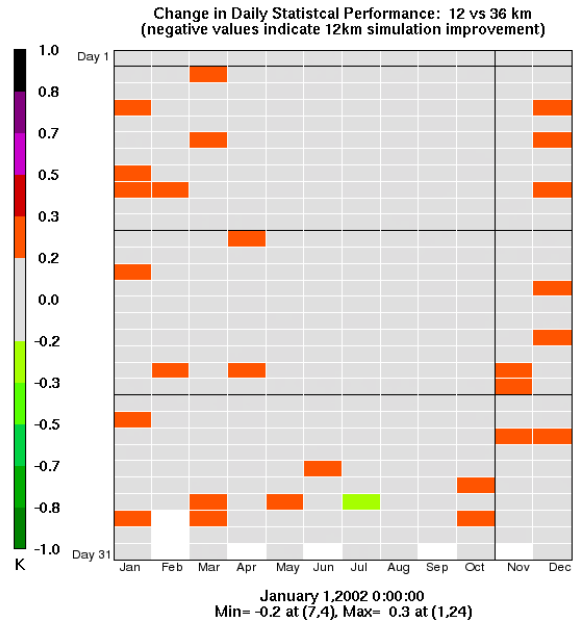


Figure 6.5. Twelve km domain daily averaged statistical performance for selected wind metrics in relation to the 36 km grid for the OhioVal subdomain.

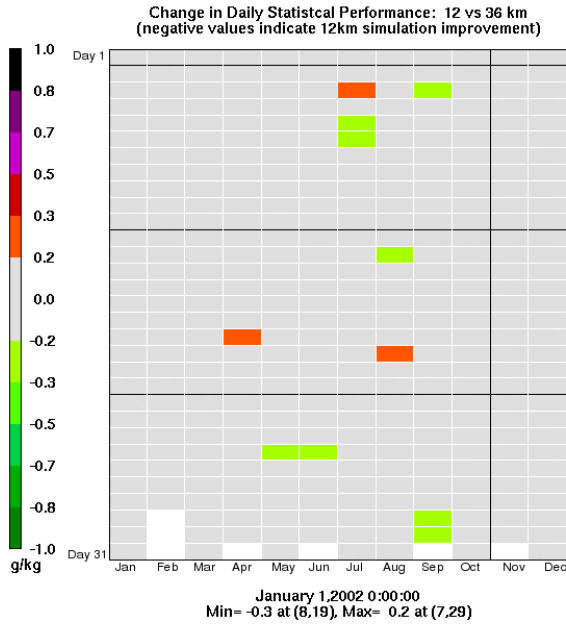
Temperature Gross Error Difference - ohioval Grid



Temperature RMSE Difference - ohioval Grid



Humidity Gross Error Difference - ohioval Grid



Humidity RMSE Difference - ohioval Grid

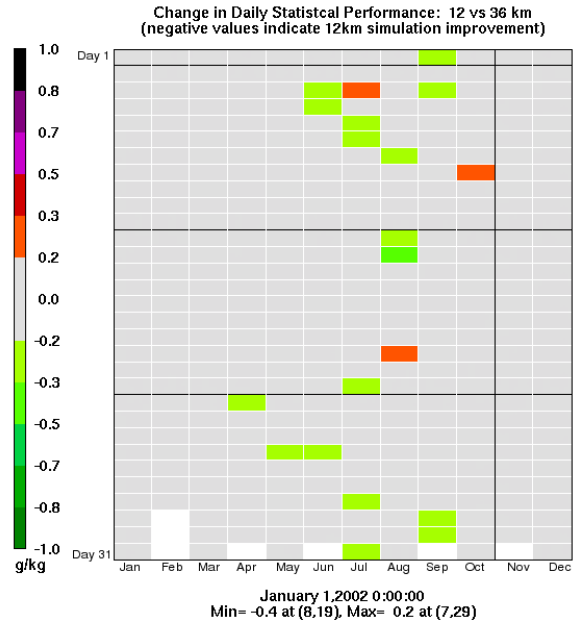
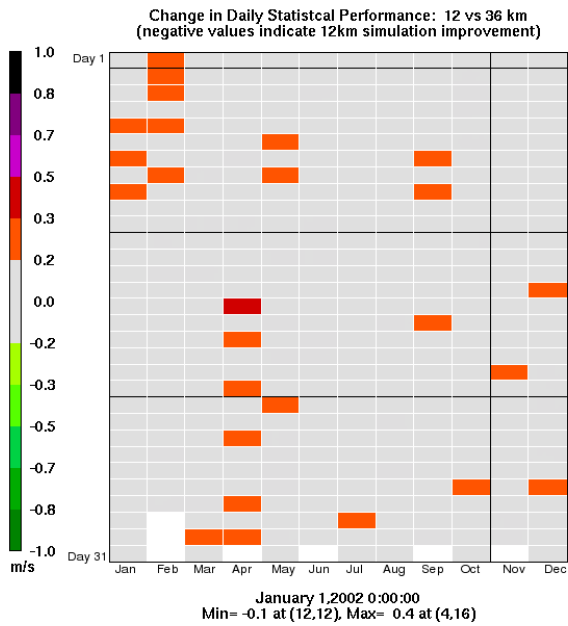
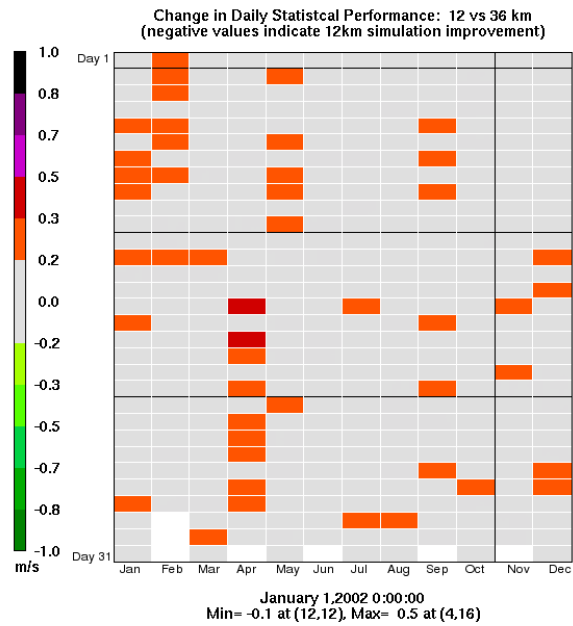


Figure 6.6. Twelve km domain daily averaged statistical performance for selected temperature and mixing ratio metrics in relation to the 36 km grid for the OhioVal subdomain.

Wind Spd Gross Error Difference - Iowa Grid



Wind Spd RMSE Difference - Iowa Grid



Wind Dir Gross Error Difference - Iowa Grid

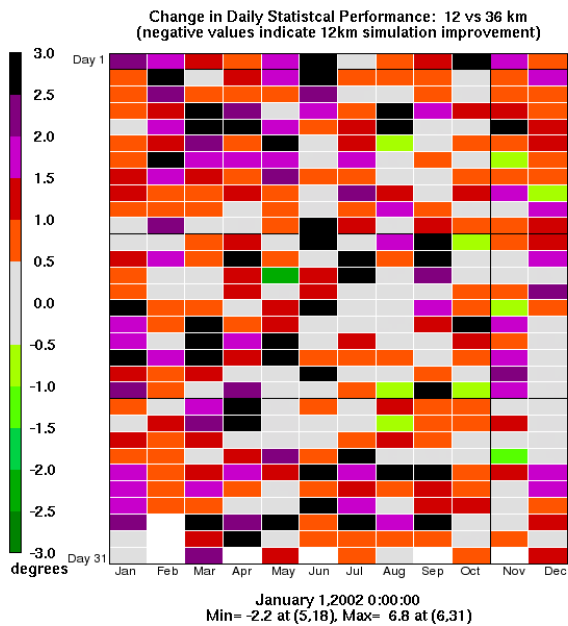
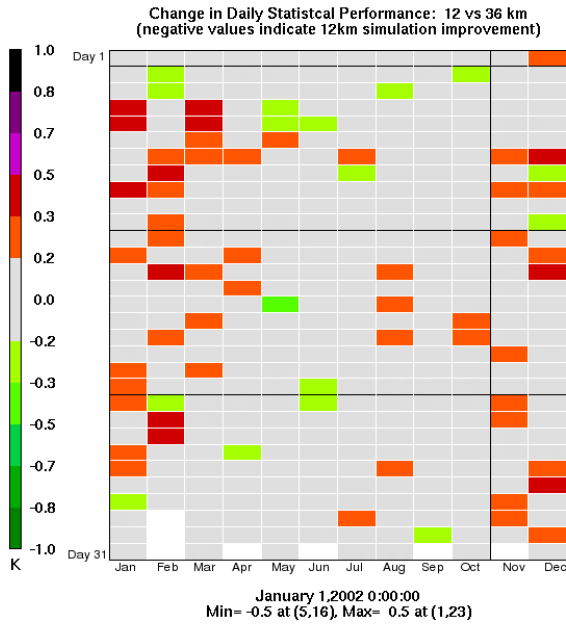
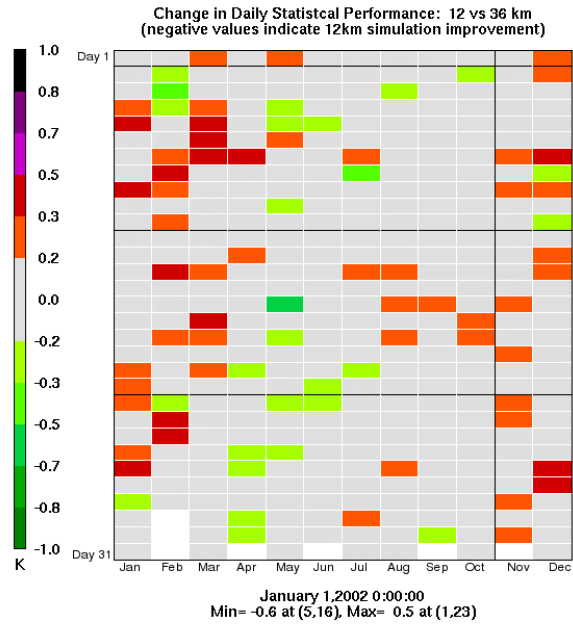


Figure 6.7. Twelve km domain daily averaged statistical performance for selected wind metrics in relation to the 36 km grid for the Iowa subdomain.

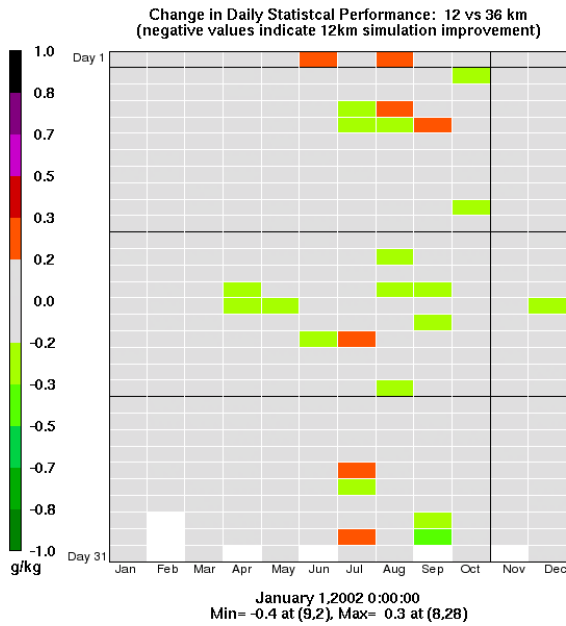
Temperature Gross Error Difference - Iowa Grid



Temperature RMSE Difference - Iowa Grid



Humidity Gross Error Difference - Iowa Grid



Humidity RMSE Difference - Iowa Grid

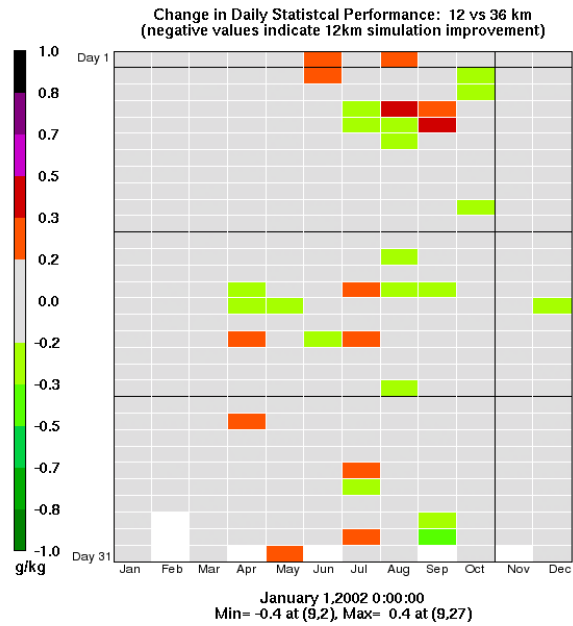


Figure 6.8. Twelve km domain daily averaged statistical performance for selected temperature and mixing ratio metrics in relation to the 36 km grid for the Iowa subdomain.

6.2 HOURLY STATISTICS

Additional comparisons between the 36 and 12 km simulations are provided below through review of hourly timeseries. Modeled (both 36 and 12 km) versus observed conditions are plotted below, with the associated bias also depicted. The hourly time series evaluation eliminates the statistical smoothing associated with the daily averaging periods. These charts also serve as the diurnal profile data source referenced in previous chapters, however, the discussion below will primarily focus upon differences between the 12 and 36 km simulations.

Assessing the timeseries from a winter (January) and summer (June) monthly subset of the annual simulation for the Great Lakes region (Figures 6.9 - 6.10) leads to a general conclusion that improvement occurs in the daytime wind speed biases with implementation of the 12 km grid, while nighttime disbenefits are observed. At 12 km resolution, the wintertime cold bias is even more pronounced versus the 36 km domain, as nighttime low temperatures dip further below observed values (Figure 6.11). The ultimate cause for the low temperature bias is unknown, but this is not an uncommon feature of MM5 simulations (Ad-Hoc Meteorological Modelers Meeting group discussion, 2007). For the GL region, no significant differences are found in either temperature or humidity during the summer month of June (Figure 6.12). Appendix C provides additional January and June hourly 12 versus 36 km statistical charts for the Great Lakes, OhioVal, CenrapN, and Iowa subdomains.

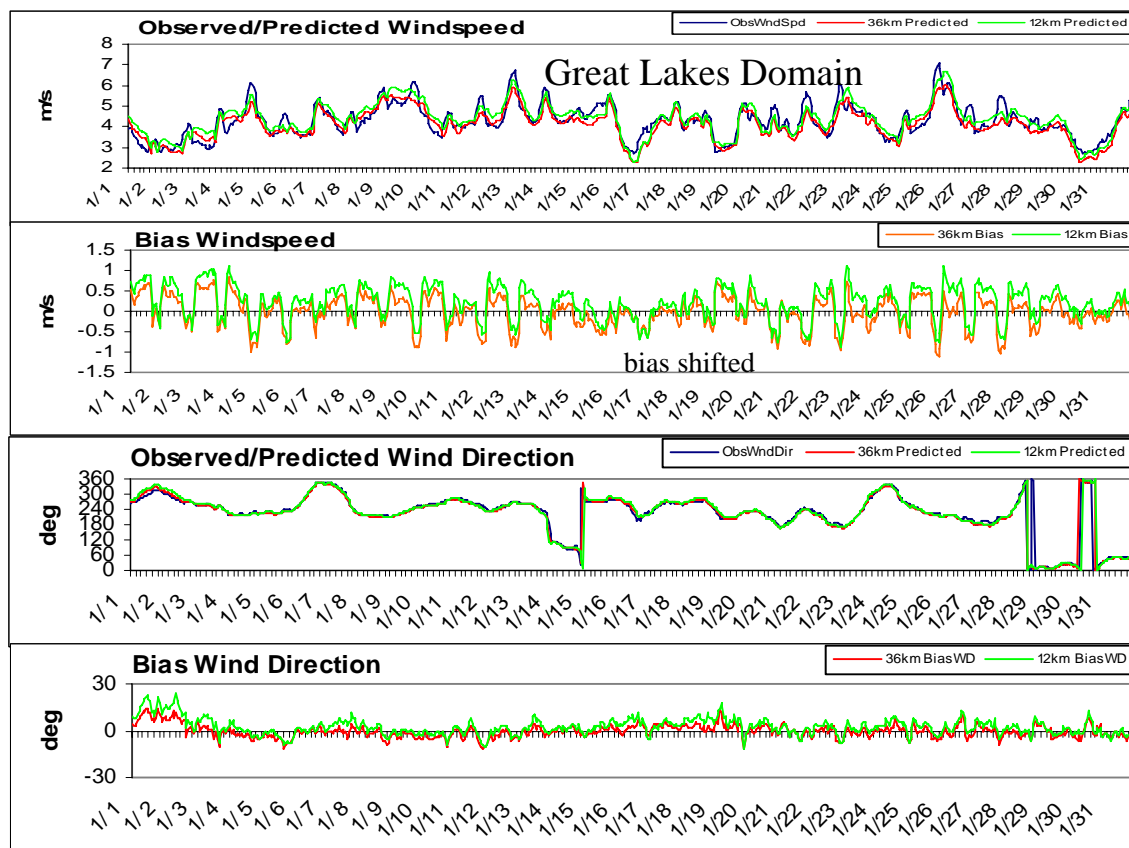


Figure 6.9. Twelve and 36 km hourly wind vector statistics for the Great Lakes subdomain for January, 2002.

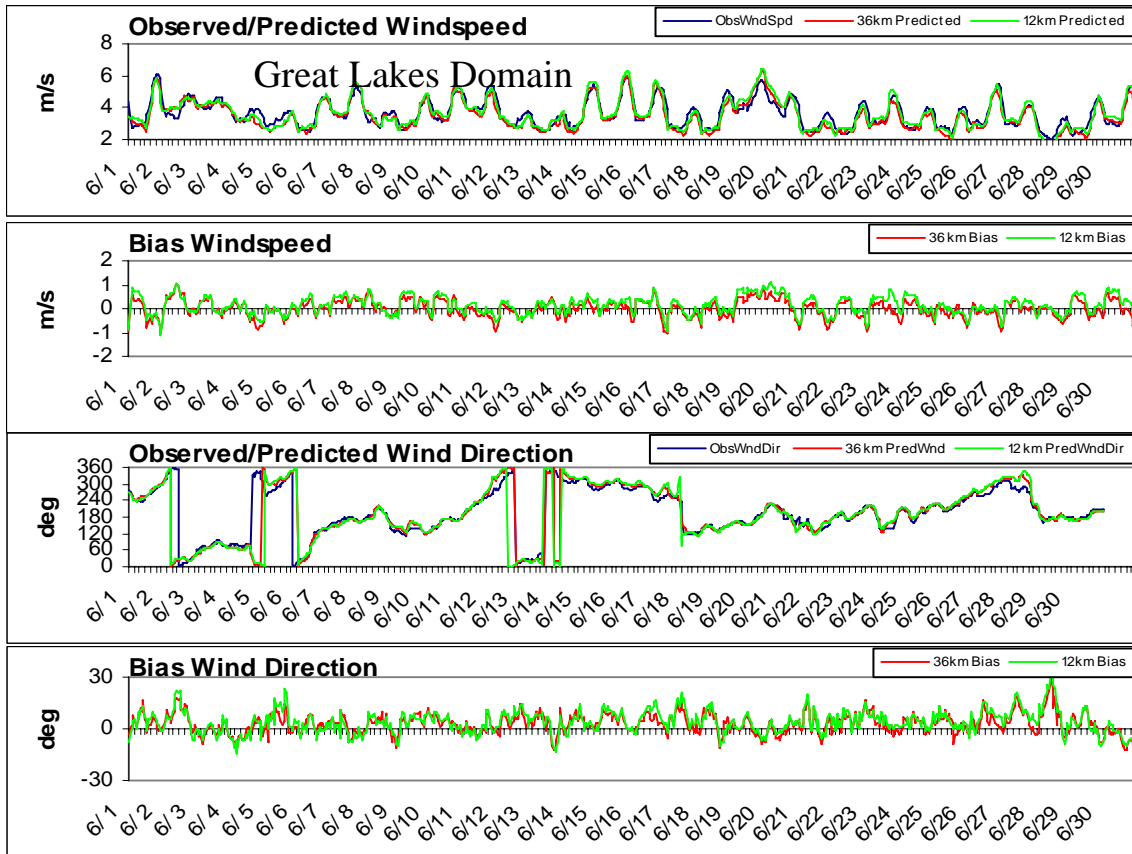


Figure 6.10. Twelve and 36 km hourly wind vector statistics for the Great Lakes subdomain for June, 2002.

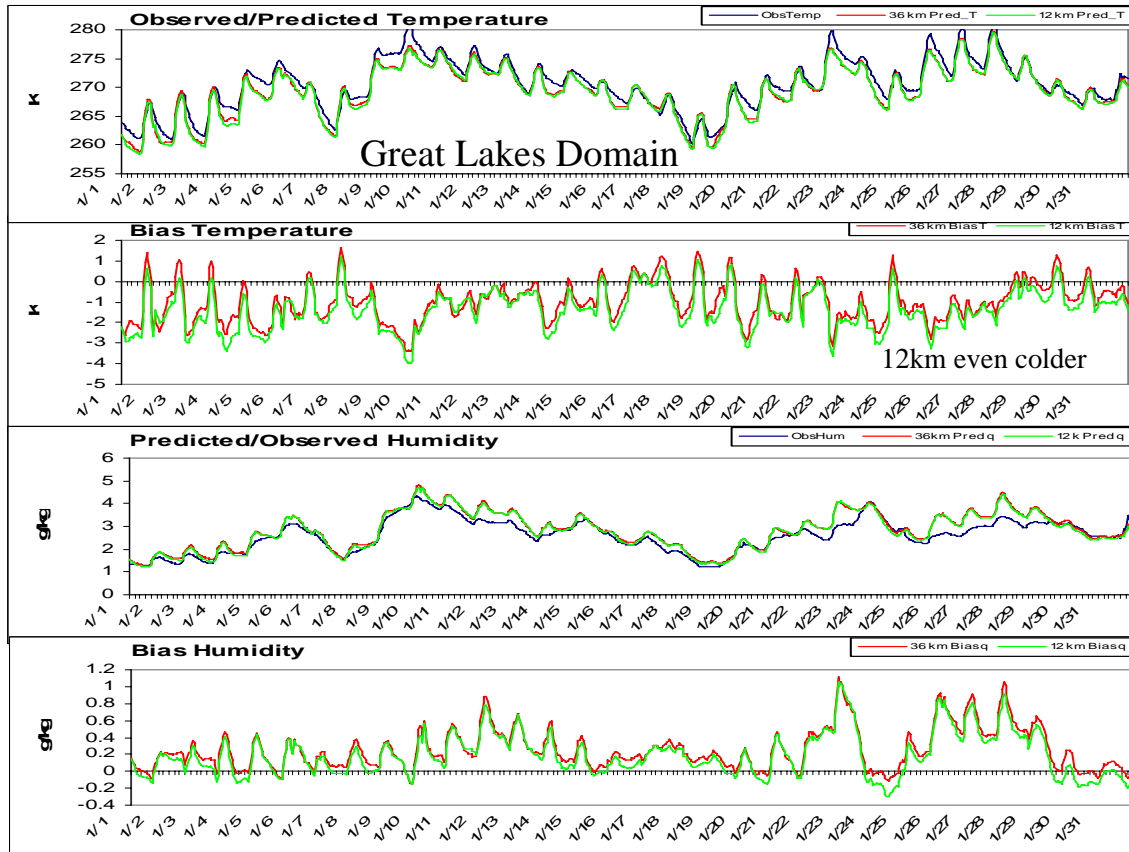


Figure 6.11. Twelve and 36 km hourly temperature and moisture statistics for the Great Lakes subdomain for January, 2002.

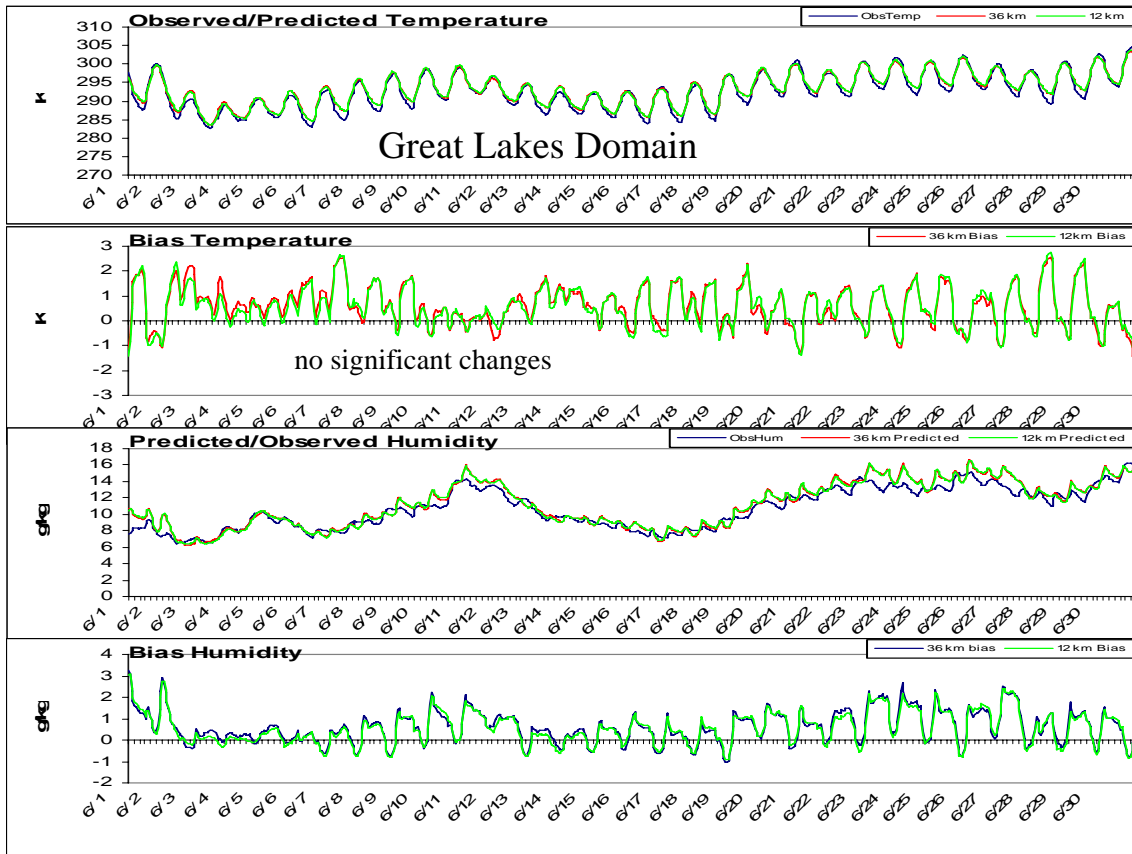


Figure 6.12. Twelve and 36 km hourly temperature and moisture statistics comparison for the Great Lakes subdomain for June, 2002.

7. UPPER AIR EVALUATION

7.1 SOUNDINGS

A comprehensive assessment of model performance cannot be completed through the evaluation of surface statistical measures alone. A rigorous evaluation requires the examination of additional features such as precipitation fields, PBL depths, and vertical profiles of temperature, moisture, and wind vectors. As readily available tools have not been identified which yield objective measures of such parameters, evaluations are typically subjective. A precipitation evaluation of the 36 km dataset has been completed by Kirk Baker (Baker et al., 2004) and is summarized below. In combination with the precipitation evaluation, the most efficient method available for an upper air analysis is to focus upon radiosonde observations. To aid in the review of upper air feature, the IDNR created the RAOBPLOT software tool that efficiently displays modeled versus observed radiosonde upper air measurements. With twice-daily soundings available from approximately 70 observing stations, roughly 51,100 modeled versus observed soundings are available for examination from the 36 km annual simulation alone. Clearly a complete examination is resource prohibitive. The volume of data available, in combination with only inefficient subjective methods for evaluations highlights a current deficiency in annual scale regional modeling applications. While inelegant, the immediately practicable solution requires a targeted review of specific data.

A brief review of the modeled versus observed sounding for many sites in the Central U.S. was conducted, with no terminal deficiencies discovered. A more focused evaluation upon the Davenport, Iowa, station was completed over the simulated summer months, with the following conclusions reached: Upper level wind vectors are well simulated. The temperature fields below approximately 900 mb yielded a tendency toward underprediction at 0Z, while the moisture fields were generally overstated during the same region and time. At 12Z, temperatures were generally underpredicted below 900 mb. In terms of estimated PBL depths, the mixed layer commonly appears shallower than observed. While error is never desired, in terms of modeling air quality (in a conservative sense) a shallow PBL is preferred versus excessive depth. A sample of the observed versus modeled sounding produced by RAOBPLOT is provided in Figure 7.1.

7.2 PRECIPITATION

Kirk Baker with the Lake Michigan Air Directors Consortium was provided a complete copy of the 36 km meteorological dataset and subsequently completed a model performance evaluation examining precipitation fields. In summary, both rainfall totals and precipitation spatial coverage are generally well simulated in the fall, winter, and springtime periods. As is common with many MM5 simulations, summertime precipitation events produce an excess of precipitation. Rainfall patterns also exhibit greater spatial coverage than observed. Additional detail, including graphical representation of predicted and observed rainfall, is available in Baker et al., 2004.

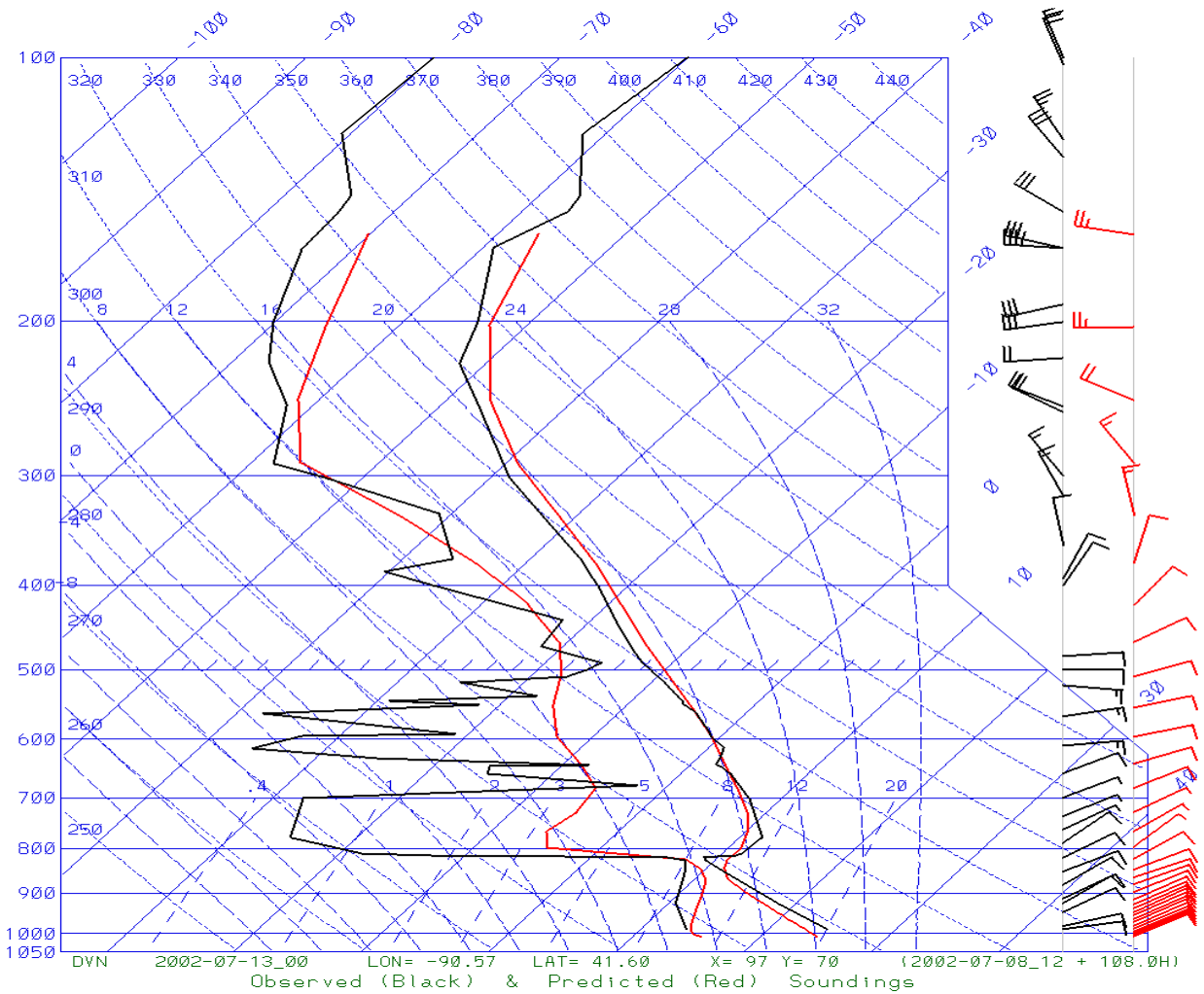


Figure 7.1. Sample ROABPLOT observed versus predicted (36 km domain) sounding for Davenport Iowa, on July 13, 2007, at 0Z. Wind speed and directions are accurately simulated throughout the depth of the sounding. The temperature profile performance is more than adequate. As is common, a positive moisture bias exists at (and above the surface), while the estimated PBL depth remains too shallow.

7.3 PBL DEPTHS

Additional upper air analyses included a limited comparison of the 36 and 12 km predicted PBL heights. Figure 7.2 provides an example comparison. As expected, the degree of agreement between the 36 and 12 km results exceeds variability. Areas in Western Illinois and Eastern Texas (among others) do display deviations. In Eastern Texas, MM5 predicts a precipitation event (which is weakly supported by observations, see Figures 7.3 - 7.4). The reduction in PBL heights in Western Illinois would appear to be precipitation driven as well, but no convective or non-convective rainfall was predicted by MM5 during this time. The observed radar reflectivities also suggests no precipitation occurred during this time. In summary, the 12 km grid yields improved feature detail yet the accuracy of such fields, across a continental scale annual simulation, is difficult to assess within a reasonable timeframe.

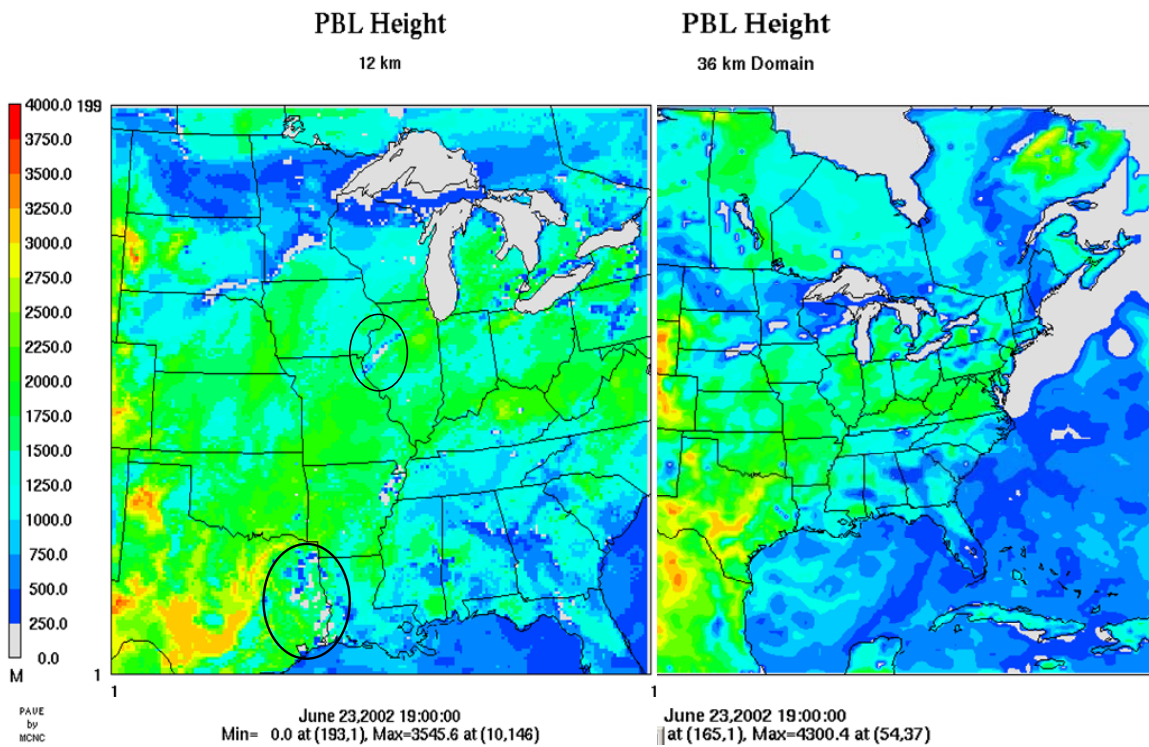


Figure 7.2. PBL heights predicted by MM5 for June 23, 2002, at 19Z. for the 12 and 36 km modeling domains.

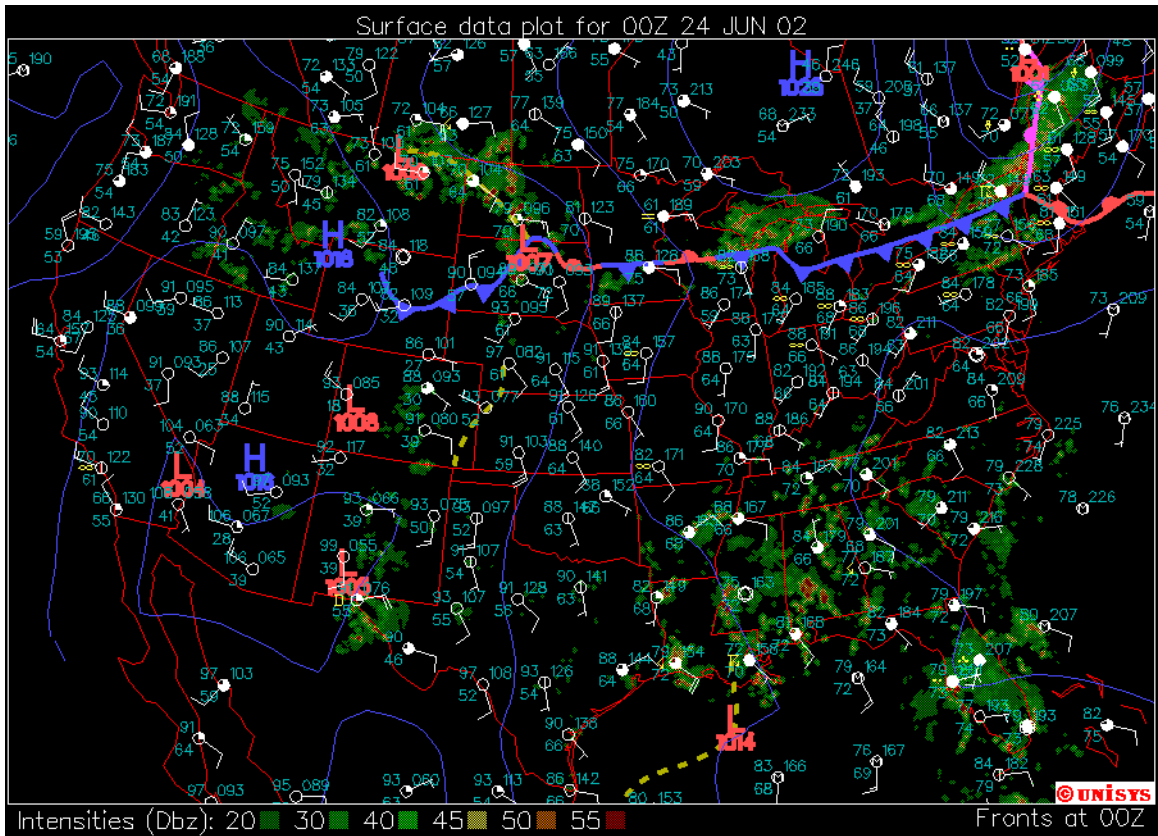


Figure 7.3. Observed conditions on June 24, 0Z.

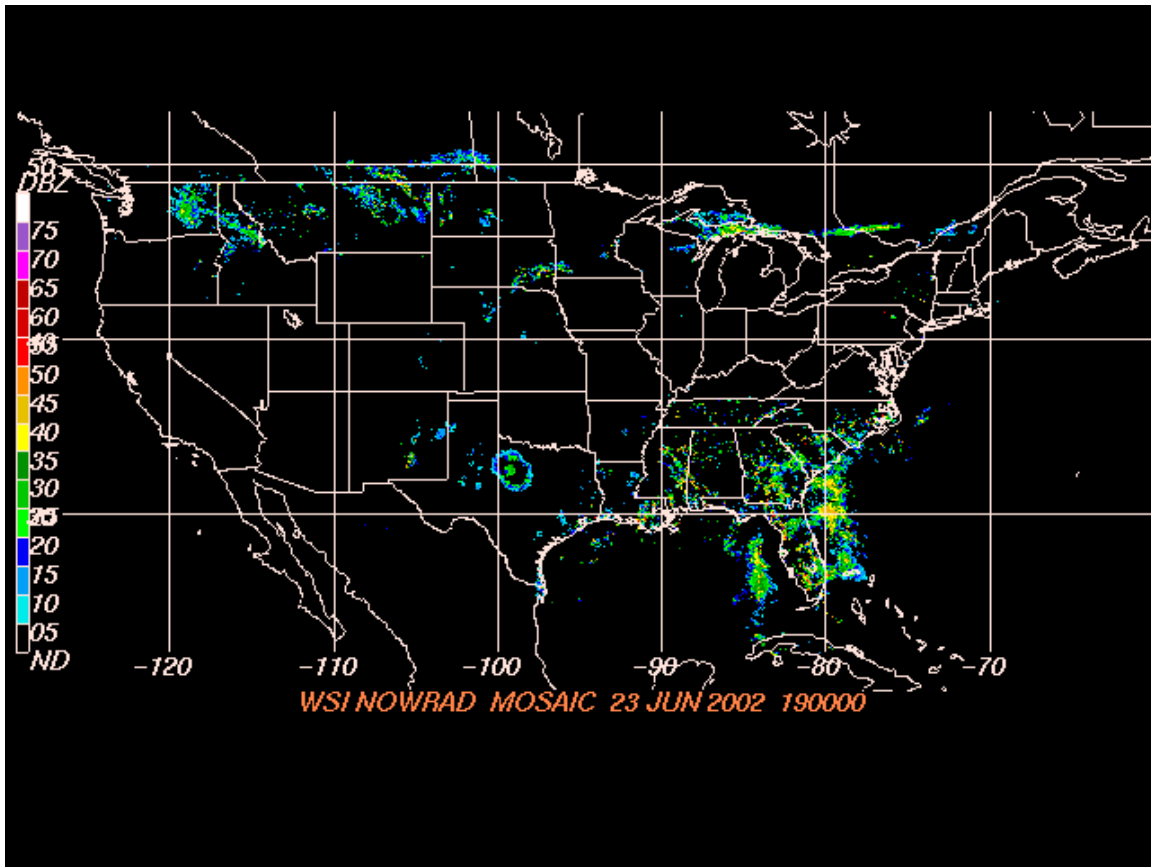


Figure 7.3. Radar reflectivity on June 23, 2002 at 19Z.

8. CONCLUSIONS

In the northern half of the Central U.S. through the Ohio River valley, the surface statistical evaluation reveals a dominant wintertime cold bias, with cool conditions typically present in the evening hours, while overly aggressive nighttime lows and weak high temperatures also contribute to the cold bias. The summer months exhibit a warm bias, attributable to the overprediction of nighttime temperatures. Wind speed and direction predictions over the central and northern Central U.S. exhibit low statistical error and provide for an increase in model confidence. Continuing the evaluation into the Western U.S. yields a reduction in model confidence, as error measures increase across all fields. As discussed, this result is not completely unexpected given complex Western topography. Regions within the Eastern U.S. demonstrate prediction skill above Western regions, yet statistical accuracy falls below that found in the Midwest.

Expanding the evaluation into upper air features reveals no fundamental flaws jeopardizing the adequacy of the simulation in terms of air quality modeling. A tendency to slightly underpredict summertime PBL depths over Eastern Iowa was discovered. In subjective terms, such error is acceptable as perfect model performance is unattainable. A similar conclusion is reached for the precipitation shortfalls discussed by Baker et al., 2004.

Within the Central U.S., increasing the horizontal resolution from 36 to 12 km yielded no benefits from a surface-feature statistical evaluation perspective. Within the Great Lakes subdomain, the 12 km simulation appears to improve daytime wind speed predictions, however, nighttime predictions suffer. Overall, wind speed error showed little variability between the 36 and 12 km domains. Beyond the statistical evaluation, additional field detail is resolved by the 12 km domain as expected. As in the upper air analysis for the 36 km grid, no fundamental flaws were identified in review of 12 km upper air features.

In summary, the statistical evaluation yields results predominantly within acceptable guidelines for the principal regions of interest (the States near and within LADCO and the northern two-thirds of CENRAP). Concurrently, no major simulation deficiencies were revealed during the upper air review. The 36 and 12 km Iowa DNR 2002MM5v363 datasets are thus judged acceptable for use in regional scale air quality modeling studies focused within the central United States.

9. REFERENCES

- Anthes, R. A. and T. T. Warner, 1978: The Development of Mesoscale Models Suitable for Air Pollution and Other Mesometeorological Studies. *Monthly Weather Review*, **106**, 1045-1078.
- Baker, K., 2002: MM5 Sensitivity for the National RPO Grid, Presented at the Ad-Hoc Meteorological Modeling Meeting, Des Plaines, IL, 2002.
- Baker, Kirk, Matthew Johnson and Steven King, 2004: Meteorological Modeling Performance Summary For Application to PM2.5/Haze/Ozone Modeling Projects. http://ladco.org/tech/photo/docs/mm5_protocol_dec2004.pdf
- Chen, F., and J. Dudhia, 2001: Coupling an advanced land-surface/hydrology model with the Penn State/NCAR MM5 modeling system. Part I: Model implementation and sensitivity. *Monthly Weather Review*, **129**, 569-585.
- Dudhia, J., 1993: A Non-hydrostatic Version of the Penn State/NCAR Mesoscale Model: Validation Tests and Simulation of an Atlantic Cyclone and Cold Front. *Monthly Weather Review*, **121**, 1493-1513.
- Emery, C., and Edward Tai, 2001: Meteorological Modeling and Performance Evaluation of the September 13-20, 1999 Ozone Episode. Prepared for the Texas Near Non-Attainment Areas through the Alamo Area Council of Governments, by ENVIRON International Corp, Novato, CA.
- McNally, Dennis, 2003: Annual Application of MM5 for Calendar Year 2001. Prepared for Pat Dolwick, USEPA, March 31st 2003.
- Olerud, Donald, K. Alapaty, and N. Wheeler, 2000: Meteorological Modeling of 1996 for the United States with MM5. Prepared for Normal Possiel, Client Representative, U.S. EPA/OAQPS. EPA Task Order Number CAA689805
- Olerud, Don and Aaron Sims, 2004: Draft Protocol for Annual MM5 Modeling in Support of VISTAS (Visibility Improvement – State and Tribal Association) (DRAFT), Prepared for Mr. Mike Abraczinskas, VISTAS Technical Analysis Workgroup.
- Pleim, J. E., and J. S. Chang, 1992: A non-local closure model for vertical mixing in the convective boundary layer. *Atmospheric Environment*, **26A**, 965-981.
- Stauffer, D. R., and N. L. Seaman, 1990: Use of Four Dimensional Data Assimilation in a Limited-Area Mesoscale Model. Part I: Experiments with Synoptic Data. *Monthly Weather Review*, **118**, 1250-1277.

- Stauffer, D. R., and N. L. Seaman. 1991: Use of Four Dimensional Data Assimilation in a Limited-Area Mesoscale Model. Part II: Effects of Data Assimilation within the Planetary Boundary Layer. *Monthly Weather Review*, **119**, 734-754
- Tesche, T. W. 1994. "Evaluation Procedures for Regional Emissions, Meteorological, and Photochemical Models." Presented at the 86th Annual Meeting of the Air and Waste Management Association, 14-18 June, Denver, CO.
- Xiu, A., and J. E. Pleim, 2000: Development of a land surface model. Part I: Application in a mesoscale meteorology model. *Journal of Applied Meteorology*, **40**, 192-209.

APPENDIX A

Temporal structure example for the 2002 annual simulation.

Start BLOCK	End BLOCK	Start (Z)	End (Z)	Filename	Metstat Usable	
					Start (Z)	End (Z)
12/28/2001 12:00	1/2/2002 12:00	12/28/2001 12:00	12/28/2001 12:00	MMOUT_DOMAIN1_00		
		12/28/2001 13:00	12/29/2001 12:00	MMOUT_DOMAIN1_01	12/29/2001 0:00	12/29/2001 12:00
		12/29/2001 13:00	12/30/2001 12:00	MMOUT_DOMAIN1_02	12/29/2001 13:00	12/30/2001 12:00
		12/30/2001 13:00	12/31/2001 12:00	MMOUT_DOMAIN1_03	12/30/2001 13:00	12/31/2001 12:00
		12/31/2001 13:00	1/1/2002 12:00	MMOUT_DOMAIN1_04	12/31/2001 13:00	1/1/2002 12:00
		1/1/2002 13:00	1/2/2002 12:00	MMOUT_DOMAIN1_05	1/1/2002 13:00	1/1/2002 23:00
1/1/2002 12:00	1/6/2002 12:00	1/1/2002 12:00	1/1/2002 12:00	MMOUT_DOMAIN1_00		
		1/1/2002 13:00	1/2/2002 12:00	MMOUT_DOMAIN1_01	1/2/2002 0:00	1/2/2002 12:00
		1/2/2002 13:00	1/3/2002 12:00	MMOUT_DOMAIN1_02	1/2/2002 13:00	1/3/2002 12:00
		1/3/2002 13:00	1/4/2002 12:00	MMOUT_DOMAIN1_03	1/3/2002 13:00	1/4/2002 12:00
		1/4/2002 13:00	1/5/2002 12:00	MMOUT_DOMAIN1_04	1/4/2002 13:00	1/5/2002 12:00
		1/5/2002 13:00	1/6/2002 12:00	MMOUT_DOMAIN1_05	1/5/2002 13:00	1/5/2002 23:00
1/5/2002 12:00	1/10/2002 12:00	1/5/2002 12:00	1/5/2002 12:00	MMOUT_DOMAIN1_00		
		1/5/2002 13:00	1/6/2002 12:00	MMOUT_DOMAIN1_01	1/6/2002 0:00	1/6/2002 12:00
		1/6/2002 13:00	1/7/2002 12:00	MMOUT_DOMAIN1_02	1/6/2002 13:00	1/7/2002 12:00
		1/7/2002 13:00	1/8/2002 12:00	MMOUT_DOMAIN1_03	1/7/2002 13:00	1/8/2002 12:00
		1/8/2002 13:00	1/9/2002 12:00	MMOUT_DOMAIN1_04	1/8/2002 13:00	1/9/2002 12:00
		1/9/2002 13:00	1/10/2002 12:00	MMOUT_DOMAIN1_05	1/9/2002 13:00	1/9/2002 23:00

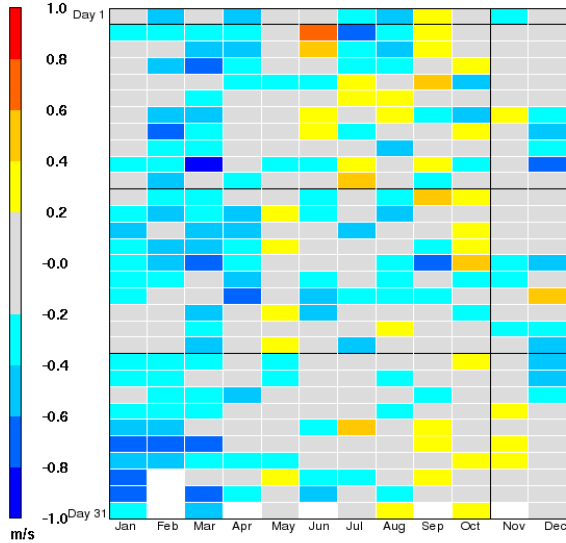
APPENDIX B

Daily averaged metrics from the 36 km simulation.

Eastern Subdomains

Wind Spd Bias - NE Grid

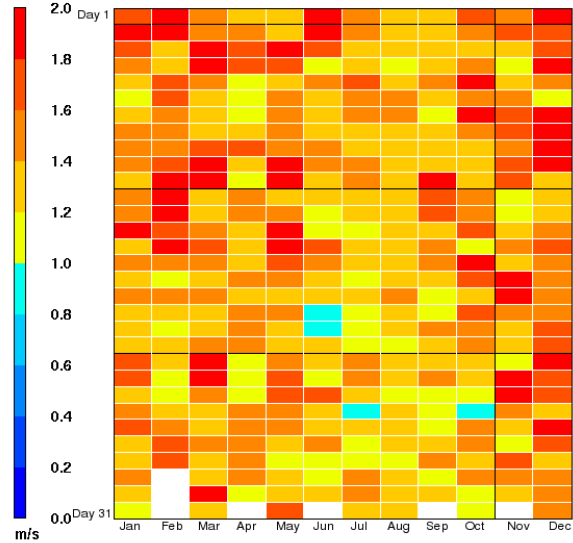
Annual MM5v363 2002 Daily Metrics: 36 km
Iowa DNR



January 1, 2002 0:00:00
Min= -1.1 at (3,22), Max= 0.6 at (6,30)

Wind Spd Gross Error - NE Grid

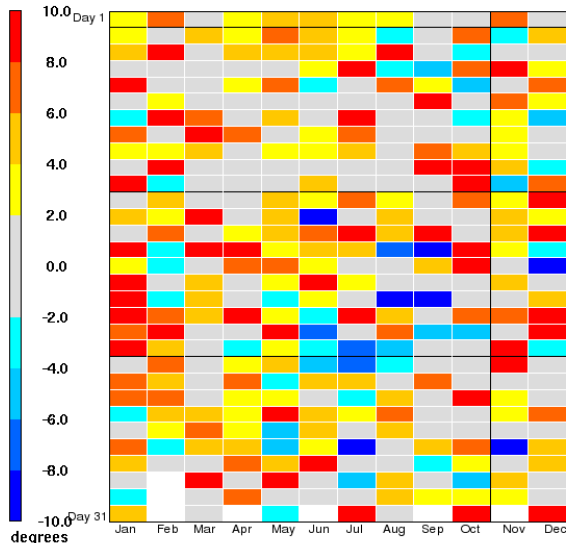
Annual MM5v363 2002 Daily Metrics: 36 km
Iowa DNR



January 1, 2002 0:00:00
Min= 0.9 at (6,13), Max= 2.5 at (3,22)

Wind Dir Bias - NE Grid

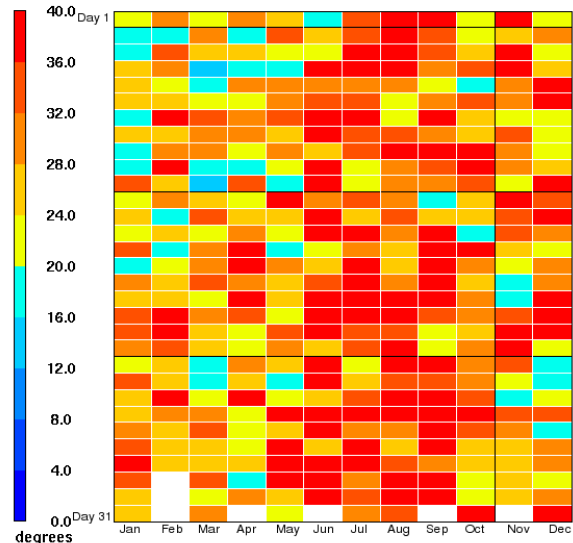
Annual MM5v363 2002 Daily Metrics: 36 km
Iowa DNR



January 1, 2002 0:00:00
Min= -10.9 at (11,5), Max= 16.6 at (8,29)

Wind Dir Gross Error - NE Grid

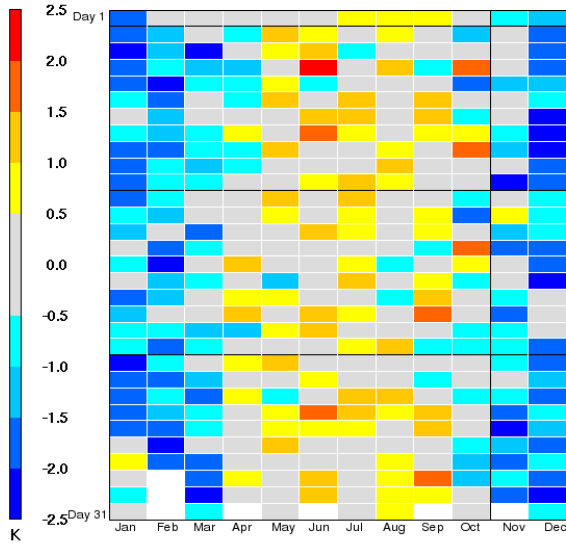
Annual MM5v363 2002 Daily Metrics: 36 km
Iowa DNR



January 1, 2002 0:00:00
Min= 13.9 at (3,21), Max= 63.8 at (9,16)

Temperature Bias - NE Grid

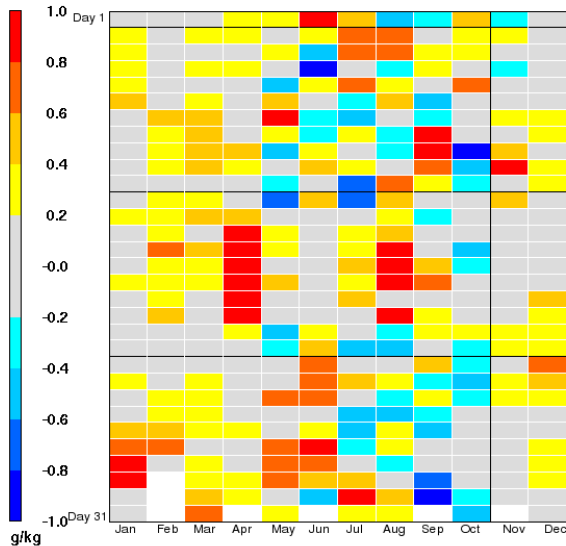
Annual MM5v363 2002 Daily Metrics: 36 km
Iowa DNR



January 1, 2002 0:00:00
Min= -2.5 at (2,5), Max= 2.0 at (6,28)

Humidity Bias - NE Grid

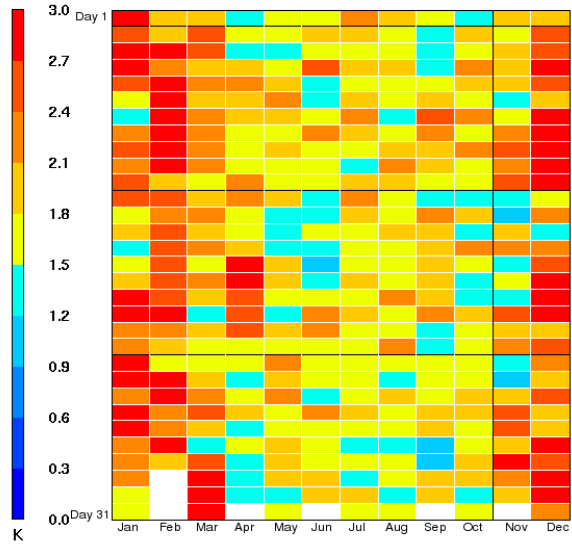
Annual MM5v363 2002 Daily Metrics: 36 km
Iowa DNR



January 1, 2002 0:00:00
Min= -1.2 at (9,2), Max= 2.7 at (4,15)

Temperature Gross Error - NE Grid

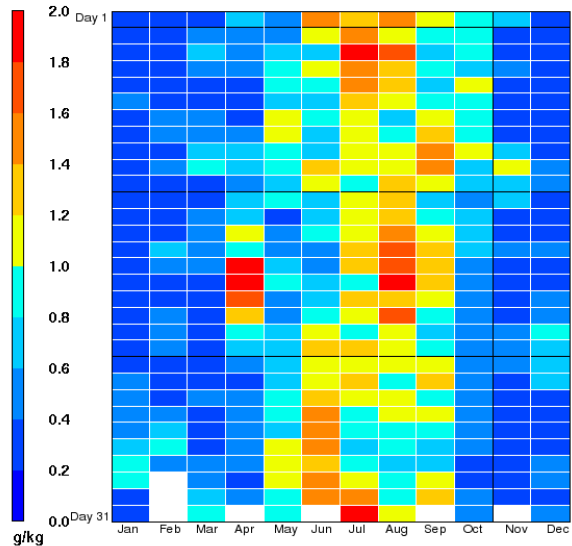
Annual MM5v363 2002 Daily Metrics: 36 km
Iowa DNR



January 1, 2002 0:00:00
Min= 1.0 at (11,19), Max= 3.5 at (1,9)

Humidity Gross Error - NE Grid

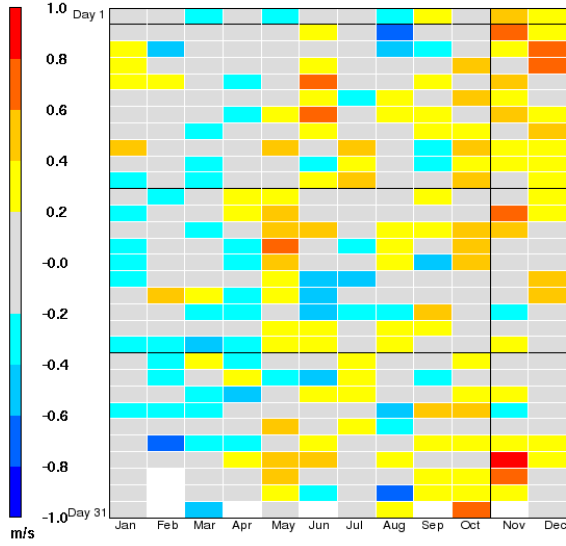
Annual MM5v363 2002 Daily Metrics: 36 km
Iowa DNR



January 1, 2002 0:00:00
Min= 0.2 at (1,24), Max= 2.7 at (4,15)

Wind Spd Bias - MidAtlantic Grid

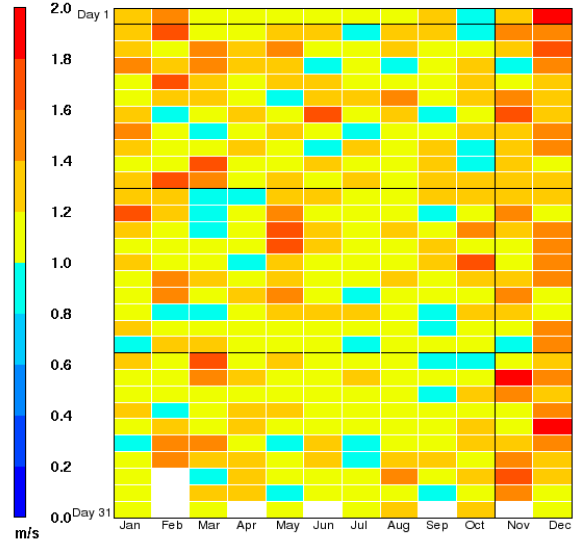
Annual MM5v363 2002 Daily Metrics: 36 km
Iowa DNR



January 1, 2002 0:00:00
Min= -0.7 at (2,5), Max= 0.9 at (11,4)

Wind Spd Gross Error - MidAtlantic Grid

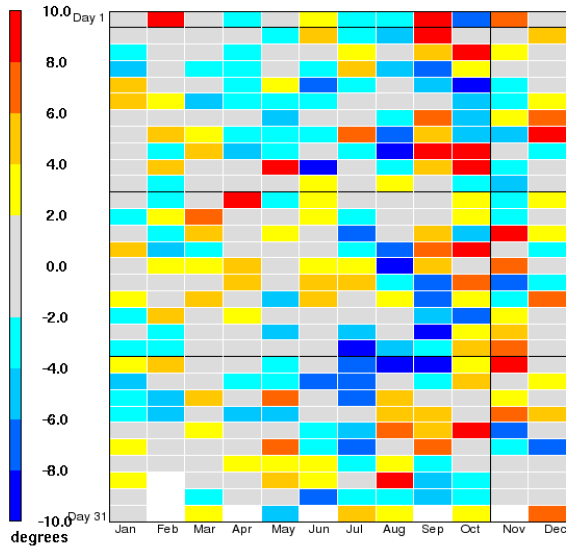
Annual MM5v363 2002 Daily Metrics: 36 km
Iowa DNR



January 1, 2002 0:00:00
Min= 0.8 at (11,11), Max= 1.9 at (12,6)

Wind Dir Bias - MidAtlantic Grid

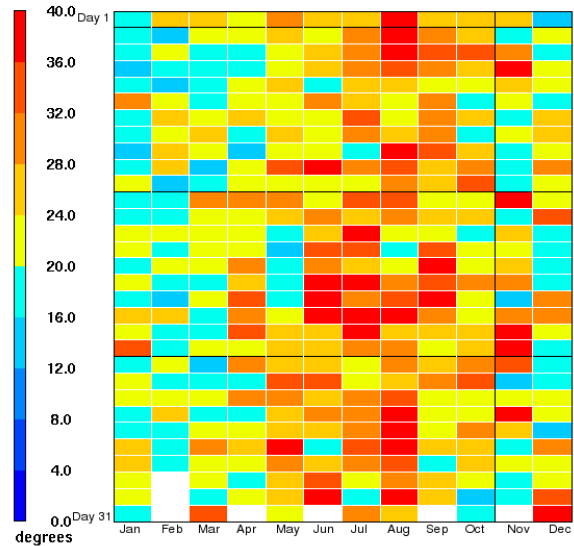
Annual MM5v363 2002 Daily Metrics: 36 km
Iowa DNR



January 1, 2002 0:00:00
Min= -11.3 at (10,27), Max= 18.2 at (9,30)

Wind Dir Gross Error - MidAtlantic Grid

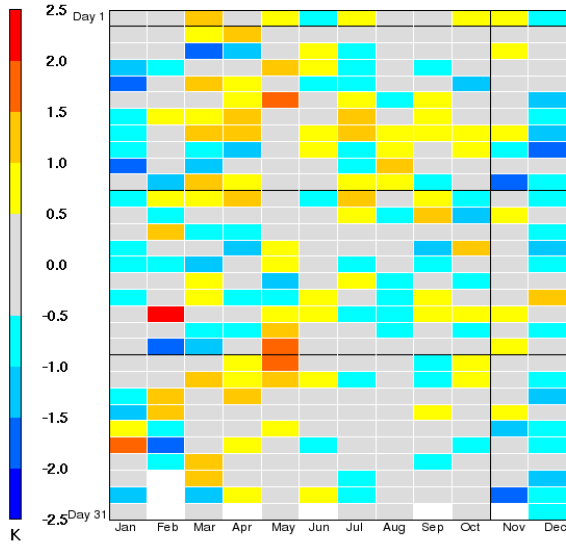
Annual MM5v363 2002 Daily Metrics: 36 km
Iowa DNR



January 1, 2002 0:00:00
Min= 12.7 at (2,27), Max= 50.1 at (8,6)

Temperature Bias - MidAtlantic Grid

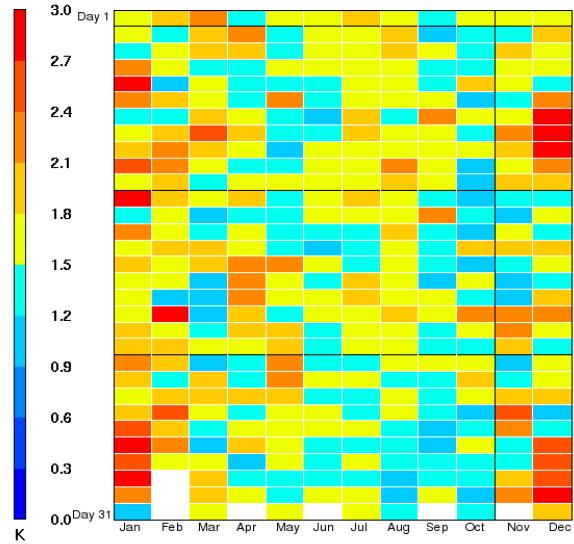
Annual MM5v363 2002 Daily Metrics: 36 km
Iowa DNR



January 1, 2002 0:00:00
Min= -1.9 at (1,27), Max= 2.4 at (2,13)

Temperature Gross Error - MidAtlantic Grid

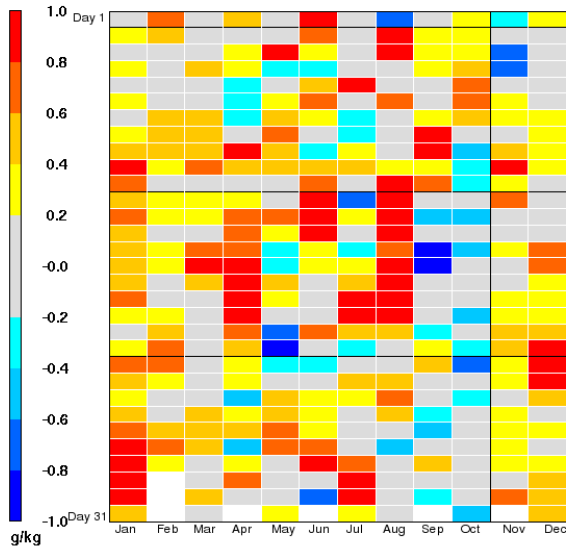
Annual MM5v363 2002 Daily Metrics: 36 km
Iowa DNR



January 1, 2002 0:00:00
Min= 1.0 at (12,7), Max= 3.2 at (1,5)

Humidity Bias - MidAtlantic Grid

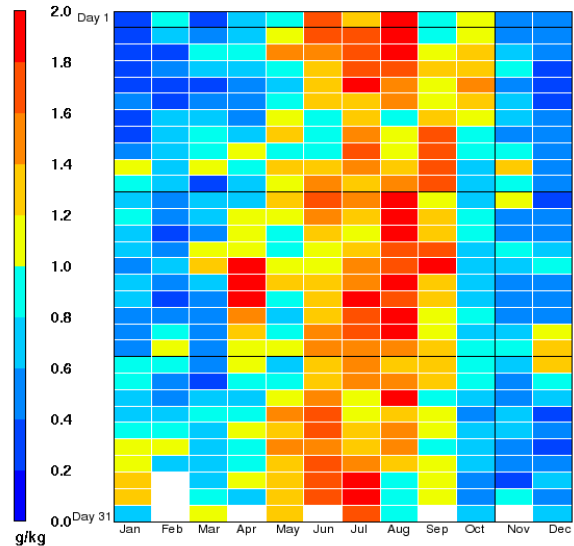
Annual MM5v363 2002 Daily Metrics: 36 km
Iowa DNR



January 1, 2002 0:00:00
Min= -1.3 at (9,16), Max= 2.7 at (4,15)

Humidity Gross Error - MidAtlantic Grid

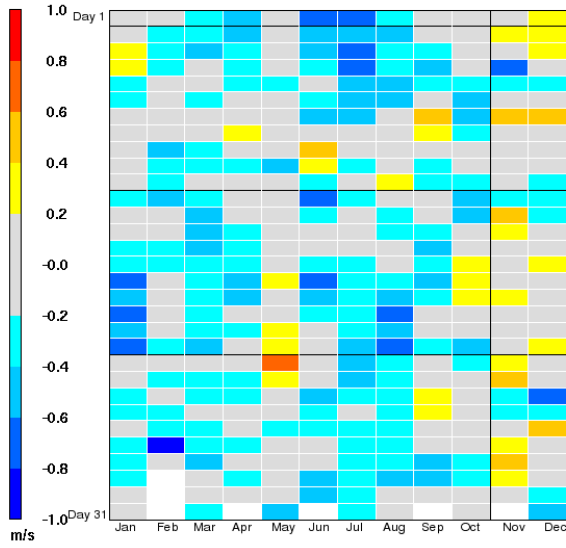
Annual MM5v363 2002 Daily Metrics: 36 km
Iowa DNR



January 1, 2002 0:00:00
Min= 0.2 at (3,27), Max= 2.8 at (4,15)

Wind Spd Bias - SE Grid

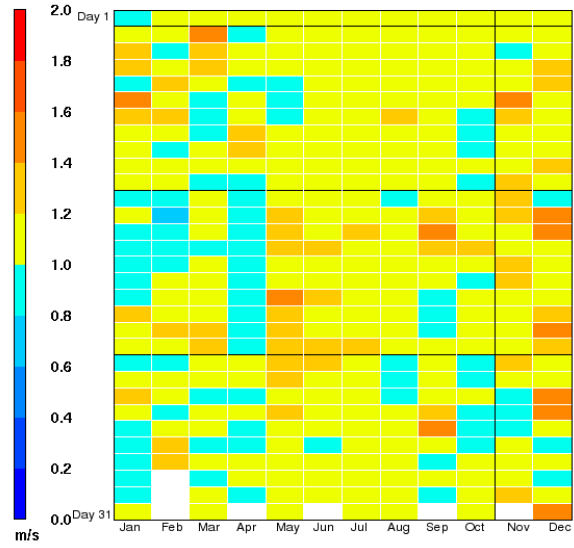
Annual MM5v363 2002 Daily Metrics: 36 km
Iowa DNR



January 1, 2002 0:00:00
Min= -0.8 at (2,5), Max= 0.6 at (5,10)

Wind Spd Gross Error - SE Grid

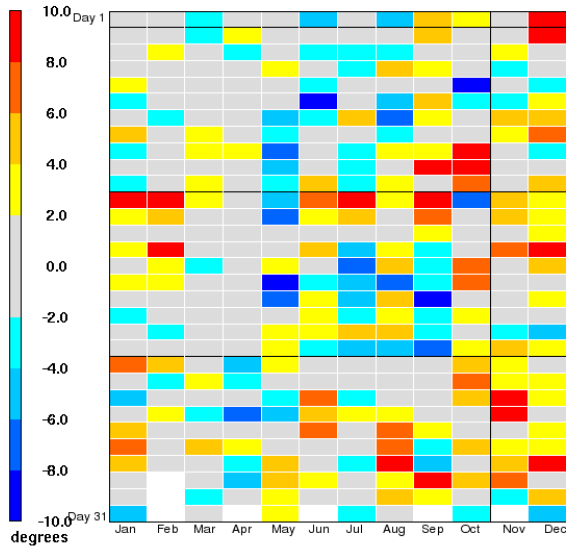
Annual MM5v363 2002 Daily Metrics: 36 km
Iowa DNR



January 1, 2002 0:00:00
Min= 0.8 at (2,19), Max= 1.5 at (12,8)

Wind Dir Bias - SE Grid

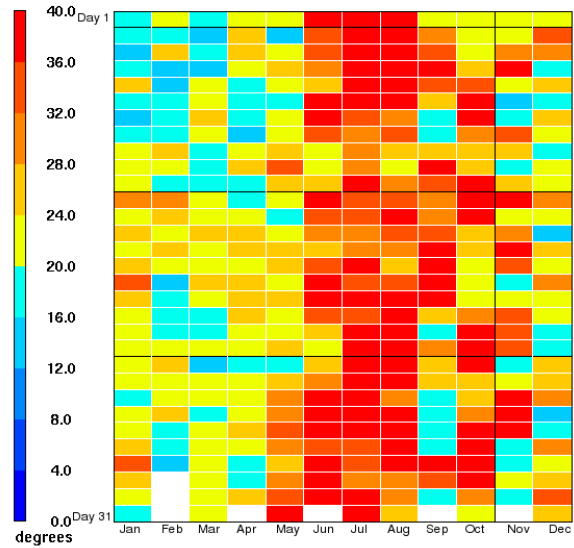
Annual MM5v363 2002 Daily Metrics: 36 km
Iowa DNR



January 1, 2002 0:00:00
Min= -9.7 at (5,15), Max= 14.5 at (8,4)

Wind Dir Gross Error - SE Grid

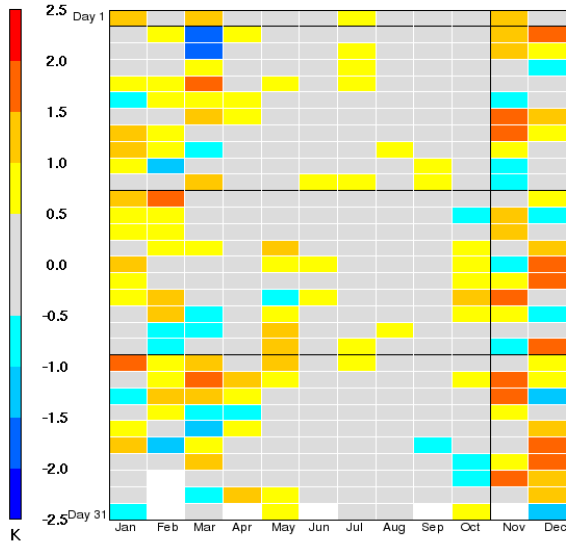
Annual MM5v363 2002 Daily Metrics: 36 km
Iowa DNR



January 1, 2002 0:00:00
Min= 12.5 at (4,24), Max= 58.5 at (7,27)

Temperature Bias - SE Grid

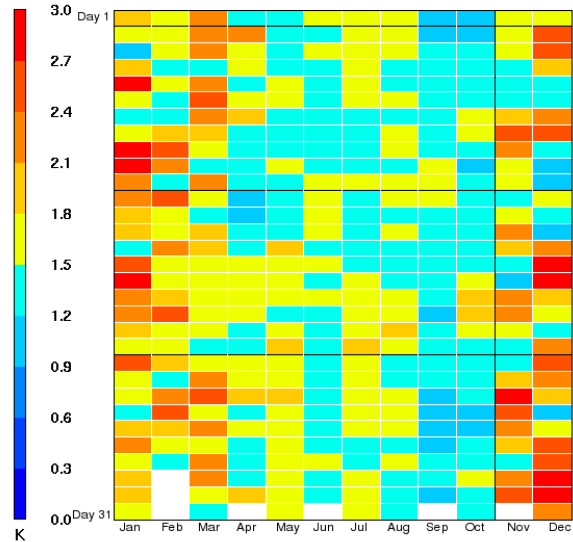
Annual MM5v363 2002 Daily Metrics: 36 km
Iowa DNR



January 1, 2002 0:00:00
Min= -2.0 at (3,30), Max= 1.9 at (12,16)

Temperature Gross Error - SE Grid

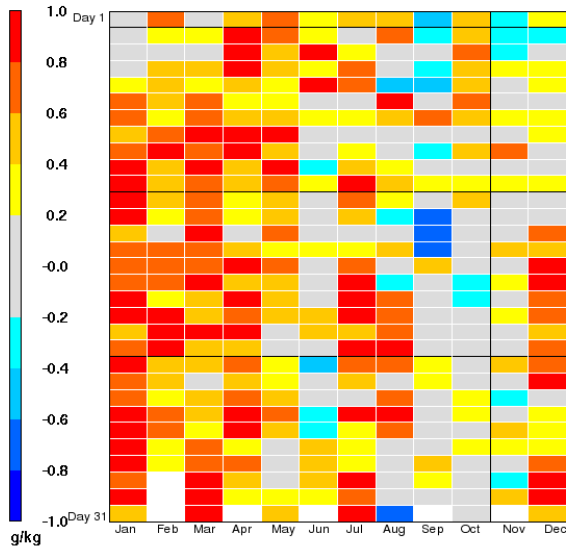
Annual MM5v363 2002 Daily Metrics: 36 km
Iowa DNR



January 1, 2002 0:00:00
Min= 1.0 at (9,7), Max= 3.5 at (12,2)

Humidity Bias - SE Grid

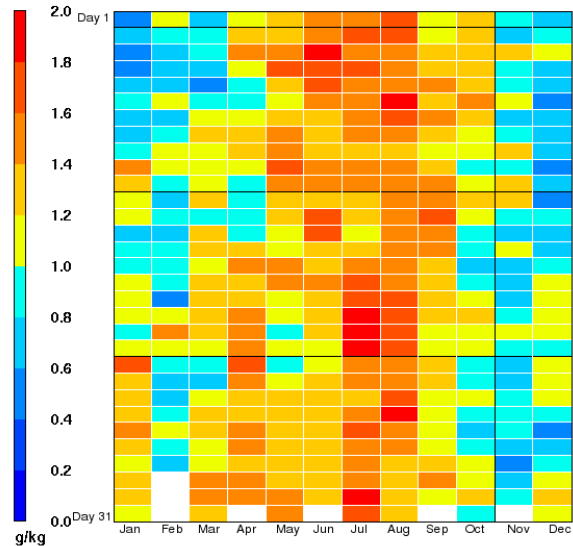
Annual MM5v363 2002 Daily Metrics: 36 km
Iowa DNR



January 1, 2002 0:00:00
Min= -0.8 at (6,1), Max= 1.6 at (1,10)

Humidity Gross Error - SE Grid

Annual MM5v363 2002 Daily Metrics: 36 km
Iowa DNR

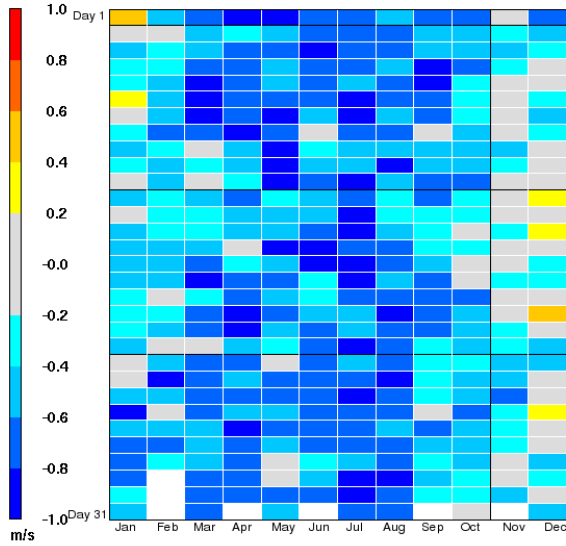


January 1, 2002 0:00:00
Min= 0.4 at (1,28), Max= 2.0 at (6,29)

Western Subdomains

Wind Spd Bias - PacificNW Grid

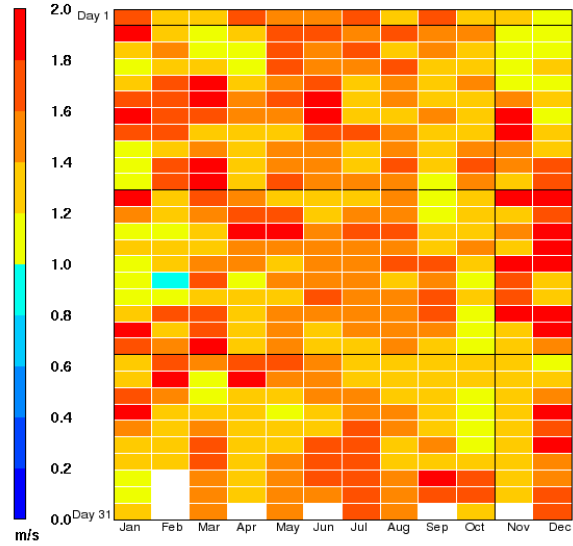
Annual MM5v363 2002 Daily Metrics: 36 km
Iowa DNR



January 1, 2002 0:00:00
Min= -1.0 at (3,27), Max= 0.5 at (1,31)

Wind Spd Gross Error - PacificNW Grid

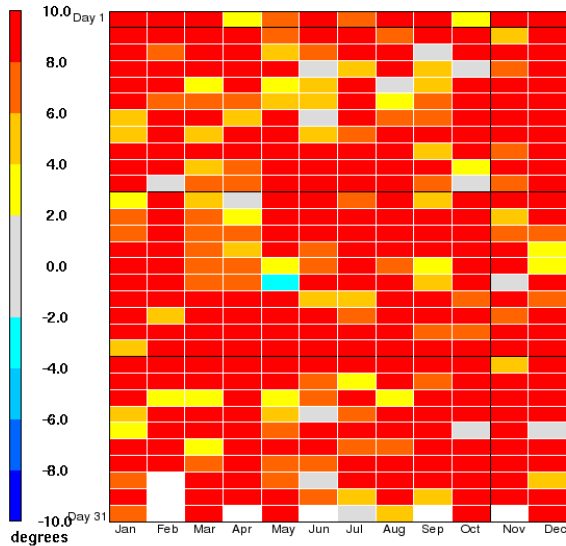
Annual MM5v363 2002 Daily Metrics: 36 km
Iowa DNR



January 1, 2002 0:00:00
Min= 1.0 at (2,15), Max= 2.4 at (12,16)

Wind Dir Bias - PacificNW Grid

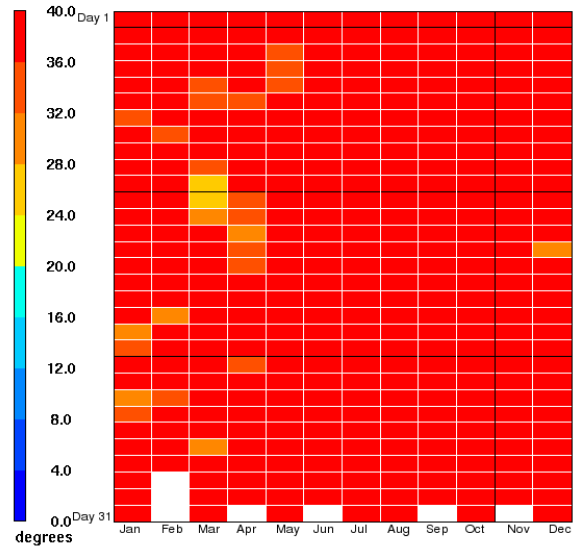
Annual MM5v363 2002 Daily Metrics: 36 km
Iowa DNR



January 1, 2002 0:00:00
Min= -2.3 at (5,15), Max= 24.3 at (3,10)

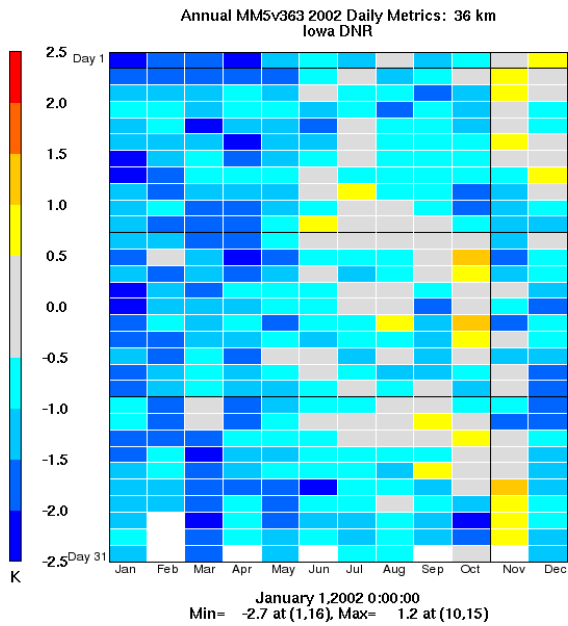
Wind Dir Gross Error - PacificNW Grid

Annual MM5v363 2002 Daily Metrics: 36 km
Iowa DNR

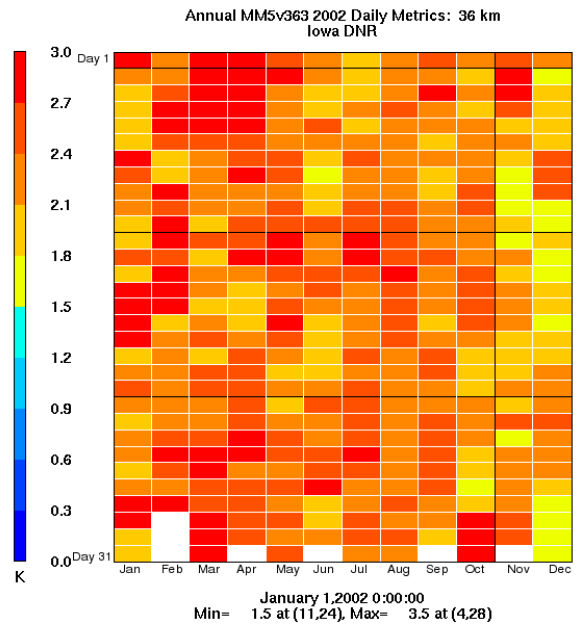


January 1, 2002 0:00:00
Min= 27.9 at (3,21), Max= 75.7 at (10,7)

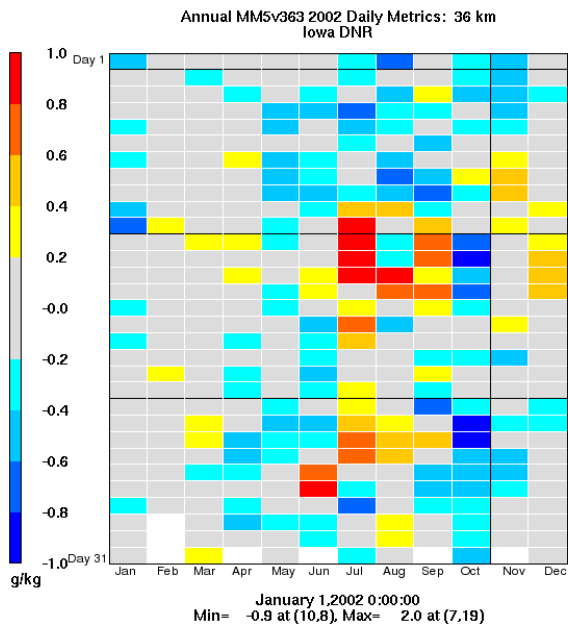
Temperature Bias - PacificNW Grid



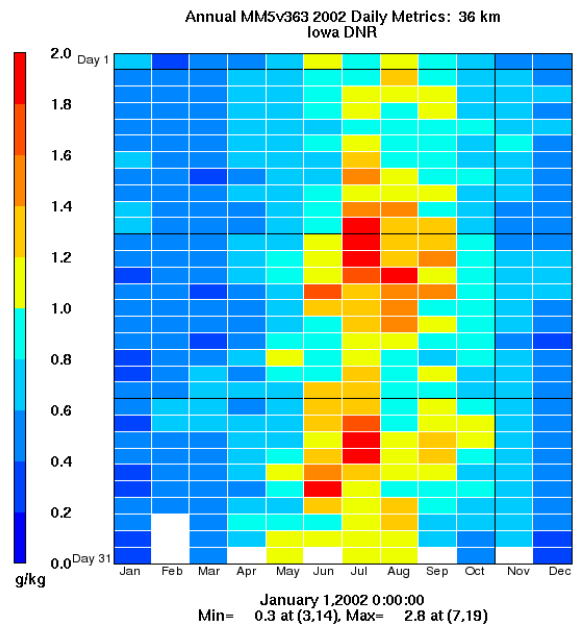
Temperature Gross Error - PacificNW Grid



Humidity Bias - PacificNW Grid

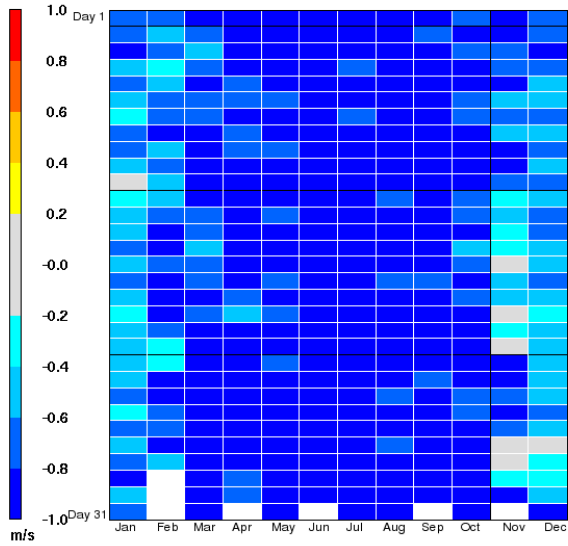


Humidity Gross Error - PacificNW Grid



Wind Spd Bias - SW Grid

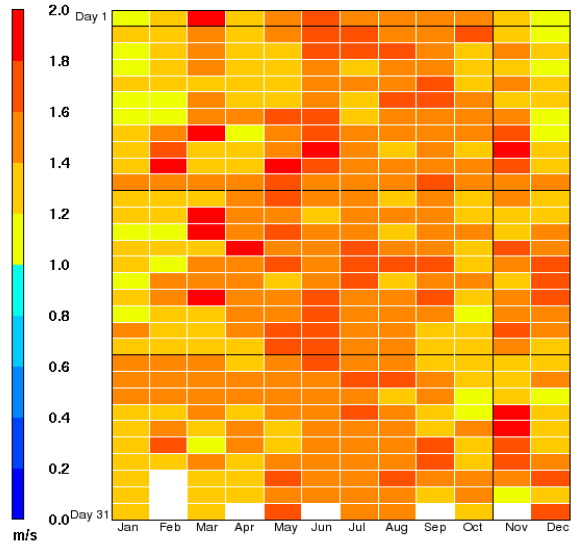
Annual MM5v363 2002 Daily Metrics: 36 km
Iowa DNR



January 1, 2002 0:00:00
Min= -1.5 at (5,22), Max= -0.1 at (11,13)

Wind Spd Gross Error - SW Grid

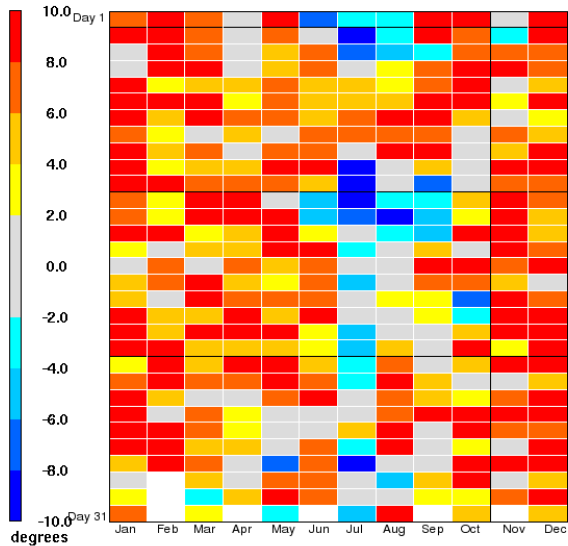
Annual MM5v363 2002 Daily Metrics: 36 km
Iowa DNR



January 1, 2002 0:00:00
Min= 1.0 at (12,25), Max= 2.1 at (4,17)

Wind Dir Bias - SW Grid

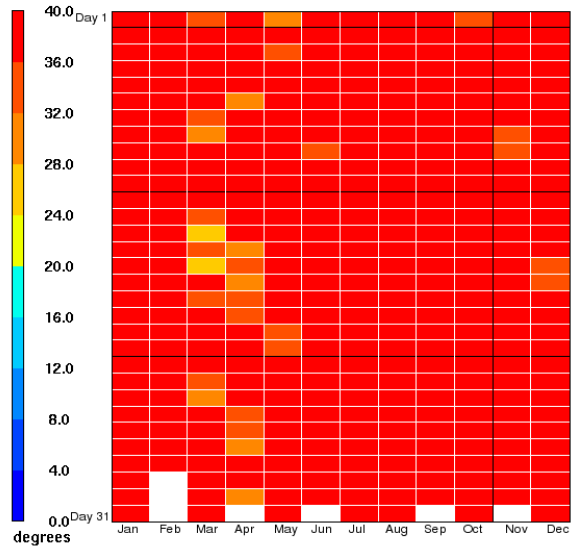
Annual MM5v363 2002 Daily Metrics: 36 km
Iowa DNR



January 1, 2002 0:00:00
Min= -11.4 at (7,4), Max= 20.5 at (12,11)

Wind Dir Gross Error - SW Grid

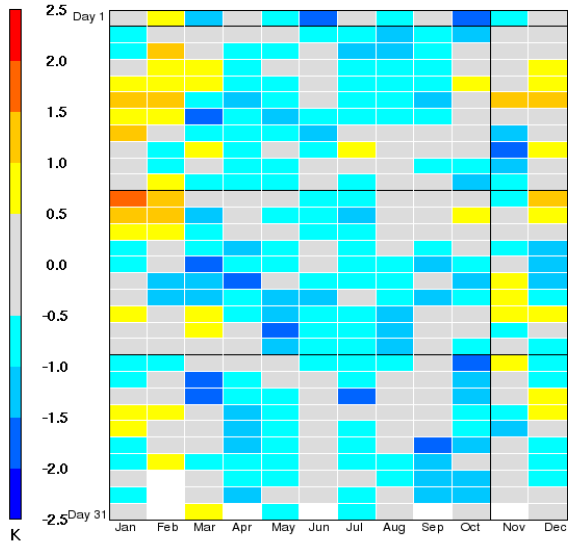
Annual MM5v363 2002 Daily Metrics: 36 km
Iowa DNR



January 1, 2002 0:00:00
Min= 25.3 at (3,18), Max= 65.8 at (12,25)

Temperature Bias - SW Grid

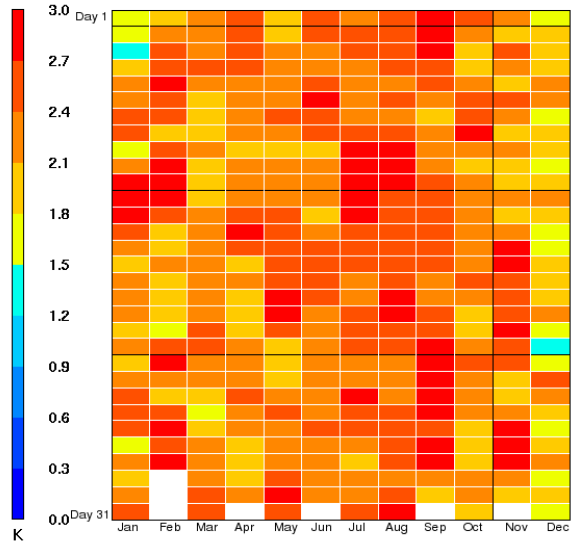
Annual MM5v363 2002 Daily Metrics: 36 km
Iowa DNR



January 1, 2002 0:00:00
Min= -1.9 at (10,31), Max= 1.5 at (1,20)

Temperature Gross Error - SW Grid

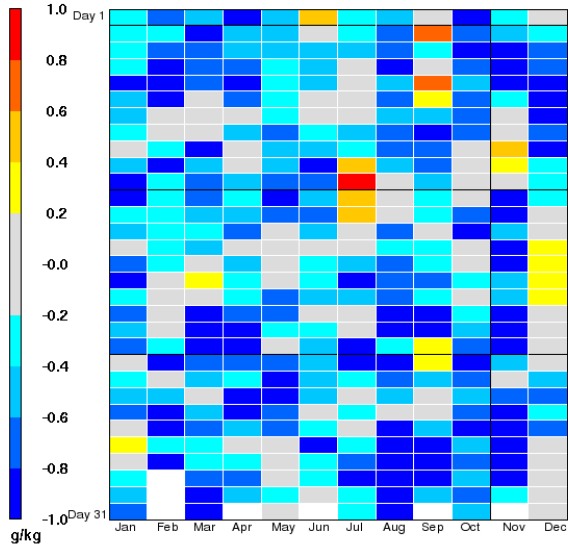
Annual MM5v363 2002 Daily Metrics: 36 km
Iowa DNR



January 1, 2002 0:00:00
Min= 1.5 at (1,29), Max= 3.2 at (1,20)

Humidity Bias - SW Grid

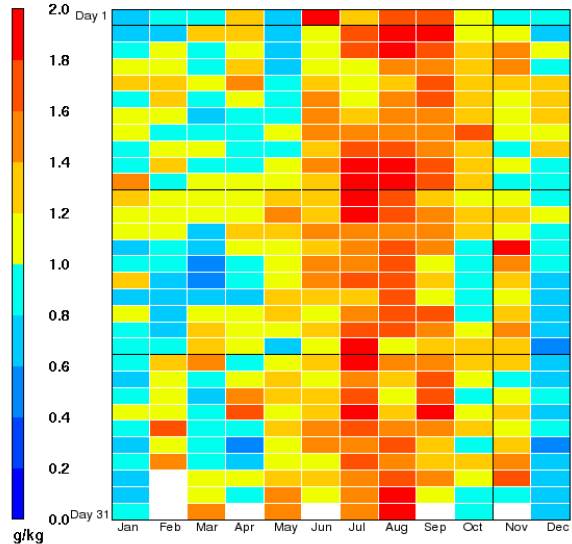
Annual MM5v363 2002 Daily Metrics: 36 km
Iowa DNR



January 1, 2002 0:00:00
Min= -1.5 at (11,3), Max= 1.2 at (7,21)

Humidity Gross Error - SW Grid

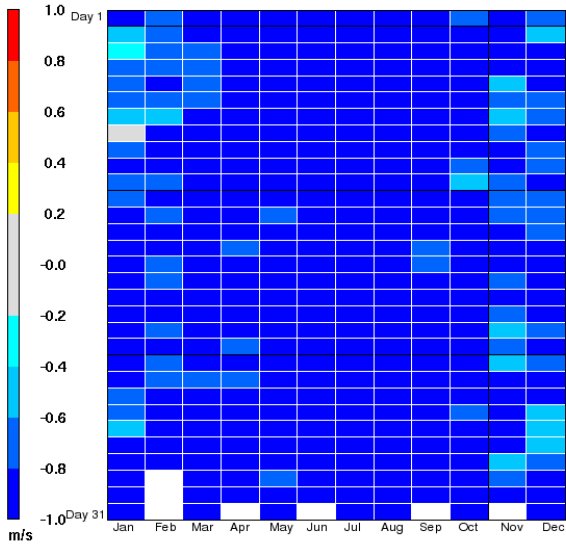
Annual MM5v363 2002 Daily Metrics: 36 km
Iowa DNR



January 1, 2002 0:00:00
Min= 0.5 at (12,11), Max= 2.4 at (7,21)

Wind Spd Bias - DessertSW Grid

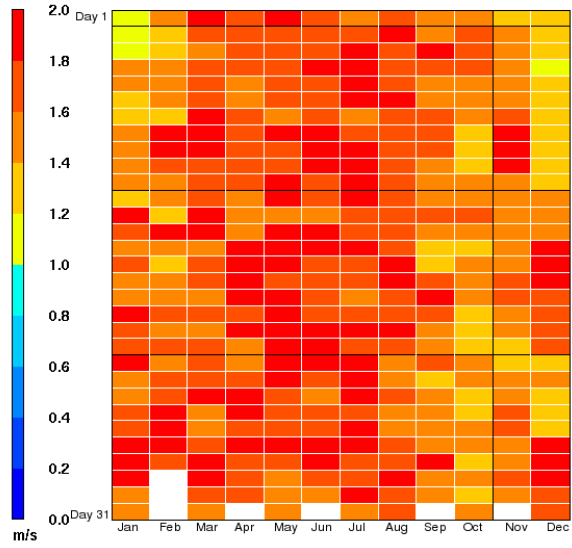
Annual MMSv363 2002 Daily Metrics: 36 km
Iowa DNR



January 1, 2002 0:00:00
Min= -1.9 at (6,3), Max= -0.1 at (1,24)

Wind Spd Gross Error - DessertSW Grid

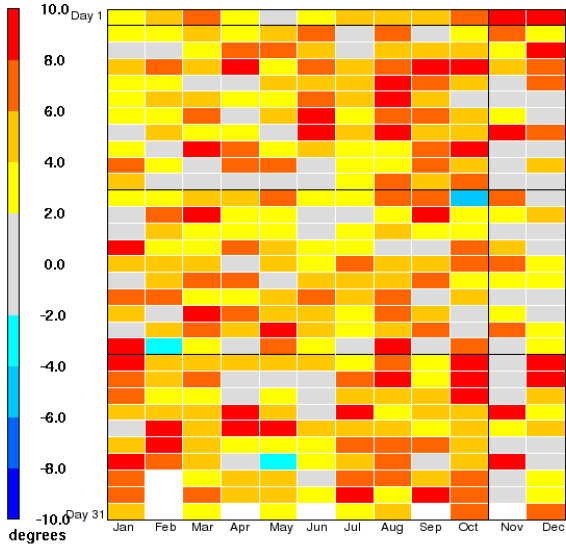
Annual MMSv363 2002 Daily Metrics: 36 km
Iowa DNR



January 1, 2002 0:00:00
Min= 1.0 at (1,30), Max= 2.5 at (4,5)

Wind Dir Bias - DessertSW Grid

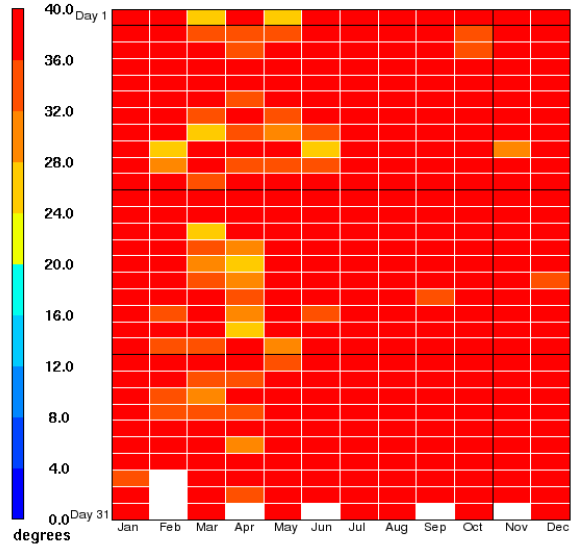
Annual MMSv363 2002 Daily Metrics: 36 km
Iowa DNR



January 1, 2002 0:00:00
Min= -5.2 at (10,20), Max= 12.0 at (8,27)

Wind Dir Gross Error - DessertSW Grid

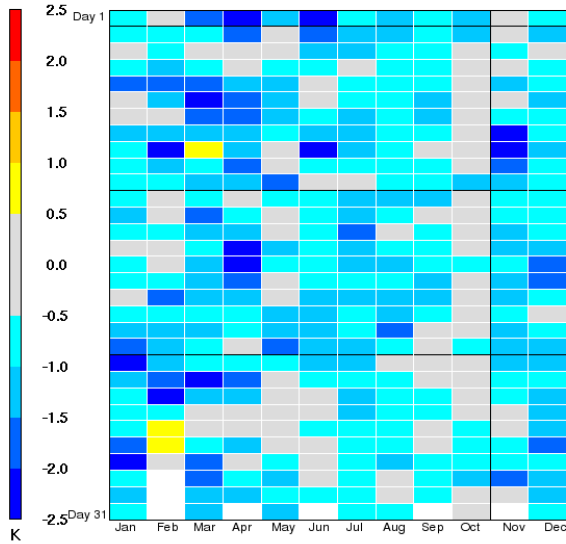
Annual MMSv363 2002 Daily Metrics: 36 km
Iowa DNR



January 1, 2002 0:00:00
Min= 24.4 at (4,16), Max= 56.2 at (5,4)

Temperature Bias - DessertSW Grid

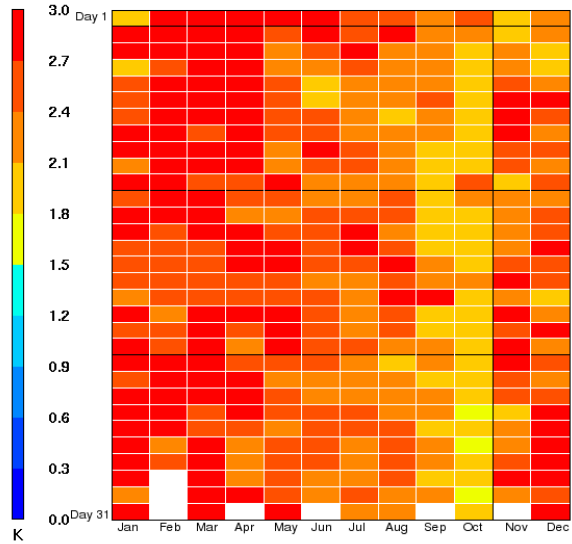
Annual MM5v363 2002 Daily Metrics: 36 km
Iowa DNR



January 1, 2002 0:00:00
Min= -2.8 at (4,17), Max= 0.9 at (3,23)

Temperature Gross Error - DessertSW Grid

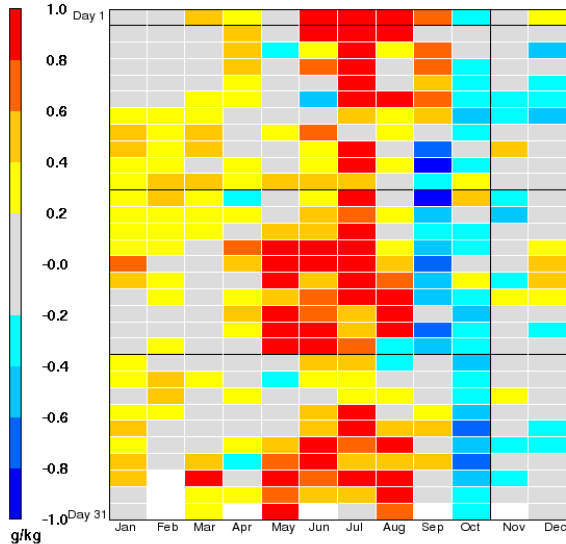
Annual MM5v363 2002 Daily Metrics: 36 km
Iowa DNR



January 1, 2002 0:00:00
Min= 1.7 at (10,2), Max= 3.8 at (3,11)

Humidity Bias - DessertSW Grid

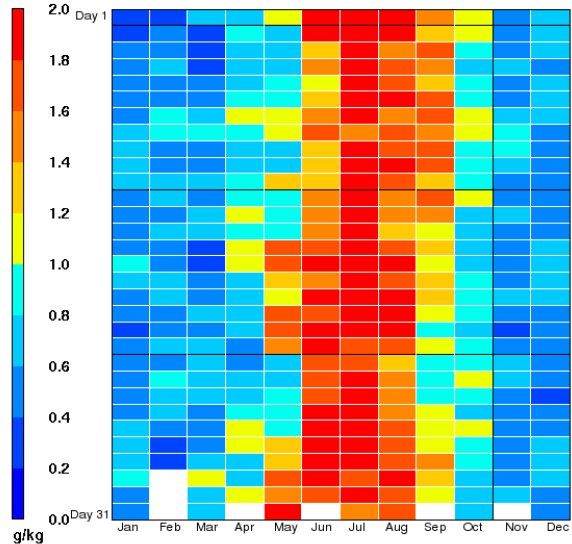
Annual MM5v363 2002 Daily Metrics: 36 km
Iowa DNR



January 1, 2002 0:00:00
Min= -0.9 at (9,22), Max= 2.8 at (6,31)

Humidity Gross Error - DessertSW Grid

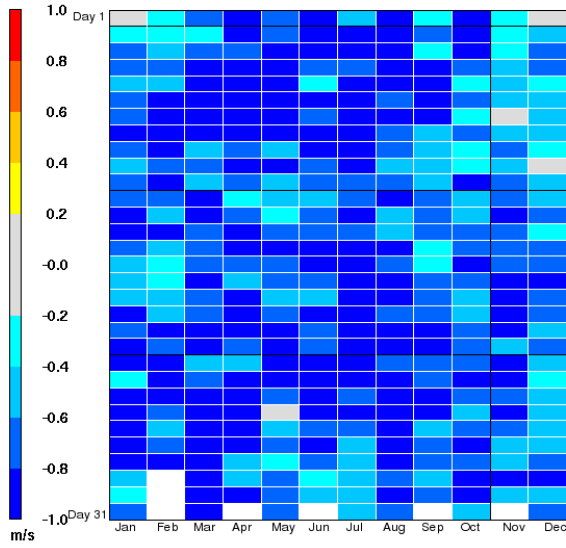
Annual MM5v363 2002 Daily Metrics: 36 km
Iowa DNR



January 1, 2002 0:00:00
Min= 0.2 at (3,29), Max= 3.2 at (6,31)

Wind Spd Bias - North Grid

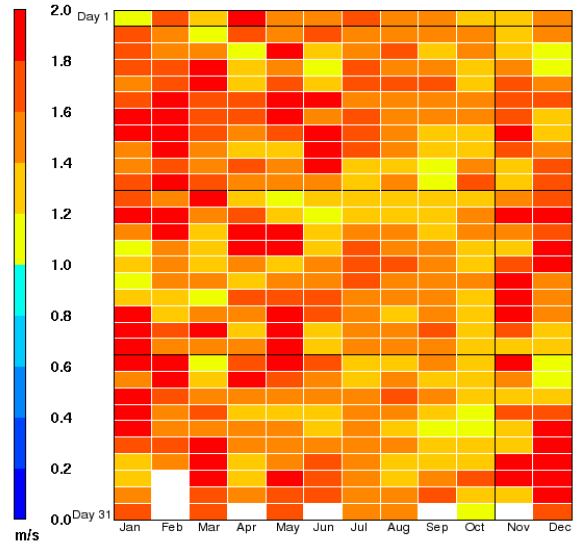
Annual MMSv363 2002 Daily Metrics: 36 km
Iowa DNR



January 1, 2002 0:00:00
Min= -1.6 at (1,19), Max= -0.1 at (11,25)

Wind Spd Gross Error - North Grid

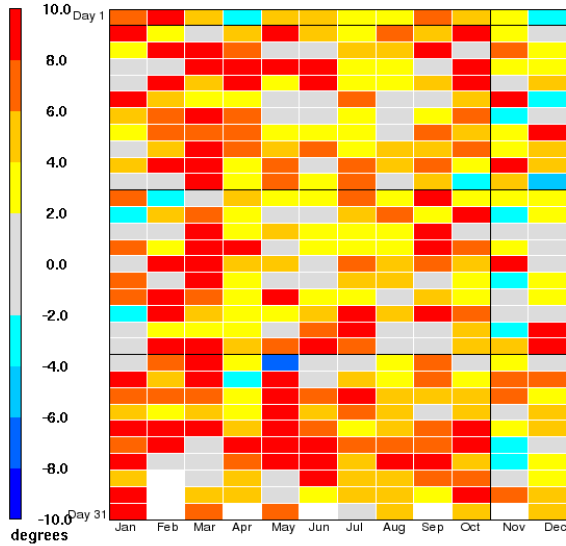
Annual MMSv363 2002 Daily Metrics: 36 km
Iowa DNR



January 1, 2002 0:00:00
Min= 1.0 at (12,10), Max= 2.7 at (2,21)

Wind Dir Bias - North Grid

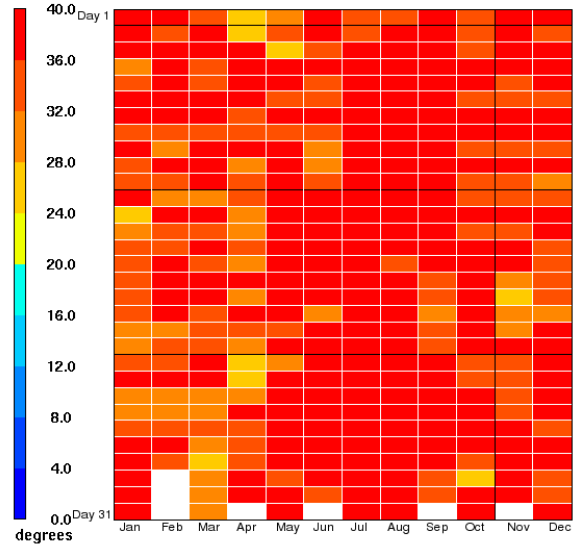
Annual MMSv363 2002 Daily Metrics: 36 km
Iowa DNR



January 1, 2002 0:00:00
Min= -7.1 at (5,10), Max= 16.3 at (3,10)

Wind Dir Gross Error - North Grid

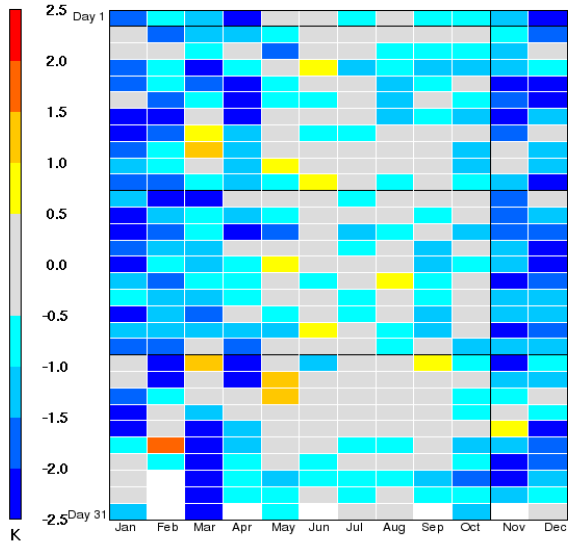
Annual MMSv363 2002 Daily Metrics: 36 km
Iowa DNR



January 1, 2002 0:00:00
Min= 25.5 at (4,30), Max= 54.6 at (5,5)

Temperature Bias - North Grid

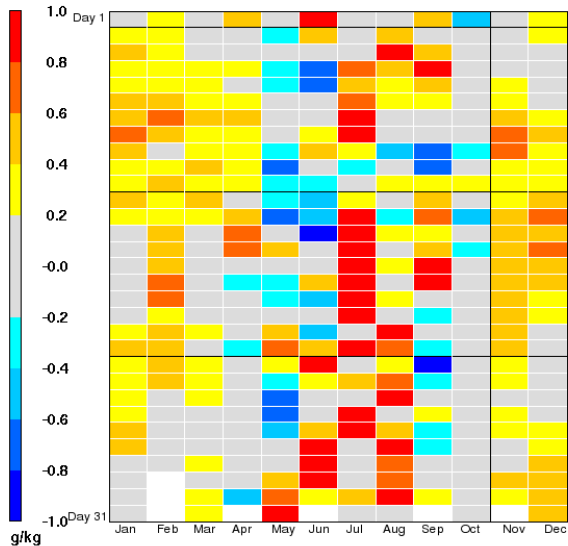
Annual MM5v363 2002 Daily Metrics: 36 km
Iowa DNR



January 1,2002 0:00:00
Min= -3.5 at (4,26), Max= 1.8 at (2,5)

Humidity Bias - North Grid

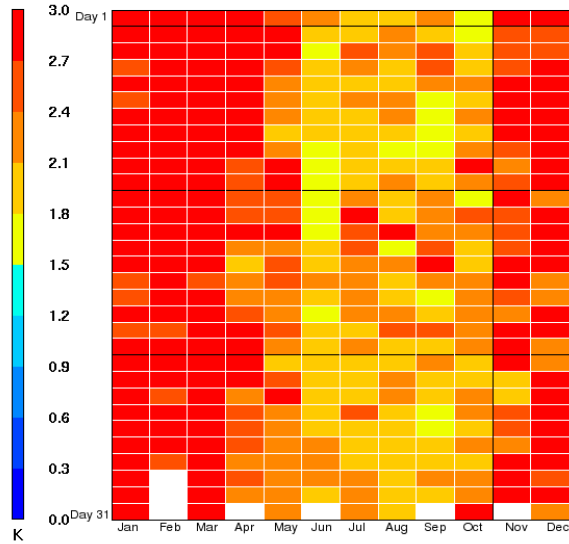
Annual MM5v363 2002 Daily Metrics: 36 km
Iowa DNR



January 1,2002 0:00:00
Min= -0.8 at (6,18), Max= 2.3 at (7,18)

Temperature Gross Error - North Grid

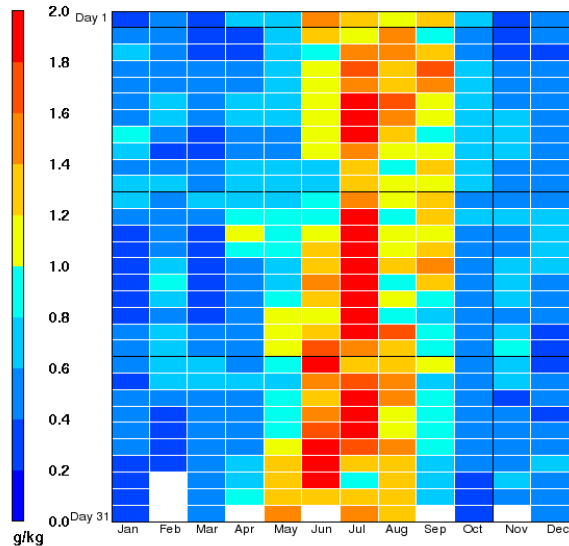
Annual MM5v363 2002 Daily Metrics: 36 km
Iowa DNR



January 1,2002 0:00:00
Min= 1.6 at (6,22), Max= 4.4 at (3,21)

Humidity Gross Error - North Grid

Annual MM5v363 2002 Daily Metrics: 36 km
Iowa DNR

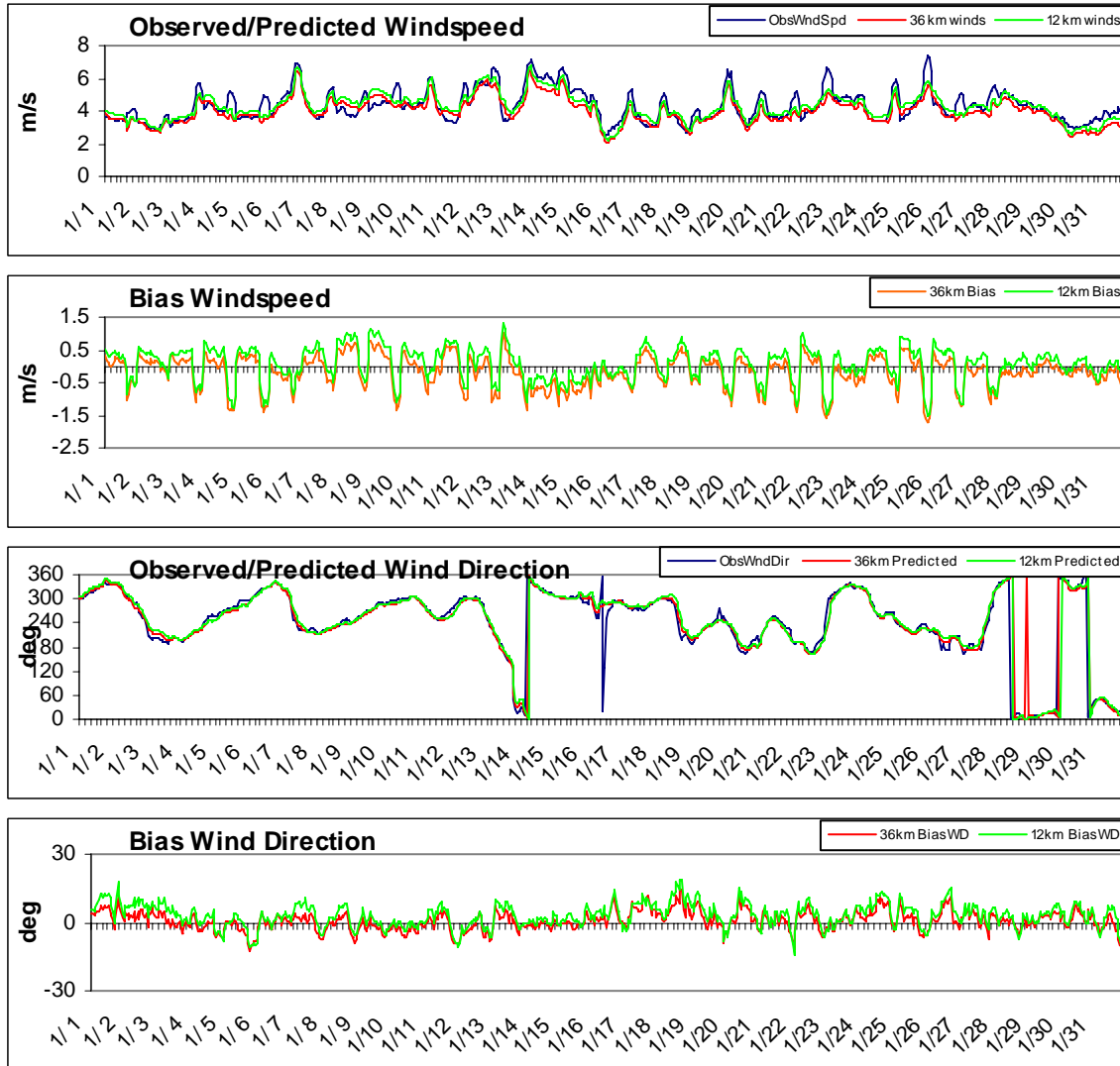


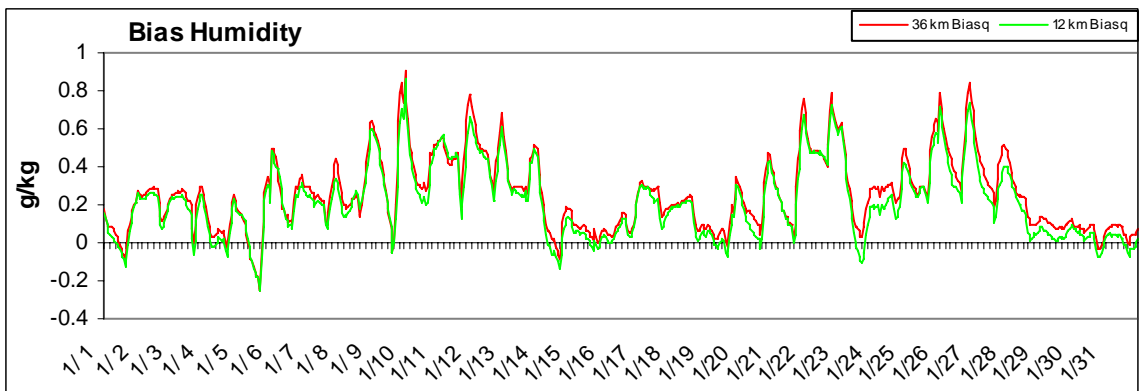
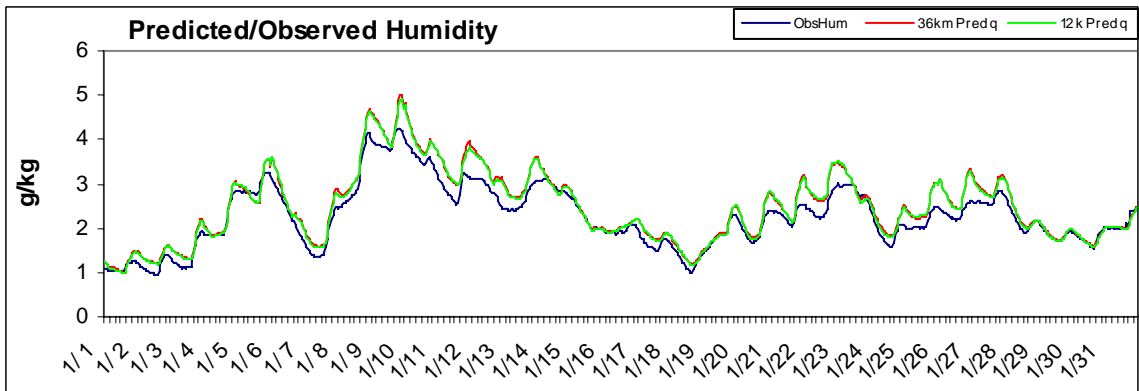
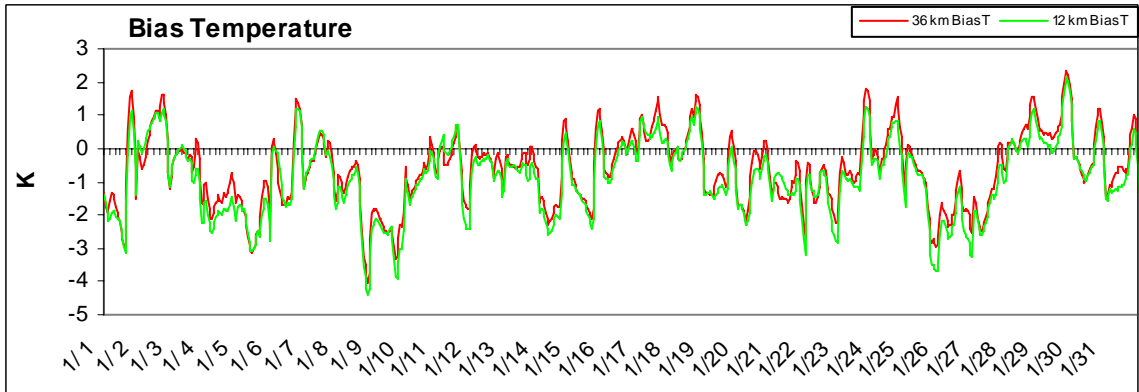
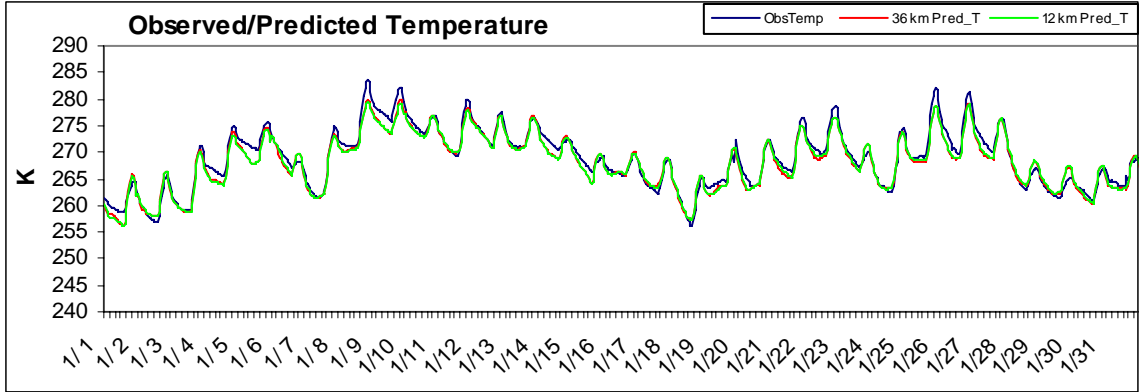
January 1,2002 0:00:00
Min= 0.2 at (2,5), Max= 2.9 at (7,18)

APPENDIX C

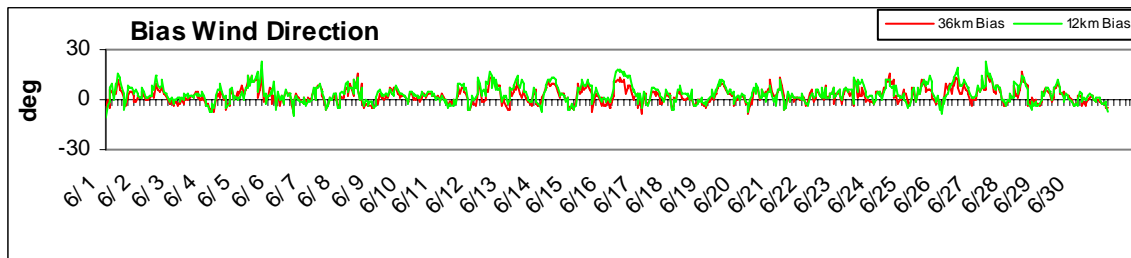
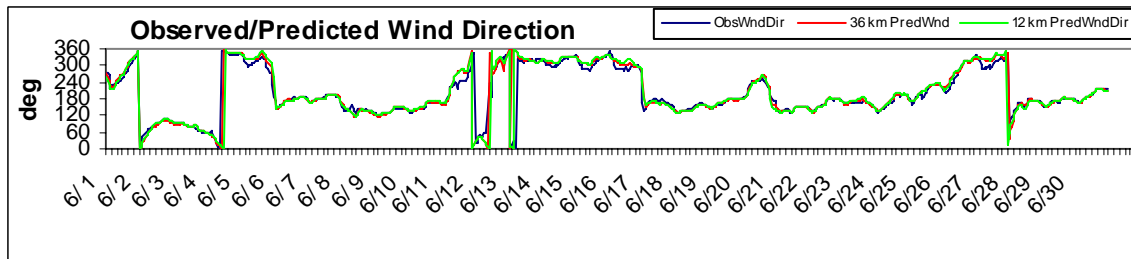
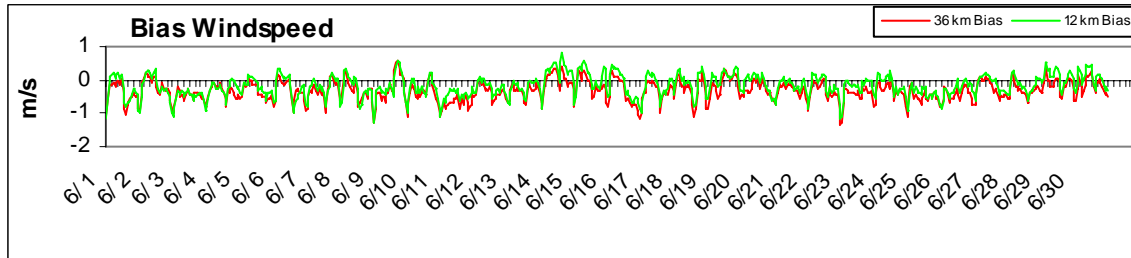
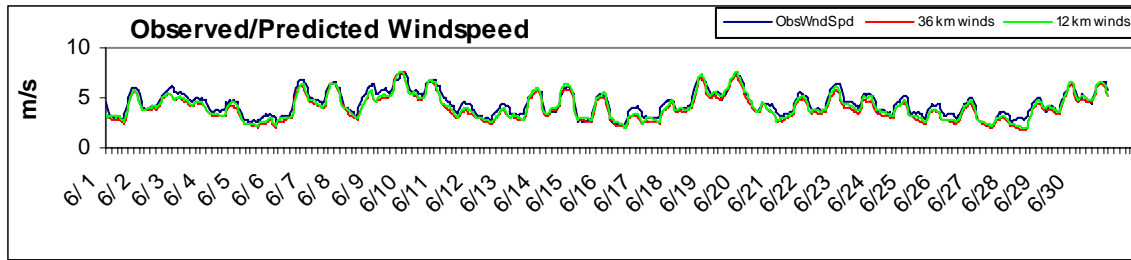
Hourly statistical results for both the 36 and 12 km grids.

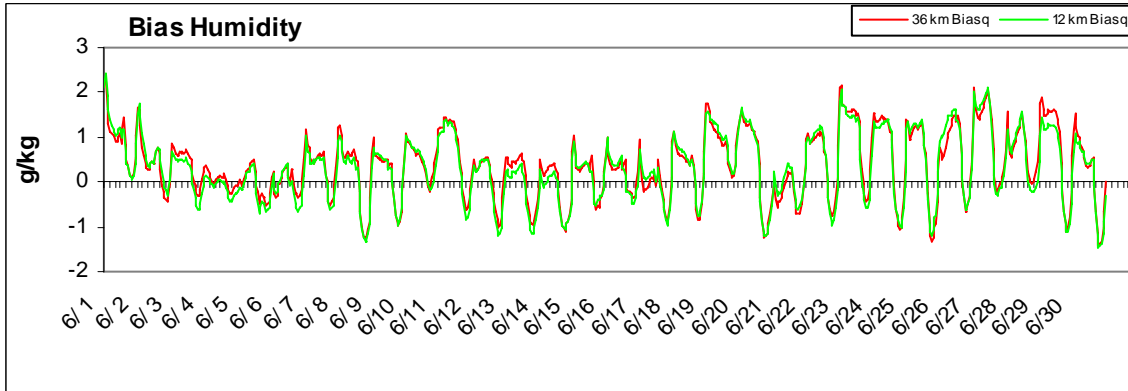
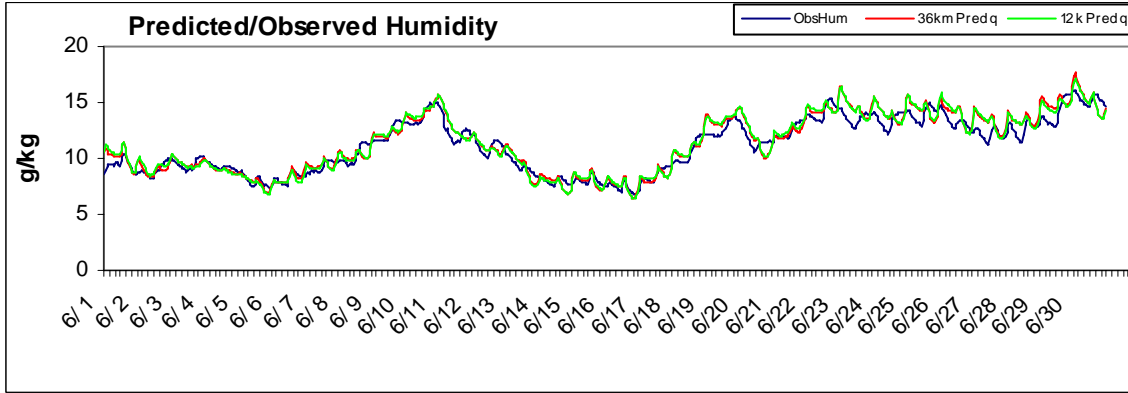
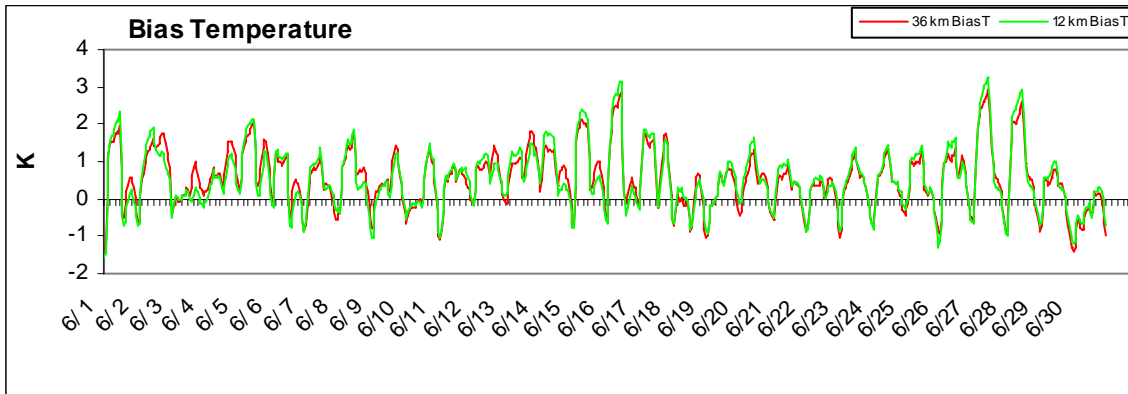
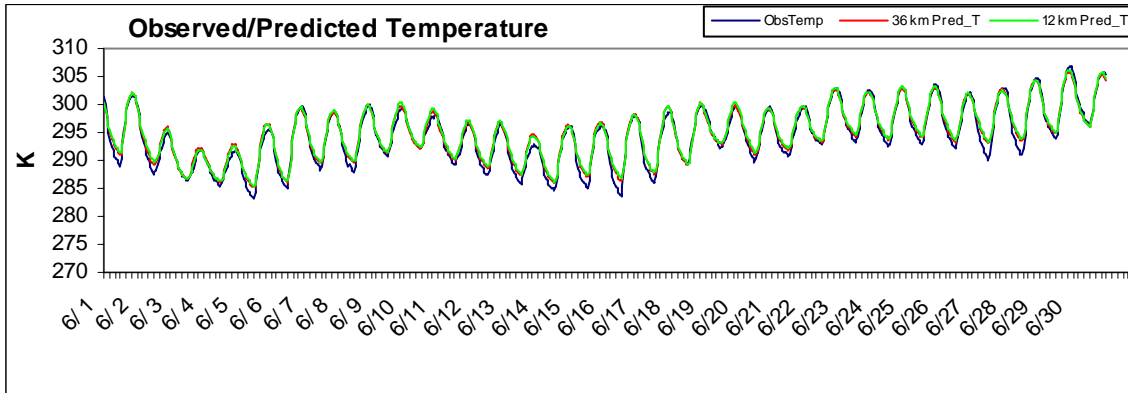
CenrapN: January 2002



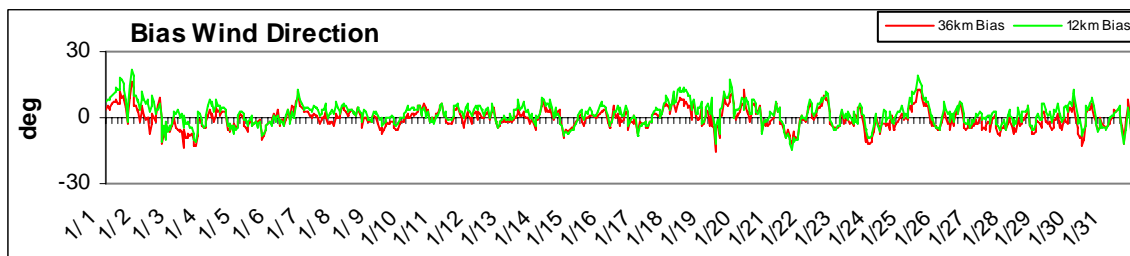
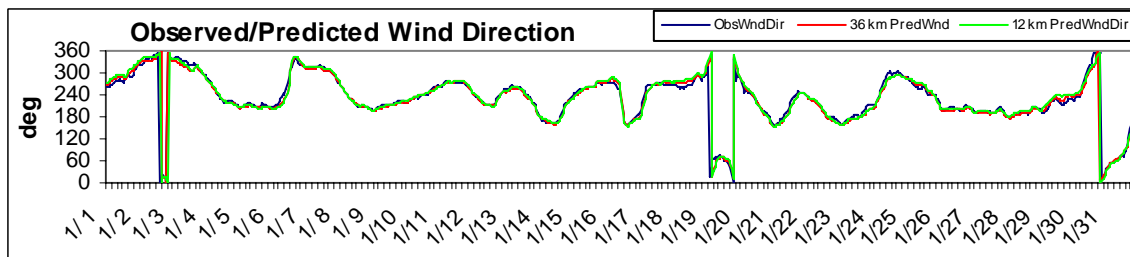
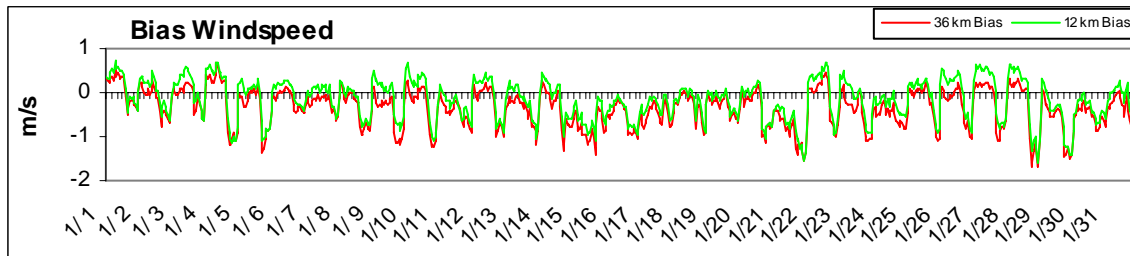
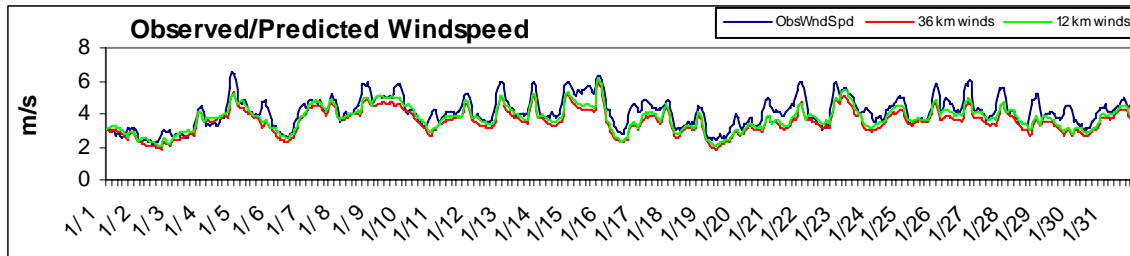


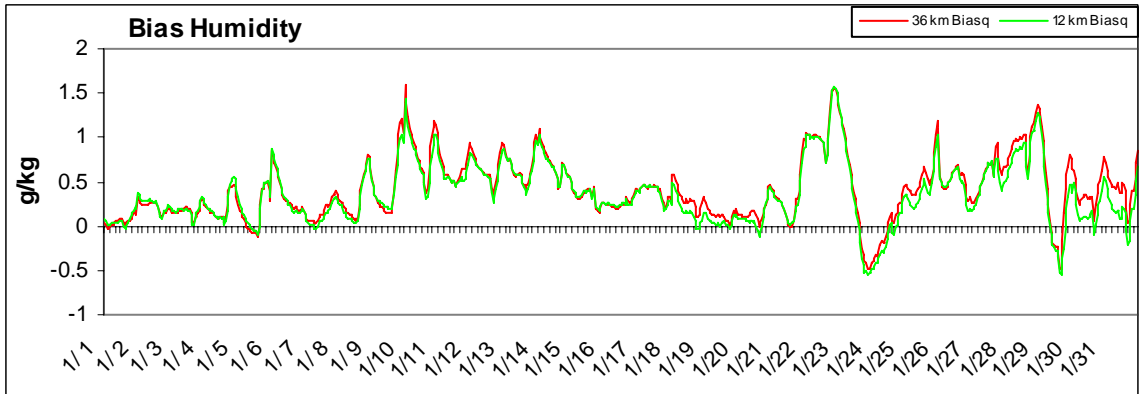
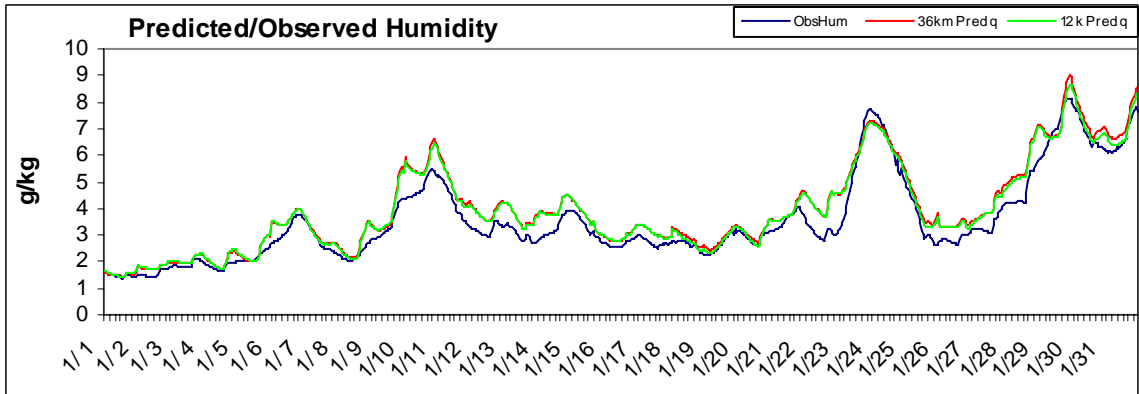
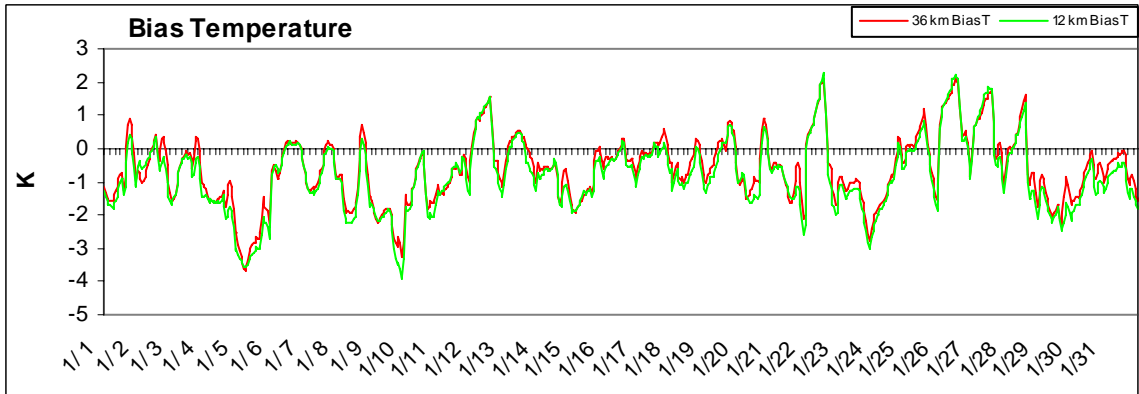
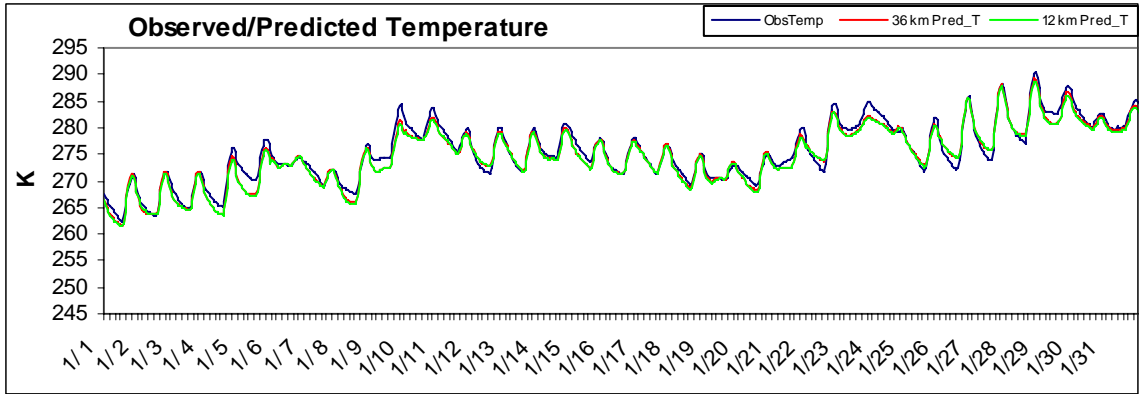
CenrapN: June 2002



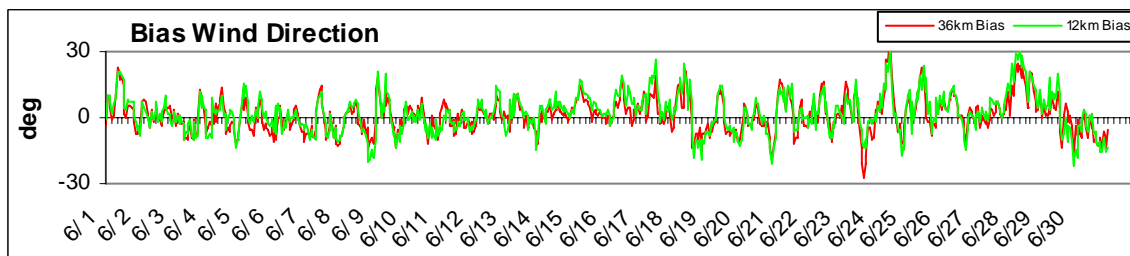
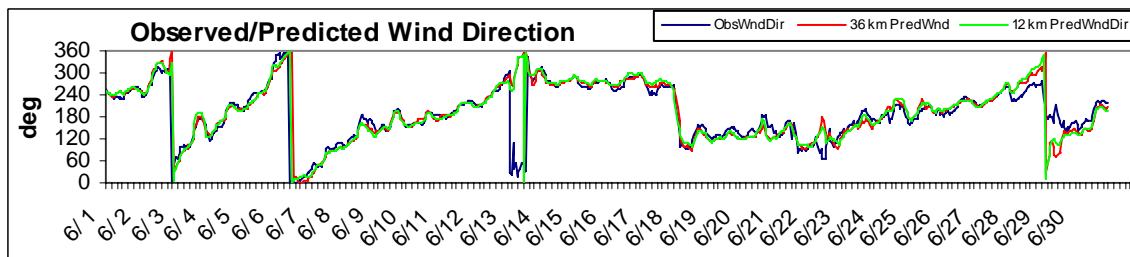
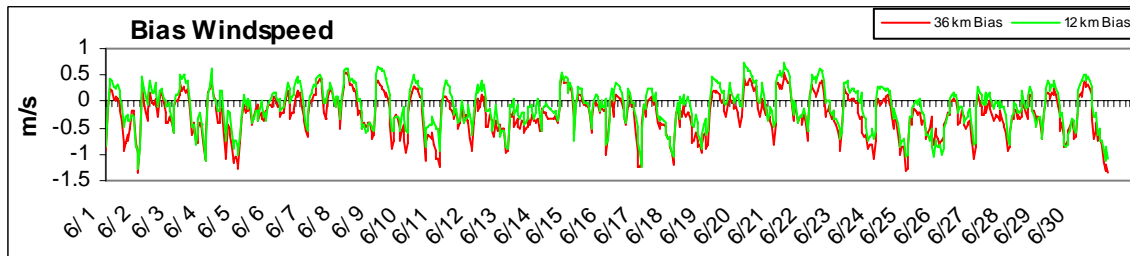
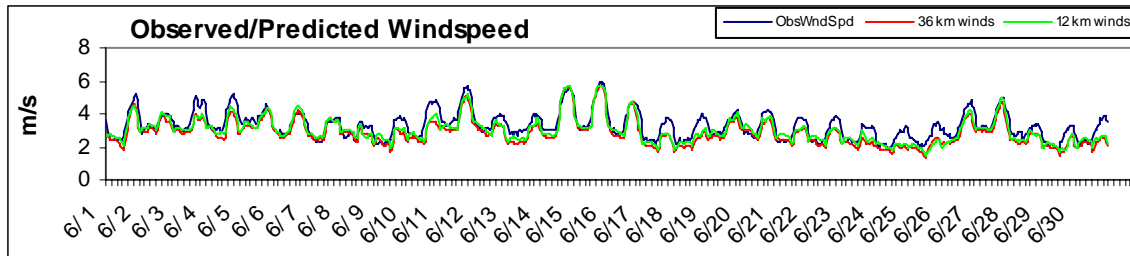


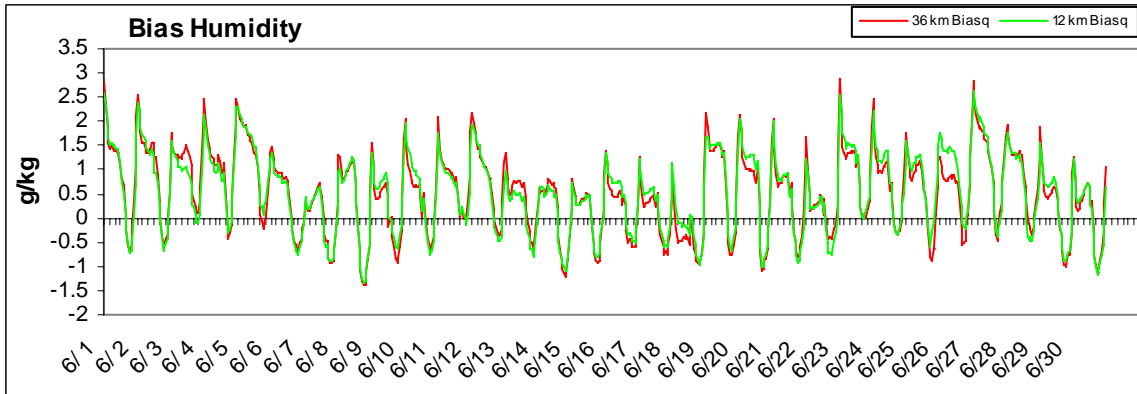
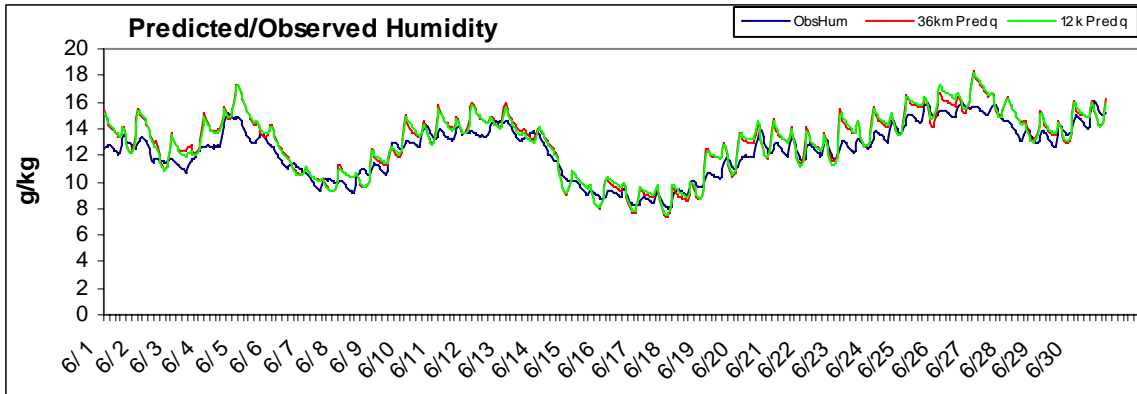
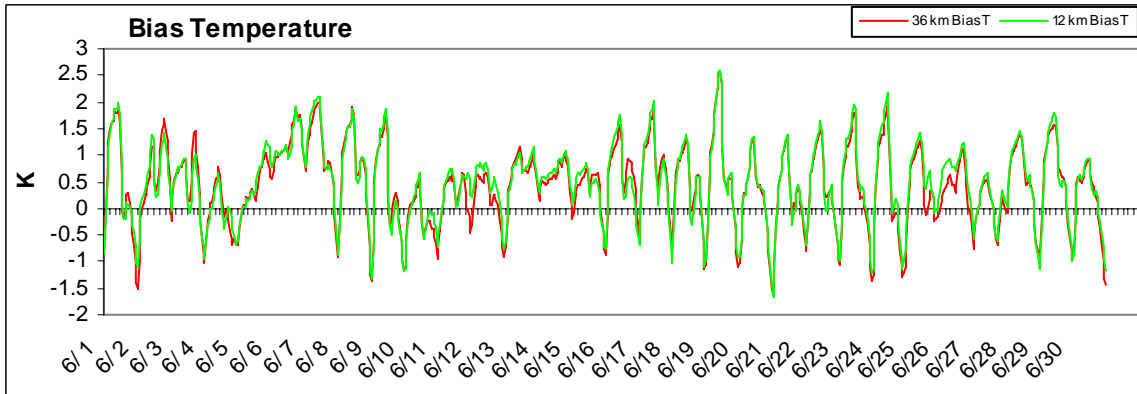
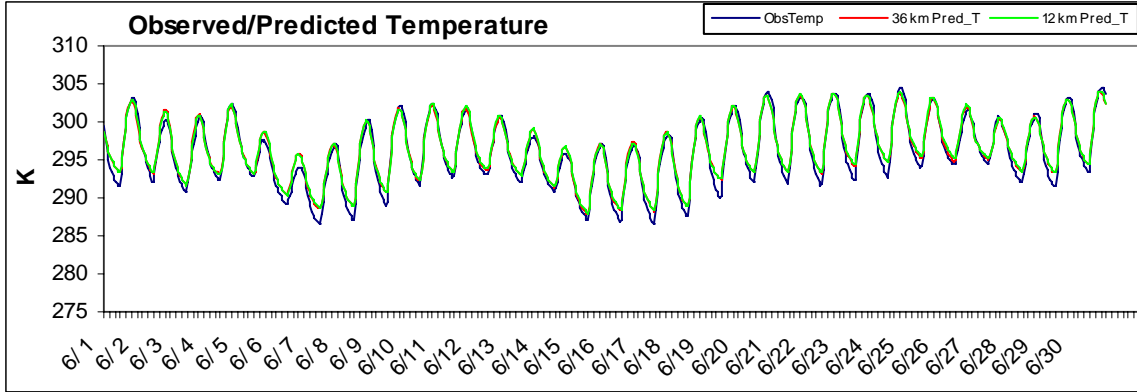
OhioVal: January 2002



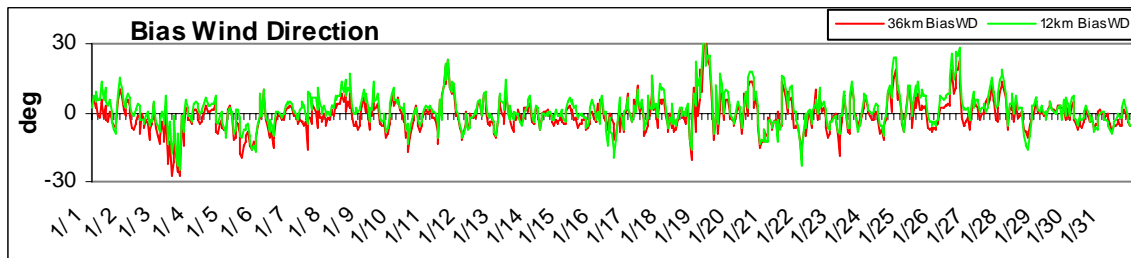
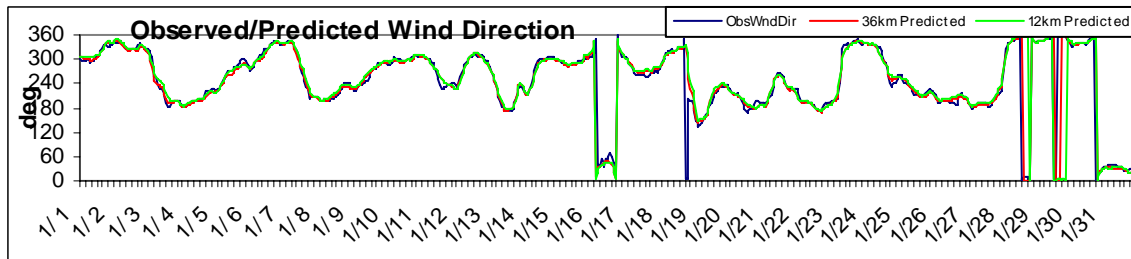
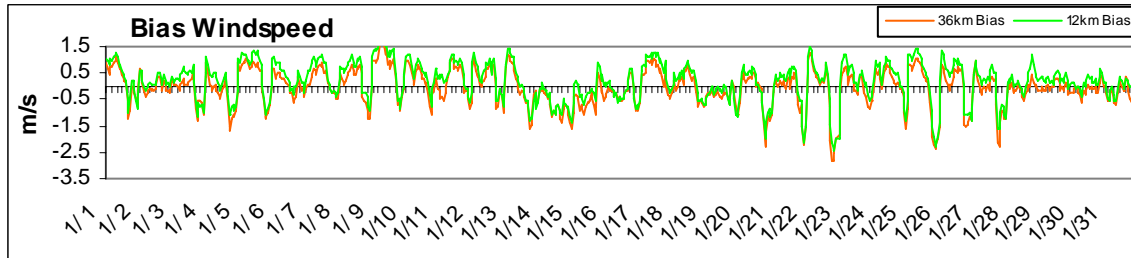
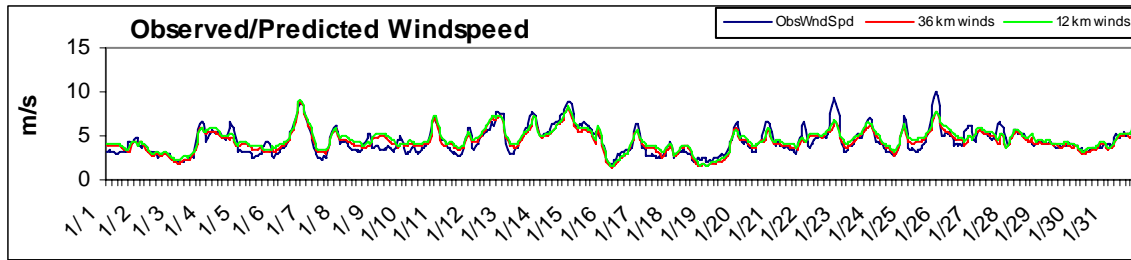


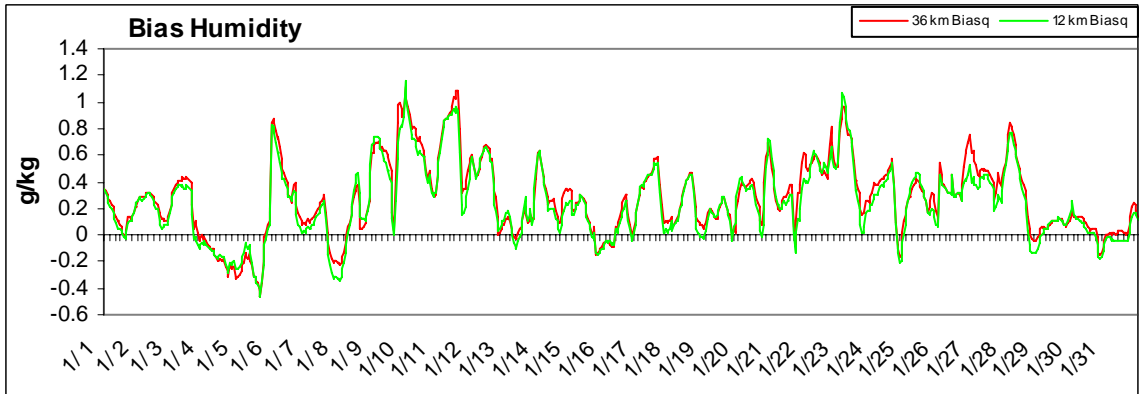
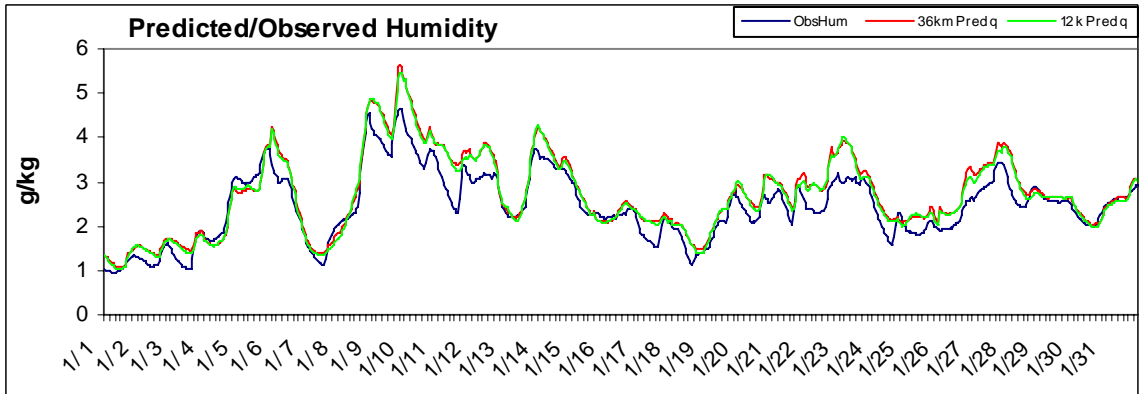
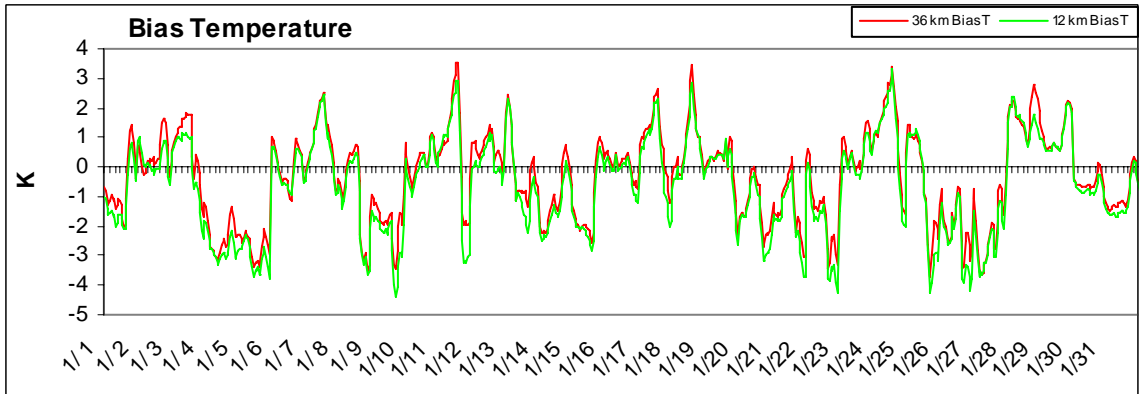
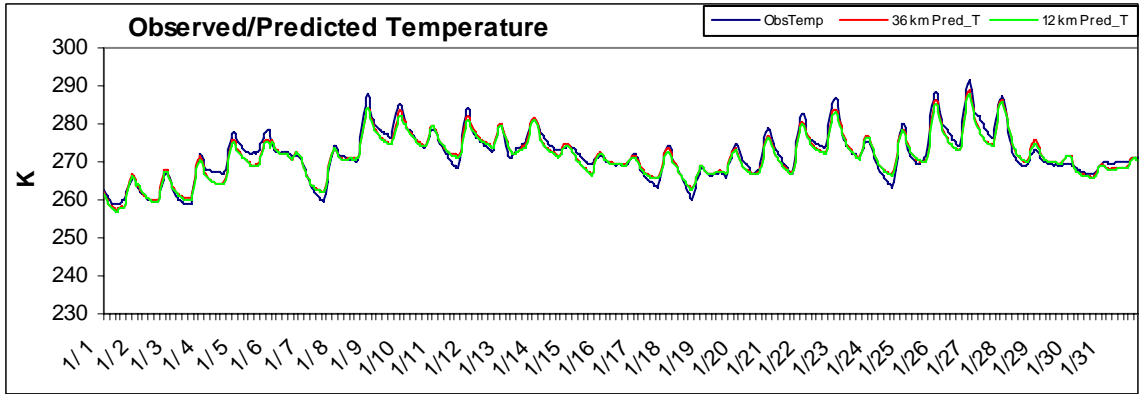
OhioVal: June 2002





Iowa: January 2002





Iowa: June 2002

